

Data Analysis Report

Advanced Data Analysis of Shallow Groundwater Dynamics in the Loxahatchee River Floodplain

Sponsoring Agency:
South Florida Water Management District
Coastal Ecosystems Division
SFWMD Identifier: PO4500030399



Rafael Muñoz-Carpena, David Kaplan and Axel Ritter

Agricultural and Biological Engineering Department
University of Florida
P.O. Box 110570, Gainesville, FL 32611-0570

July 2009

Executive Summary

In November 2008, the South Florida Water Management District (SFWMD) contracted with the University of Florida (UF) to perform data processing for 2008 and analysis of data from June 2005 to December 2008 for a series of twelve shallow groundwater wells in the Loxahatchee River Basin. This report details the data analysis methods and results.

Highlights of the draft data analysis include:

1. River stages in the Northwest Fork of the Loxahatchee River correlate well with shallow groundwater elevations, both in upriver and tidal locations, further confirming the reliability of the final groundwater datasets.
2. Trends in shallow groundwater EC can be observed over individual tidal cycles as well as over longer seasonal time periods. In general, the EC values recorded were low upstream and increased with proximity to Jupiter Inlet and the Atlantic Ocean.
3. On Transects with multiple wells, observed EC was generally greatest closest to the river and decreased with distance towards the upland.
4. Dynamic factor models (DFM) were developed for water table elevation (WTE) and groundwater electrical conductivity (GWEC) in the Loxahatchee River floodplain.
5. A baseline DFM for WTE required six common trends, i.e., independent patterns of unexplained variability, to best describe the dynamics of WTE in the Northwest Fork of the Loxahatchee River. This indicates the complex and multifaceted nature of the WTE variability in the area.
6. Using appropriate explanatory variables (regional groundwater elevation, net recharge at two distributed locations, and river stages at Lainhart Dam and at RM9.1), common trends were reduced from six to three. This indicates that a large amount of the initial unexplained variability can be explained by other measured environmental factors, and that these effectively control the groundwater dynamics in the area.
7. Managed environmental variables (in this case, stage at Lainhart Dam) only explain WTE variability over a short geographic range compared with other effects (tides, rainfall, ET) that have a widespread effect in the watershed. Spatially variable rainfall patterns over short distances played a large role in WTE variation.
8. Factor loadings were low relative to regression coefficients, allowing for the development of a multilinear regression mode (i.e., with no common trends) for WTE that produced acceptable results for most wells. However, common trends were still important to achieve adequate model fits for some wells.
9. A baseline DFM for GWEC required nine common trends, again indicating the complex and multifaceted nature of the GWEC variability in the area. Alternate

baseline DFMs were created using the seven most variable GWEC series aggregated to weekly totals to improve interpretation of the model.

10. The original suite of explanatory variables applied to WTE did not improve model performance when applied to GWEC, but two calculated variables—cumulative flow debt (CFD) and cumulative salt surplus (CSS)—were used to some benefit in the DFM.
11. The final model for GWEC used three common trends and three explanatory variables (net recharge calculated with rain from the S46 structure; CFD using a critical flow of $2.5 \text{ m}^3 \text{ s}^{-1}$ (88 cfs); and CSS calculated from the SWEC series at Kitching Creek).
12. Factor loadings for the DFM of GWEC model were also low relative to regression coefficients, however trends were still important to achieve adequate model fits.
13. The DFMs developed herein are useful for filling data gaps during the study period; identifying the relative importance and relationships between hydrological and management variables that can improve river management plans; and assessing the effects of different restoration scenarios on the floodplain of the Northwest Fork of the Loxahatchee River.

Table of Contents

Background.....	8
Final Data Analysis Report (Deliverable 3.2).....	10
Introduction	10
Materials and Methods	12
Study Area and Experimental Setup	12
Compiled Time Series and Summary Statistics.....	16
Dynamic Factor Analysis.....	16
Hydrological Time Series and Analysis Procedure.....	18
Results and Discussion	20
Experimental Time Series and Summary Statistics.....	20
<u>Correlation with Surface Water Measurements</u>	20
<u>Water Table Elevation</u>	22
<u>Electrical Conductivity</u>	26
<u>Temperature</u>	29
<u>Wet/Dry Seasonality</u>	29
Dynamic Factor Analysis of Water Table Elevation	32
<u>Baseline DFA (no explanatory variables)</u>	32
<u>DFA with explanatory variables</u>	34
<u>Multilinear regression model (DFA with no common trends)</u>	43
Dynamic Factor Analysis of Groundwater Electrical Conductivity.....	44
<u>Baseline DFA (no explanatory variables)</u>	44
<u>Alternate Baseline DFAs</u>	47
<u>DFA with explanatory variables</u>	49
<u>Multilinear regression model (DFA with no common trends)</u>	55
Conclusions.....	56
References.....	58
Appendix I – Daily Time Series Graphs	61
Appendix II – Global and Wet/Dry Season Statistics Tables.....	77

List of Tables

TABLE 1. PROJECT TASKS AND DELIVERABLES. BOLDDED ITEMS HAVE PREVIOUSLY BEEN DELIVERED.....	9
TABLE 2. WELL LOCATIONS AND CHARACTERISTICS.	14
TABLE 3. HYDROLOGICAL TIME SERIES USED IN THE DFA.....	19
TABLE 4. CORRELATION COEFFICIENTS (R) BETWEEN GROUNDWATER WELLS AND SURFACE WATER MEASURED IN THE NORTHWEST FORK OF THE LOXAHATCHEE RIVER.	22
TABLE 5. CORRELATION COEFFICIENTS (R) BETWEEN SURFACE WATER MEASURED IN THE NORTHWEST FORK OF THE LOXAHATCHEE RIVER.....	22
TABLE 6. AIC AND C_{EFF} VALUES FOR THE DFMS WITH NO EXPLANATORY VARIABLES AND 1 – 7 COMMON TRENDS. BEST MODEL IS REPRESENTED IN BOLD NUMBERS.	32
TABLE 7. CONSTANT LEVEL PARAMETERS (μ_N), CANONICAL CORRELATION COEFICENTS ($P_{M,N}$), FACTOR LOADINGS ($\gamma_{M,N}$), REGRESSION COEFFICIENTS ($\beta_{K,N}$), AND COEFFICIENTS OF EFFICIENCY (C_{EFF}) FROM MODEL II (3 TRENDS, 5 EXPLANATORY VARIABLES). SIGNIFICANT REGRESSION PARAMETERS IN BOLD.	37
TABLE 8. CONSTANT LEVEL PARAMETERS (μ_N), MODEL PARAMETERS, AND COEFFICIENTS OF EFFICIENCY (C_{EFF}) FROM MODEL III (NO TRENDS, 5 EXPLANATORY VARIABLES). SIGNIFICANT MODEL PARAMETERS IN BOLD.	43
TABLE 9. AIC AND C_{EFF} VALUES FOR THE GWEC DFMS WITH TWELVE RESPONSE VARIABLES AND NO EXPLANATORY VARIABLES AND 1 – 10 COMMON TRENDS. THE BEST DFM (DIAGONAL MATRIX; $M=9$; $C_{EFF}=0.944$; $AIC = 2198$) IS IN BOLD.	45
TABLE 10. CANDIDATE EXPLANATORY VARIABLES USED IN THE DFA OF GROUNDWATER ELECTRICAL CONDUCTIVITY.....	49
TABLE 11. OUTPUT RESULTS FROM DFA WITH EXPLANATORY VARIABLES (MODEL II).	52

List of Figures

FIGURE 1. LOXAHATCHEE RIVER AND SURROUNDING AREA SHOWING NORTH, NORTHWEST, AND SOUTH FORKS AND MAJOR HYDRAULIC INFRASTRUCTURE.....	12
FIGURE 2. LAYOUT OF TRANSECTS AND WELLS ON THE NORTHWEST FORK OF THE LOXAHATCHEE RIVER.	13
FIGURE 3. METEOROLOGICAL AND SURFACE WATER (STAGE/EC) MONITORING LOCATIONS.....	15
FIGURE 4. AVERAGE DAILY RIVER STAGE AT LAINHART DAM (BLUE) AND AVERAGE DAILY GROUNDWATER ELEVATION AT WELL T1W1 (RED). NOTE: DIFFERENT Y-AXIS SCALES.....	21
FIGURE 5. 15-MINUTE RIVER STAGE AT RM 9.1 (BLUE) AND AVERAGE DAILY GROUNDWATER ELEVATION AT WELLS IN THE FLOODPLAIN OF TRANSECT 7 (RED, GREEN, YELLOW) FOR A 2-MONTH PERIOD IN 2007. NOTE: DIFFERENT Y-AXIS SCALES.....	21
FIGURE 6. ANNUAL AVERAGE WATER TABLE ELEVATION (FT, NAVD88) FOR ALL 12 WELLS IN THE PROJECT.	23
FIGURE 7. AVERAGE DAILY WATER TABLE ELEVATION (FT, NAVD88) IN HIGHER ELEVATION WELLS OVER THE PERIOD OF RECORD.	24
FIGURE 8. AVERAGE DAILY WATER TABLE ELEVATION (FT, NAVD88) IN LOWER ELEVATION WELLS OVER THE PERIOD OF RECORD.	24
FIGURE 9. AVERAGE DAILY WATER TABLE ELEVATION (FT, NAVD88) OF WELLS ON TRANSECT 7. NOTE MAINTENANCE OF LARGE FRESHWATER HEAD IN UPLAND WELL (T7W4).	25
FIGURE 10. AVERAGE DAILY WATER TABLE ELEVATION (FT, NAVD88) OF WELLS ON TRANSECT 8. NOTE MAINTENANCE OF HIGHER HEAD IN UPLAND WELL (T8W3). DATA GAP IN 2007 IS DUE TO WATER TABLE FALLING BELOW PROBE LEVEL.....	25
FIGURE 11. AVERAGE DAILY WATER TABLE ELEVATION (FT, NAVD88) OF WELLS ON TRANSECT 9.....	26
FIGURE 12. ANNUAL AVERAGE EC (S/M) FOR 12 WELLS IN THE PROJECT AND RIVER EC NEAR TRANSECTS 1 AND 7. THE DOTTED RED LINE INDICATES THE 2 PPT (0.3125 S/M) SALINITY THRESHOLD IDENTIFIED FOR THE PROTECTION OF BALD CYPRESS HEALTH.	27
FIGURE 13. DAILY AVERAGE EC (S/M) IN THE RIVER AT RM 9.1 (NEAR TRANSECT 7) AND IN THE 4 WELLS ON THAT	

TRANSECT. NOTE RIVER SALINITY FAR EXCEEDS GROUNDWATER SALINITY IN DRY SEASONS.	27
FIGURE 14. AVERAGE DAILY EC (S/M) FOR 4 WELLS ON TRANSECT 7.....	28
FIGURE 15. AVERAGE DAILY EC (S/M) FOR 3 WELLS ON TRANSECT 8.....	28
FIGURE 16. AVERAGE DAILY EC (S/M) FOR 3 WELLS ON TRANSECT 9.....	29
FIGURE 17. SEASONAL RAINFALL TOTALS RECORDED AT THE S-46 GAUGING STATION ON THE SOUTHWEST FORK OF THE LOXAHATCHEE RIVER. ERROR BARS INDICATE PLUS/MINUS ONE STANDARD DEVIATION.	29
FIGURE 18. ANNUAL RAINFALL SUMS FOR RAIN GAUGES AT S-46 STRUCTURE AND WEATHER STATION JDWX. 2006 IS NOT SHOWN FOR JDWX BECAUSE OF INCOMPLETE RECORDS AT THIS STATION DURING THIS YEAR.	30
FIGURE 19. AVERAGE WET/DRY SEASON WATER TABLE ELEVATION (FT, NAVD88). ERROR BARS INDICATE PLUS/MINUS ONE STANDARD DEVIATION.	31
FIGURE 20. AVERAGE WET/DRY SEASON GROUNDWATER EC (S/M). ERROR BARS INDICATE PLUS/MINUS ONE STANDARD DEVIATION.	31
FIGURE 21. AKAIKE INFORMATION CRITERIA (AIC) VERSUS NASH-SUTCLIFFE COEFFICIENT OF EFFICIENCY (<i>CEFF</i>) WITH INCREASING NUMBER OF COMMON TRENDS ($M = 1-7$) USING (A) A DIAGONAL ERROR COVARIANCE MATRIX AND (B) A SYMMETRIC, NON-DIAGONAL ERROR COVARIANCE MATRIX.....	32
FIGURE 22. FACTOR LOADINGS FOR THE MODEL WITH SIX TRENDS AND NO EXPLANATORY VARIABLES. THE IMPORTANCE OF EACH TREND TO THE MODEL CAN BE SEEN INDIVIDUALLY FOR EACH INPUT TIME SERIES (IN THIS CASE, WTE).....	33
FIGURE 23. THE THREE MOST IMPORTANT TRENDS TO MODEL I (LEFT) AND THEIR ASSOCIATED CANONICAL CORRELATION COEFFICIENTS (RIGHT). PANEL (A) SHOWS HIGH CORRELATION TO UPLAND AND UPSTREAM WELLS; (B) IS MOST ASSOCIATED WITH FLOODPLAIN WELLS; (C) HAS LOW CORRELATIONS EXCEPT FOR WELLS T8W1 AND T8W3.	34
FIGURE 24. NET RECHARGE (NR; CUMULATIVE RAINFALL – CUMULATIVE ET) FOR THE TWO RAINFALL TIME SERIES USED IN THE DFM. NOTE THAT NR_S46 SHOWS A STEADY DRYING PATTERN OVER THE ~4-YEAR PERIOD, WHILE NR_JDWX SHOWS A WETTING TREND.	35
FIGURE 25. AIC VERSUS <i>CEFF</i> FOR MODELS I, II, AND SEVERAL ALTERNATE DFMS.	36
FIGURE 26. REGRESSION PARAMETERS AND FACTOR LOADINGS FOR MODEL II ($M=3, K=5$). REGRESSION PARAMETERS (A-E) ARE SHOWN WITH THEIR STANDARD ERRORS, WITH BLACK BARS INDICATING SIGNIFICANCE.	38
FIGURE 27. COMMON TRENDS AND ASSOCIATED $P_{M,N}$ VALUES FOR MODEL II.....	40
FIGURE 28. OBSERVED AND MODELED TIME SERIES FOR UPLAND WELLS. <i>CEFF</i> RANGES FROM 0.86 TO 1.0.	41
FIGURE 29. OBSERVED AND MODELED TIME SERIES FOR FLOODPLAIN WELLS. <i>CEFF</i> RANGES FROM 0.78 TO 0.98.	42
FIGURE 30. OBSERVED VERSUS PREDICTED NORMALIZED WTE AND THE 1:1 LINE.....	42
FIGURE 31. FIGURE 32. OBSERVED (SYMBOLS) AND MODELED (LINES) NORMALIZED WTE FOR (A) WELL T3-W1; (B) WELL (T7-W1); AND (C) WELL T7-W3 OBTAINED FROM MODEL III USING 5 EXPLANATORY VARIABLES AND NO TRENDS.....	43
FIGURE 32. AKAIKE INFORMATION CRITERIA (AIC) VERSUS NASH-SUTCLIFFE COEFFICIENT OF EFFICIENCY (<i>CEFF</i>) WITH DIAGONAL (LEFT) AND NON-DIAGONAL ERROR MATRICES FOR THE BASELINE DFM USING TWELVE RESPONSE VARIABLES.....	44
FIGURE 33. THE THREE MOST IMPORTANT TRENDS TO MODEL I-A (LEFT) AND THEIR ASSOCIATED CANONICAL CORRELATION COEFFICIENTS (RIGHT). PATTERNS OF SHARED VARIATION AMONG GWEC IN THE TWELVE WELLS ARE UNCLEAR.	46
FIGURE 34. GWEC IN THE TWELVE WELLS IN THE LOXAHATCHEE RIVER. LOW MAGNITUDE AND LOW VARIATION WELLS (T1W1, T3W1, T7W4, T8W3, AND T9W3) SHOWN IN BLACK.	47
FIGURE 35. AKAIKE INFORMATION CRITERIA (AIC) VERSUS NASH-SUTCLIFFE COEFFICIENT OF EFFICIENCY (<i>CEFF</i>) FOR MODEL I-B (SEVEN RESPONSE VARIABLES; LEFT) AND MODEL I-C WEEKLY GWEC (SEVEN RESPONSE VARIABLES; RIGHT). BOTH USED DIAGONAL ERROR COVARIANCE MATRICES.....	48
FIGURE 36. CALCULATED CUMULATIVE FLOW DEBT (CFD) FOR FIVE CRITICAL FLOW LEVELS ($1 - 3 \text{ M}^3 \text{ S}^{-1}$).....	50
FIGURE 37. CALCULATED CUMULATIVE SALT SURPLUS (CSS) FOR FOUR SWEC STATIONS.	51
FIGURE 38. REGRESSION PARAMETERS AND FACTOR LOADINGS FOR MODEL II ($M=3, 3$ EXPLANATORY VARIABLES). REGRESSION PARAMETERS ARE SHOWN WITH THEIR STANDARD ERRORS.	52

FIGURE 39. COMMON TRENDS AND ASSOCIATED $P_{M,N}$ VALUES FOR MODEL II..... 53

FIGURE 40. OBSERVED AND MODELED TIME SERIES FOR FLOODPLAIN WELLS. *CEFF* RANGES FROM 0.58 TO 1.0.
..... 54

FIGURE 41. OBSERVED VERSUS PREDICTED NORMALIZED GWEC FOR THE MODEL WITH NO COMMON TRENDS
(MODEL III). PANEL (A) SHOWS THE BEST FIT (*CEFF* = 0.43, R^2 = 0.45); (B) SHOWS THE WORST (*CEFF* = -0.51;
 R^2 = 0.44)..... 55

Background

The Loxahatchee River and Estuary are located in southeastern coast of Florida. Historically, the Northwest Fork of the Loxahatchee River was primarily a freshwater system. In 1947, the river inlet at Jupiter was dredged for navigation and has remained permanently open since that time. Drainage patterns within the basin have also been altered significantly due to land development, road construction, such as, Florida Turnpike, and construction of the C-18 and other canals. These anthropogenic activities along with sea level rise have resulted in significant adverse impacts on the ecosystem, including increased saltwater encroachment and undesired vegetation changes in the floodplain. The problem of saltwater intrusion and vegetation degradation in the Loxahatchee River may be partly induced by diminished freshwater input, from both surface water and ground water into the River system.

Finding the characteristics of each hydrologic components and their relationship is important to develop restoration plan for the ecosystem in the Loxahatchee River Basin. In past years, a Loxahatchee floodplain groundwater well network and soil moisture monitoring stations along two transects have been established and the associated data have been collected. In this report, the data collected from the wells includes temperature, water pressure, barometric pressure, DO, and electric conductivity (EC) from January to December 2008, which are raw data in binary format. The overall objective of this project is to process and document groundwater data of 2008 to a format for meaningful use, and to conduct hydrologic analysis based on the ground water data together with soil moisture data and river stage data from June 2005 to December 2008.

The objectives of the project include:

- Process and document the ground water data collected from 12 wells in Loxahatchee River Basin (January to December 2008)
- Conduct hydrologic data analysis based on the ground water, soil moisture, and river stage (June 2005 – January 2008)

To achieve these objectives, specific tasks and deliverables were developed, which are summarized in Table 1. A project kick-off meeting (**Task 1**) was held on December 3rd, 2008 at the offices of the South Florida Water Management District (SFWMD). At this meeting, the University of Florida (UF) introduced the staff needed to complete this work and made a PowerPoint presentation (**Deliverable 1.1**) to the District engineers/scientists including a detailed overview of the project objectives, plans, methods, schedule and required deliverables. During this kick-off meeting and discussions, the Consultant and the District agreed on a Project Work Plan that described the objectives for each task in detail, the major questions being addressed by each task, and the rationale for the task.

During the meeting, UF prepared kick-off meeting minutes specifying all points of the project work plan and the main points discussed in the meeting, including all inputs from the District engineers/scientists. These draft minutes were submitted to District staff on December 8th, 2008 and were approved by the district on December 9th, 2008 to serve as the Final Project Work Plan (**Deliverable 1.2**).

Table 1. Project tasks and deliverables. Bolded items have previously been delivered.

TASK	DELIVERABLE
1. Project Kick-off Meeting and Project Work Plan	1.1 Power Point Presentation 1.2 Agreement document with key points of Project Work Plan
2. Process and Document 2008 Groundwater Data	2.1 Draft of Data Processing Report
	2.2 Final Data Processing Report
3. Advanced Groundwater data Analysis with Soil and River Data	3.1 Draft of Data Analysis Report
	3.2 Final Data Analysis Report

This report presents **Deliverable 3.2 (Final Data Analysis Report)**, detailing progress made and issues encountered. Specifically, compiled time series and summary statistics of water table elevation (WTE) and groundwater electrical conductivity (EC) data from 2005 – 2008 are presented here. Additionally, UF performed correlation analyses and Dynamic Factor Analysis (DFA) on the 12 WTE and groundwater EC time series processed in Task 2 and the previous scope of work. Detailed descriptions of data processing and quality assurance/quality control (QA/QC) methods appear in the Final Data Processing Report (Task 2.2) and are not repeated here.

Final Data Analysis Report (Deliverable 3.2)

Introduction

The Loxahatchee River is located on the lower eastern coast of Florida, USA (26° 59' N, 80° 9' E), and its watershed drains approximately 240 square miles in Palm Beach and Martin Counties. The Northwest Fork of the Loxahatchee River and its watershed are unique in that they contain a diverse array of terrestrial and aquatic ecosystems including coastal pine scrub, pinelands, xeric oak scrub, hardwood hammocks, freshwater marshes, wet prairies, cypress swamps, mangrove swamps, seagrass beds, tidal flats, oyster beds, and coastal dunes (Treasure Coast Planning Council, 1999) in an increasingly urbanized area. However, a changing hydroperiod and salinity regime in the river and its floodplain over the last century has been linked to undesired vegetative changes in the floodplain forest (SFMWD, 2005). Of primary concern is the loss of the bald cypress ecosystem and transition to mangrove-dominated communities as saltwater moves further upriver and into the floodplain forest.

The health of the Loxahatchee River and its adjacent ecosystems is a priority for many residents, visitors, agencies, and political leaders. As such, a number of planning efforts have been initiated over the past 20 years, including the Loxahatchee River National Wild and Scenic River Management Plan, the North Palm Beach County Comprehensive Everglades Restoration Plan (CERP) Project, and the Minimum Flows and Levels Rule (among others) (SFWMD, 2005). Minimum Flows and Levels (MFLs) are designed to protect the ecology and water resources of a river and are linked to the concept of protecting valued ecosystem components (VECs) from “significant harm” (SFWMD, 2002). An MFL for the Northwest Fork of the Loxahatchee River was adopted in April 2003 to protect the river’s remaining freshwater floodplain swamp community as well as other downstream estuarine resources including oysters (*Crassostrea virginica*) and several sea grasses (all identified as VECs). However, these management efforts have focused solely on the river channel, and have not addressed saltwater intrusion into the floodplain.

Saltwater intrusion has been described as the “landward and upward displacement of the freshwater-saltwater interface in coastal aquifers, and increased saline water penetration in deltaic and estuarine areas” (Knighton et al., 1991) and as the invasion of fresh or brackish surface water or groundwater by water with higher salinity (USGS, 2001). The dynamics of saltwater intrusion are controlled by the interactive effects of tidal activity, wind speed and direction, density gradient caused by salinity, and the timing and volume of fresh surface water and groundwater discharge (which are, in turn, functions of rainfall, evapotranspiration, and myriad watershed and aquifer properties). With diurnal tidal cycles, stochastic annual weather cycles, and decadal climate cycles, the dynamic behavior of saltwater intrusion is surely “non-linear and complex” (Wang, 1998). Saltwater intrusion can also be associated with accelerated sea-level rise, hurricanes, or severe drought, and can quickly lead to catastrophic loss of coastal wetlands (Wanless et al., 1994).

Description and modeling of hydroperiod, groundwater elevation and salinity, soil moisture, and soil porewater salinity are essential to understanding the hydrological and ecological functioning of the floodplain forest (e.g., Mitsch and Gosselink, 2000) where the valued ecosystems components live (and die, as the case may be). However, finding direct

relationships between basic hydrological inputs (rainfall, river stage, river salinity, etc.) is not always straightforward (Ritter et al., 2009) because of the complex interactions between surface water, groundwater, and porewater in a variably saturated matrix with heterogeneous soils, vegetation, and topography. Depth, duration, frequency, and salinity of tidal flooding is a function of distance to the ocean, distance away from the river channel, local elevation (microtopography), volume of freshwater flow, and direction, volume, and salinity of groundwater fluxes.

Analysis of long-term monitoring of soil moisture and porewater salinity (Mortl, 2006; Kaplan et al., 2007); groundwater elevation and salinity (Muñoz-Carpena et al., 2008); upstream river flow and salinity; downstream surface water elevation and salinity; and meteorological data in order to characterize the temporal variation of hydrological and water quality variables may improve understanding of system dynamics. However, investigating relationships between multivariate time series using visual inspection and comparative statistics is difficult, subjective, and may not appropriately characterize the system (Ritter et al., 2007). Thus, an alternate method for identifying common trends and causal factors is required.

Dynamic Factor Analysis (DFA) is a dimension reduction technique, originally developed for the interpretation of economic time series (Geweke, 1977). DFA is a multivariate application of classic time series analysis and can be a powerful tool for the modeling of short, incomplete, non-stationary time series in terms of common trends and explanatory variables (Zuur et al., 2003a). With DFA, underlying temporal variation in observed data (input time series) is modeled as linear combinations of common trends (unexplained variability), a constant level (or intercept) parameter, zero or more explanatory variables (additional observed time series), and noise (Zuur et al., 2003b). Like other time series models, DFA aims to maintain a good fit while minimizing the number of common trends, and thus, model selection is made using Akaike's information criterion (AIC), which includes a penalty for each additional estimated parameter (Akaike, 1974; Zuur et al., 2003b).

The ability to model time series as a combination of common trends *and* explanatory variables is especially useful for analyzing complex environmental systems, where DFA can help assess what explanatory variables (if any) affect the time series of interest, and thus may be worthy of closer attention. DFA has been successfully applied in hydrology to identify common trends in groundwater levels (Kovacs et al., 2004; Ritter and Muñoz-Carpena, 2006), soil moisture dynamics (Ritter et al., 2009), and interactions between hydrological variables and groundwater quality trends (Muñoz-Carpena et al., 2005; Ritter et al., 2007). It has been used to identify trends and environmental response variables affecting squid populations (Zuur and Pierce, 2004) and commercial fisheries (Erzini, 2005; Tulp et al., 2008). DFA applications are not limited to the natural sciences: Molenaar (2006) explored the use of DFA in psychology and biomedicine and Sbarra and Ferrer (2006) have even used DFA to study the dynamics of love and anger following romantic breakups.

The objective of this task is to apply DFA to study the interactions between hydrological conditions in the floodplain and other hydrological variables obtained throughout the Loxahatchee River watershed.

Materials and Methods

Study Area and Experimental Setup

The study was conducted in the Loxahatchee River Watershed in southeastern Florida (Fig. 1), where intensive data collection and modeling efforts in support of MFL development have been underway for several years. The Loxahatchee River has three main tributaries: the North Fork, the Northwest Fork, and the Southwest Fork. These three tributaries join at the Loxahatchee Estuary Central Embayment, which connects to the Atlantic Ocean via Jupiter Inlet (Fig. 1). The watershed includes several large, protected, publicly owned areas including Jonathan Dickinson State Park (JDSP), the Loxahatchee Slough Preserve, Jupiter Ridge Natural Area, and J.W. Corbett Wildlife Management Area.

In the Northwest Fork of the Loxahatchee River, encroaching salinity and altered hydroperiods have been linked to four factors: 1) the construction of canals that direct water away from the historic watershed; 2) the construction of the C-18 canal (Fig. 1) which transferred a majority of the historic flow of the Northwest Fork to the Southwest Fork; 3) the permanent opening of the Jupiter Inlet (Fig. 1), historically an intermittent barrier to saltwater intrusion, to the Atlantic Ocean; and 4) the lowering of the regional groundwater table in the watershed by community consumption (Mortl, 2006). These hydrologic changes have been linked to changes in the vegetative composition of the floodplain, where studies have documented the retreat of bald cypress upriver since at least the turn of the twentieth century. Freshwater flow to the Northwest Fork is controlled by managing river stage at Lainhart Dam (Fig. 1).

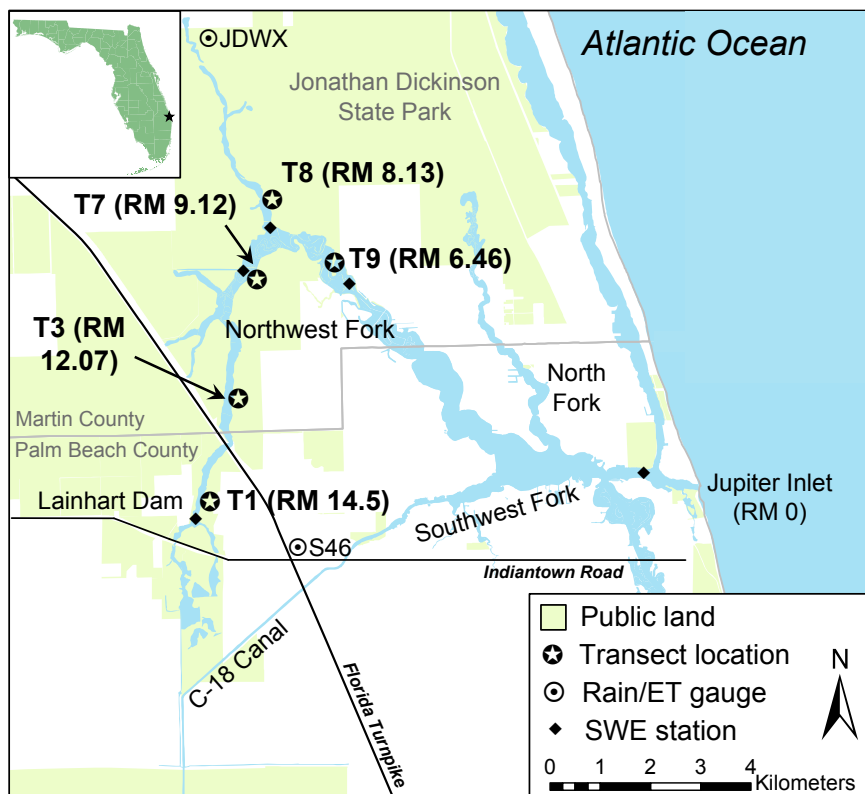


Figure 1. Loxahatchee River and surrounding area showing North, Northwest, and South Forks and major hydraulic infrastructure.

Groundwater data, including temperature, electric conductivity (EC), dissolved oxygen (DO), barometric pressure, and H₂O pressure, were collected using TROLL 9000/9500 multi-parameter water quality probe (In-Situ Inc., Ft. Collins, CO, USA) from July 2003 through January 2009 along five previously established vegetation survey transects perpendicular to the Northwest Fork of the Loxahatchee River (T1, T3, T7, T8, and T9; Fig. 2). Upriver transects T1 and T3 each have only one well, while transitional and tidal transects have multiple wells to document differences in groundwater EC from the river channel towards the upland. T7 has four wells and T8 and T9 each have three wells. Table 2 summarizes important attributes of the twelve wells in the study.

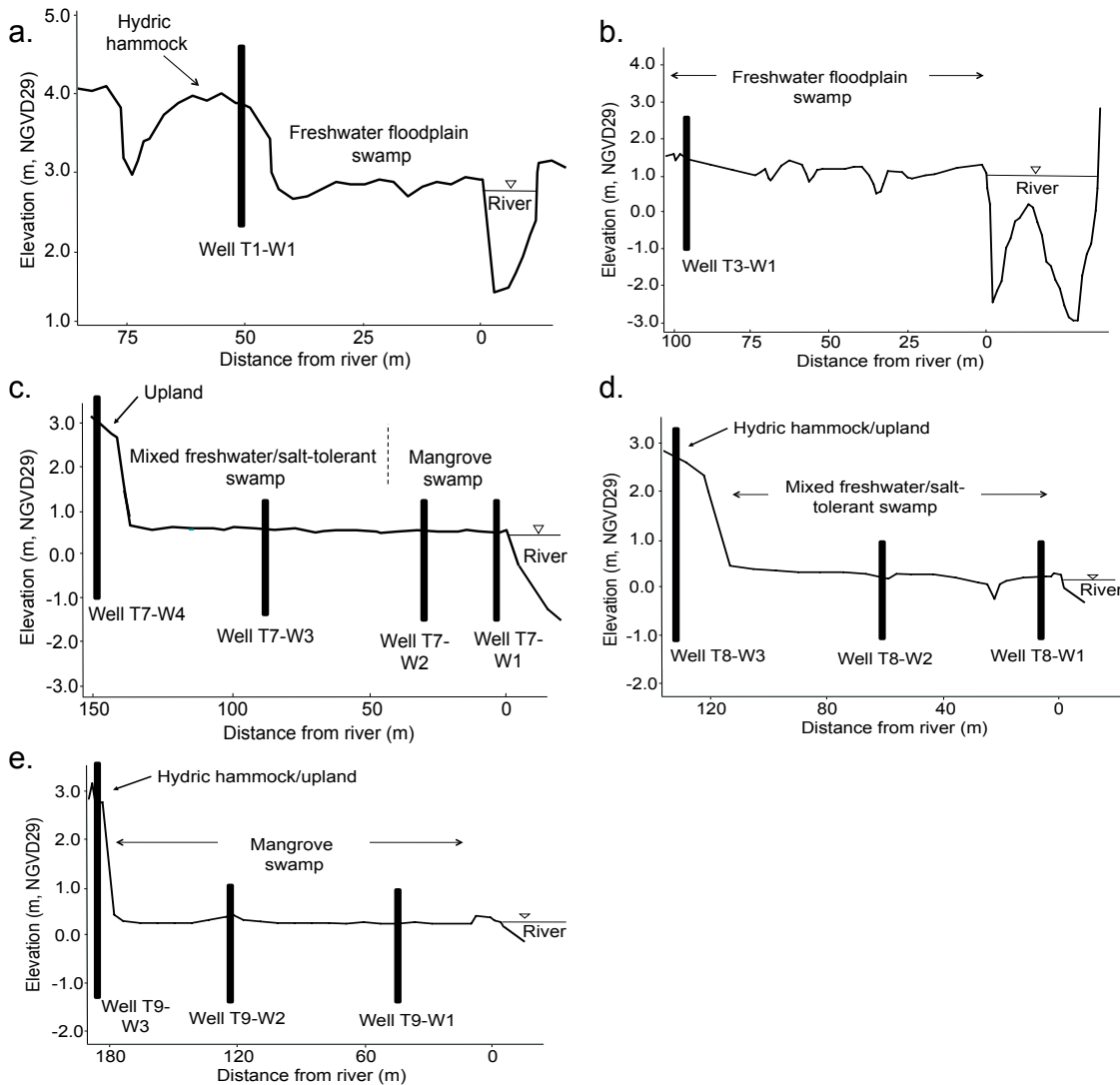


Figure 2. Layout of Transects and wells on the Northwest Fork of the Loxahatchee River.

Table 2. Well locations and characteristics.

Well	River Mile	Transect Type	Elevation (m, NGVD29)	Upland/ Floodplain
T1W1	14.5	Riverine	4.19	Upland
T3W1	12.1	Riverine	2.51	Upland
T7W1	9.1	Transitional	1.27	Floodplain
T7W2	9.1	Transitional	1.34	Floodplain
T7W3	9.1	Transitional	1.47	Floodplain
T7W4	9.1	Transitional	3.85	Upland
T8W1	8.1	Transitional	1.03	Floodplain
T8W2	8.1	Transitional	1.27	Floodplain
T8W3	8.1	Transitional	3.19	Upland
T8W1	6.5	Tidal	1.32	Floodplain
T9W2	6.5	Tidal	1.53	Floodplain
T9W3	6.5	Tidal	3.85	Upland

Transects 1 and 3 are upriver locations, not directly impacted by daily tides. Transect 1 is located 14.5 miles upstream of the river mouth (indicated as RM 14.5) and has elevations ranging from 13.74 ft (4.19 m) (referenced to the National Geodetic Vertical Datum [NGVD]) on the top of a hydric hammock to 5.44 ft (1.66 m) in the river channel (Fig. 2a). This freshwater transect is dominated by upland forest and hydric hammock at higher elevations and mature bald cypress swamp (average diameter at breast height [DBH] of 1.61 ft [0.49 m] in the floodplain) (SFWMD, 2005). Transect 3, located at RM 12.1, has several shallow braided streams in the floodplain and elevations ranging from 5.54 feet (1.69 m) in the floodplain to -9.87 ft (-3.00 m) in the river channel (Fig. 2b). This transect contains freshwater riverine swamp, but is dominated by pop ash (*Fraxinus caroliniana*) with only four large bald cypress (average DBH 3.00 ft [0.92 m]) in the canopy. Intrusion of less flood-tolerant species into the riverine floodplain in these and other riverine transects has been documented, indicating the ecological impact of shortened hydroperiod (SFWMD, 2005).

Moving downriver, transects 7, 8, and 9 all receive daily tidal flooding of varying salinity over most or all of their length. Transect 7 is in a transitional area (RM 9.1) and has elevations ranging from 10.06 feet (3.07 meters) in the upland to 1.31 feet (0.40 meters) in the floodplain (Fig. 2c). Vegetation studies indicate that this transect has been impacted by saltwater intrusion, logging, and invasion by exotic plants (SFWMD, 2006) and presently contains upper tidal swamp (dominated by red mangrove [*Rhizophora mangle*]) transitioning to freshwater riverine swamp approximately 100 ft (30 m) from the river channel. Transect 8 is located approximately 500 ft (150 m) upstream of the confluence of the Northwest Fork and Kitching Creek at RM 8.13. This transect has elevations ranging from 9.06 ft (2.76 m) in the upland to 0.77 ft (0.23 m) at the creek edge and transitions from hydric hammock in the uplands to upper tidal swamp in the floodplain (Fig. 2d). The canopy is dominated by pond apple (*Annona glabra*), wax myrtle (*Myrica cerifera*), and bald cypress, though red and white mangroves (*Laguncularia racemosa*) seedlings and sub-canopy are present, especially within a braided channel with direct connection to the creek (SFWMD, 2007). Finally, transect 9 is located at RM 6.5 on a small peninsula in the Northwest Fork and has elevations ranging from 9.48 ft (2.89 m) in the upland to 1.31 ft (0.40 m) at the river's edge (Fig. 2e). This transect consists of lower tidal swamp, dominated by red and white mangrove except on an elevated trail, which supports some sabal palm (*Sabal palmetto*). Roberts et al. (2008) documented intense

vegetation changes on this transect, with a transition from freshwater to saltwater swamp species in less than 50 years.

Along with groundwater elevation and EC in the twelve wells described above, additional meteorological and hydrological variables were measured across the watershed. Breakpoint rainfall data were recorded at the SFWMD S-46 Structure on the Southwest Fork of the Loxahatchee River and at the JDWX weather station in Jonathan Dickinson State Park (Fig. 3) and converted to daily sums. Additional meteorological data including daily ET values were recorded at the JDWX weather station. These data are publicly available and were downloaded from the SFWMD's DBHYDRO browser (Stations S46_R and JDWX; accessed at <http://www.sfwmd.gov/org/ema/dbhydro/index.html>).

Surface water elevation (i.e., river stage) and salinity (expressed as electrical conductivity at 25° C [EC], S/m) were recorded at five locations in the Northwest Fork. A SFWMD station at Lainhart Dam (adjacent to Transect 1) measures mean daily headwater stage (LNHRT_H) and calculates flow (LNHRT_W), both of which are available on the DBHYDRO browser. The Loxahatchee River District (LRD) maintains a sampling station (Datasonde Station 69) on the Northwest Fork of the Loxahatchee River at the Indiantown Road (close to Transect 1) that measures EC hourly. These data were acquired from LRD staff. USGS/SFWMD stations located at RM 9.1 (near transect 7), Kitching Creek (near transect 8), Boy Scout Dock (~0.5 river miles downstream of transect 9), and Coast Guard Station (near the Jupiter inlet) measure surface water elevation and surface and bottom salinity every 15 minutes. These data were acquired from USGS staff. Finally, daily average water table elevation data from several USGS wells near the Loxahatchee River are publicly available and were downloaded from the USGS National Water Information System (accessed at <http://waterdata.usgs.gov/nwis/>). All meteorological and surface water monitoring locations are summarized in figure 3.

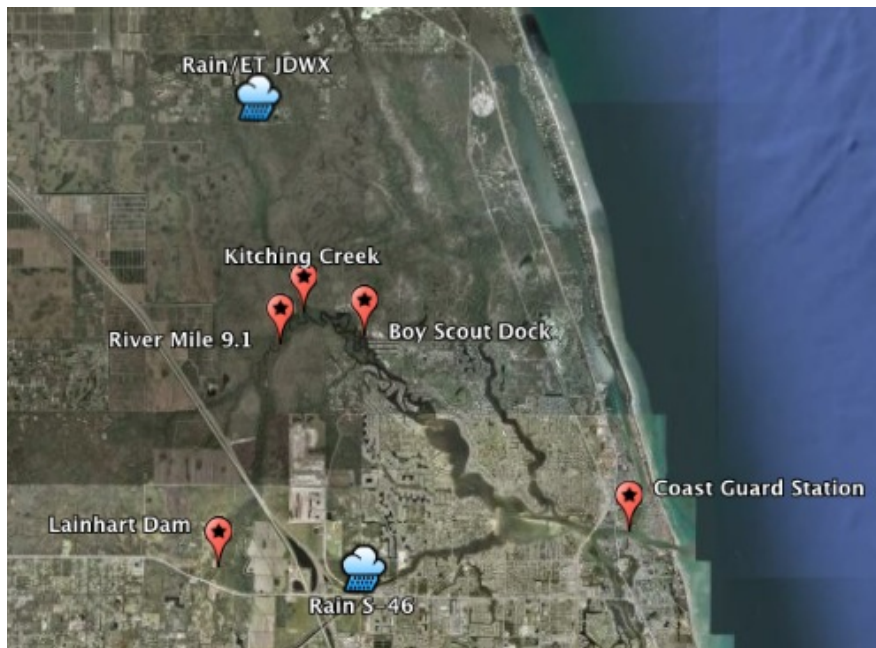


Figure 3. Meteorological and surface water (stage/EC) monitoring locations.

Compiled Time Series and Summary Statistics

After all data processing, calculation, conversion, and correction, UF uploaded all Loxahatchee River groundwater data to its hydrological database (HydroBase). HydroBase is a web-based information system for hydrological data storage, maintenance and mining. Based on industry standard Microsoft SQL server, .NET asp web services, and Java, the application contains powerful on-line web-based graphing, statistical analysis, and reporting capabilities as well as project maintenance and administration. Hydrobase is capable of quick graphical analysis and calculation of daily, weekly, monthly, quarterly, yearly, and entire period statistics including minima, maxima, mean, sum, variance, and standard deviation.

The SOW for the first phase of groundwater data processing and analysis covered the periods from June 2005 through December 2007. The second scope of work included data from December 2007 through the first download of January 2009. Where available and deemed reliable, additional groundwater elevation and EC data from 9/1/04 through 6/8/05 were added to the dataset presented here to get a more complete picture of floodplain hydrology, especially during the extreme, high water events associated with hurricanes Frances and Jeanne. This additional data was mined from the FTP site provided by the SFWMD and checked for continuity with the existing dataset, but was not subjected to the full QA/QC procedure outlined in Task 2.2. The following statistics for ground water elevation and EC data were calculated: mean annual, mean wet season, mean dry season, and average monthly distribution.

Mean annual and mean wet and dry season groundwater statistics for the Loxahatchee River were calculated using Hydrobase. For this report, wet season was defined as June 1st through October 31st and the dry season was defined as November 1st through May 31st (SFWMD, 2006). Water table depths and elevations are available in NGVD29 and NAVD88 in both feet and meters in the electronic and online data reports. Data reported in this section of the report are listed in ft NAVD88 as requested in the project scope of work.

Dynamic Factor Analysis

DFA is based on the structural time series models (Harvey, 1989), and provides for the description of a time series with N response variables using a Dynamic Factor Model (DFM) consisting of a combination of M common trends, K explanatory variables, a level or intercept parameter, and noise (Lütkepohl, 1991; Zuur et al., 2003b):

$$\begin{aligned} N \text{ time series} &= \text{linear combination of } M \text{ common patterns} + \text{level parameter} \\ &+ K \text{ explanatory variables} + \text{noise} \end{aligned} \quad [1]$$

In contrast to physically-based or mechanistic models, DFA modeling is not built upon the underlying mechanisms of a given system, but upon the common patterns among and interactions between response variables and explanatory factors. Thus, it requires no detailed information about the physical, chemical, or biological interactions that are actually occurring between input and explanatory time series (Ritter et al., 2009). In the case presented here, this means that a complete understanding of how surface water, groundwater, and other hydrological variables interact in the floodplain is not necessary.

The goal of DFA is to minimize the number of common patterns (keep M as small as possible) while still achieving a good DFM fit. The use of explanatory variables in DFA helps improve the model fit and identify what environmental factors most affect the response variables. Equation 1 may be written in mathematical form as follows:

$$s_n(t) = \sum_{m=1}^M \gamma_{m,n} \alpha_m(t) + \mu_n + \sum_{k=1}^K \beta_{k,n} v_k(t) + \varepsilon_n(t) \quad [2]$$

$$\alpha_m(t) = \alpha_m(t-1) + \eta_m(t) \quad [3]$$

where $s_n(t)$ is the size N ($1 \leq n \leq N$) vector containing the values of the response variables at time t . In this study, N represents the twelve groundwater elevation and EC time series. The $\alpha_m(t)$ is a length M ($1 \leq m \leq M$) vector containing the common unknown patterns at time t ; $\gamma_{m,n}$ are the factor loadings or weighting coefficients for each $\alpha_m(t)$ patterns; the constant level parameter μ_n shifts up or down each linear combination of common patterns; $\beta_{k,n}$ represents the fitted regression parameter for the k -th (for $1 \leq k \leq K$) explanatory variable $v_k(t)$. K corresponds here to the number of explanatory variables considered in the DFA.

The $\varepsilon_n(t)$ and $\eta_m(t)$ are (independent) Gaussian distributed noise with zero mean and unknown diagonal covariance matrix. Parameters $\gamma_{m,n}$, μ_n , in Eq. [2] are calculated using the Expectation Maximization algorithm (Dempster et al., 1977; Shumway and Stoffer, 1982; Wu et al., 1996). The $\alpha_m(t)$ patterns are modeled as a random walk (Harvey, 1989) and are estimated using the Kalman filter/smoothing algorithm and the Expectation Maximization method, while the regression parameters associated with the explanatory variables ($\beta_{k,n}$) are modeled as in linear regression (Zuur and Pierce, 2004). The error component in Eq. (2) is determined by the covariance matrix \mathbf{H} , whose elements represent information that cannot be explained by the common trends or the explanatory variables. Using a symmetric, non-diagonal \mathbf{H} can result in a smaller number of common trends required for an adequate model fit (Zuur et al., 2003a). Since it contains off-diagonal elements, a non-diagonal matrix can account for joint information between two response variables that is not otherwise explained by the other terms in the DFM. The use of the non-diagonal matrix causes the number of parameters to increase considerably, however (Highland Statistics Ltd., 2000).

Weighting factors accompanying the common trends and explanatory variables allows for identification of relevant response variable common trends and the most important hydrological components (explanatory variables) for each response variable. In other words the results from the DFA may be interpreted in terms of the canonical correlation coefficients, $\rho_{m,n}$, the regression parameters $\beta_{k,n}$, and the match between modeled and observed $s_n(t)$ values. The goodness-of-fit of the DFM was assessed by visual inspection of the observed versus predicted groundwater elevation and EC and quantified with the Nash Sutcliffe coefficient of efficiency ($-\infty \leq C_{eff} \leq 1$, Nash and Sutcliffe, 1970) and Akaike's information criterion (AIC; Akaike, 1974). For two different DFMs, the DFM with largest C_{eff} and smallest AIC is preferred.

Additionally, cross-correlation between the $s_n(t)$ response variables and the $\alpha_m(t)$ common patterns was quantified by means of the $\rho_{m,n}$ canonical correlation coefficients, such that a $\rho_{m,n}$ close to unity indicates that the corresponding common pattern is highly associated with the response variable at a given location. Finally, the weights of the k -th explanatory variable v_k upon each $s_n(t)$ are given by the regression parameters, $\beta_{k,n}$. The magnitude of the $\beta_{k,n}$ and their associated standard errors were used to assess with a t-test whether response and explanatory variables were significantly related (t-value >2).

DFA deals with missing data in the response series by using a “design matrix” to identify missing observations and modify the factor loading, regression, and error matrices. The Kalman filter and smoother algorithm then skips these missing observations (Zuur et al., 2003).

Analyses for groundwater elevation and groundwater EC were performed individually. The DFA was carried out sequentially, starting by building a DFM with only common trends such that the number of common patterns was varied until a minimum AIC was achieved (Zuur et al., 2003a). Once a minimum M was identified, different combinations of explanatory variables were incorporated in the analysis until a satisfactory combination of common patterns and explanatory variables was identified. This reduces the unexplained variability and improves description of water table elevation and EC in the floodplain. Response variables and candidates for explanatory times series variables used in the analysis are discussed in more detail in the following section.

Note that although time series and summary statistics presented below are reported in ft, NAVD88 as requested in the SOW, that the DFA analysis was performed on time series in SI units and referenced to the NGVD29 datum for ease of comparison with other available data. Since all data is normalized (mean subtracted, divided by standard deviation) before analysis, the relationships developed in the DFA are independent of datum. DFA was implemented using the Brodgar version 2.5.7 statistical package (Highland Statistics Ltd., Newburgh, UK) based on the statistical software language “R”, version 2.6.0 (R Core Development Team, 2007). Further details about DFA may be found in Zuur et al. (2003b, 2007).

Hydrological Time Series and Analysis Procedure

As mentioned above, groundwater elevation and groundwater EC were analyzed independently. A total of 46 daily time series (each with 1589 daily values) were investigated for use in these analyses (Table 3). Note that WTE data are autocorrelated (i.e., WTE at time t is related to WTE at $t-1$), while this is not true for rainfall and ET. To account for the “memory” (Ritter et al., 2009) of the WTE series, we used the difference between cumulative rainfall and cumulative ET to create the two net recharge (NR) time series. Note that rainfall is measured at S46 and JDWX, but ET is only measured at JDWX and cumulative ET from this station was used to calculate both NR series. Not all time series from each category of explanatory variables were used in the final DFMs since multicollinearity often existed between explanatory variables measured at nearby locations. The severity of multicollinearity (and resulting usefulness of a suite of explanatory variables) is determined using the variance inflation factor (VIF) for each set of explanatory variables used (Zuur et al., 2007). VIFs with values greater than five were avoided in these analyses (Ritter et al. 2009).

Table 3. Hydrological time series used in the DFA.

Variable	Series Type	No. of series	Description
WTE	Response	12	Groundwater table elevation (m NGVD29) from wells in the Loxahatchee River floodplain
GWEC	Response	12	Groundwater electrical conductivity (S/m) from wells from the Loxahatchee River floodplain
SWE	Explanatory	6	Surface water elevation (m NGVD29) from monitoring stations (Lainhart Dam, RM 9.1, Kitching Creek up/downstream, Boy Scout Dock, and Coast Guard Station) in the Loxahatchee River
SWEC	Explanatory	8	Surface water electrical conductivity (S/m) from monitoring stations (Indiantown Road, RM 9.1 [top/bottom], Kitching Creek Outlet, Boy Scout Dock [top/bottom], and Coast Guard Station [top/bottom]) in the Loxahatchee River
NR	Explanatory	2	Cumulative net recharge (cumulative rainfall – cumulative ET, mm) from weather stations at the S-46 structure and in Jonathan Dickinson State Park (NR_S46 and NR_JDWX in the Loxahatchee River watershed.
WTE_R	Explanatory	9	Groundwater table elevation (m NGVD29) from wells near the Loxahatchee River including M1001, M1024, M1048, M1234, M1255, M1261, PB565, PB689, and PB1642

Results and Discussion

Experimental Time Series and Summary Statistics

In general, recorded water table elevations, depths, groundwater temperatures, and EC values were highly variable across wells and transects, as well as over seasons and years. For example, water table elevations ranged from a maximum of 12.463 ft (3.80 m) in the upstream well on Transect 1 (T1W1) to a minimum of -2.871 ft in the tidal floodplain of Transect 8 (T8W1). EC values ranged from near zero in many upland wells to a maximum of 3.733 S/m in well T9W1 during the dry season of 2007. Some major trends are apparent, however. This section quickly summarizes the experimental data and apparent trends for the entire dataset, including preliminary correlations with other environmental data (surface water, regional groundwater), followed by a more in-depth analysis using dynamic factor analysis (DFA) to develop a dynamic factor model (DFM) of groundwater elevation and EC in the Loxahatchee River floodplain.

Timelines of average daily water table elevation, temperature, and EC are given in Appendix I. Within Appendix I, figures 1 – 12 show average daily water table elevation (ft, NAVD88); figures 13 – 24 show average daily groundwater temperature (°C); and figures 25 – 36 show average daily EC (S/m). Summary statistics, including global and wet/dry season means, minima, maxima, variances, and standard deviations of groundwater elevation and EC are given in tables 1 through 3 of Appendix II. Seasonal statistics were calculated for full or partial wet and dry seasons of 2004 through 2008 using monthly averages. Overall wet/dry season statistics were calculated using all wet/dry month averages in the period of record. Since yearly and monthly statistics for groundwater elevation, depth to water table, groundwater temperature, and groundwater EC were calculated for data from 6/8/05 through 1/5/09 in Task 2.2 of this SOW and the previous SOW, they are not re-calculated in the appendices. As mentioned above, experimental time series were extended back to 9/1/04 where available and deemed reliable, but these data are not available for all wells, so time series may have different start dates.

Correlation with Surface Water Measurements

River stages in the Northwest Fork of the Loxahatchee River (where available) correlate well with groundwater elevations recorded there, both in upriver and tidal locations, further confirming the reliability of the final groundwater datasets. For example, river stage measured at Lainhart Dam (close to Transect 1) corresponds well with groundwater elevation at T1W1 (Fig. 4) and river stage measured at RM 9.1 (close to transect 7) corresponds with the tidal wells T7W1, T7W2, and T7W3 (Fig. 5).

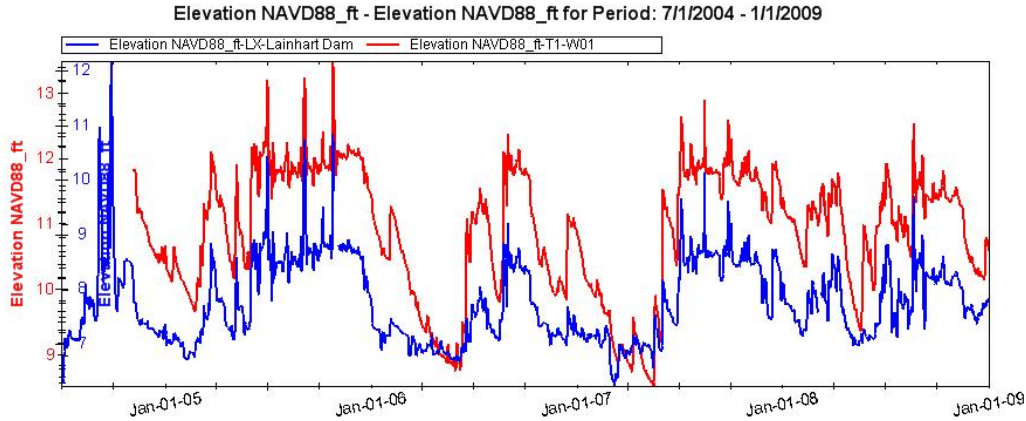


Figure 4. Average daily river stage at Lainhart Dam (blue) and average daily groundwater elevation at well T1W1 (red). Note: different y-axis scales.

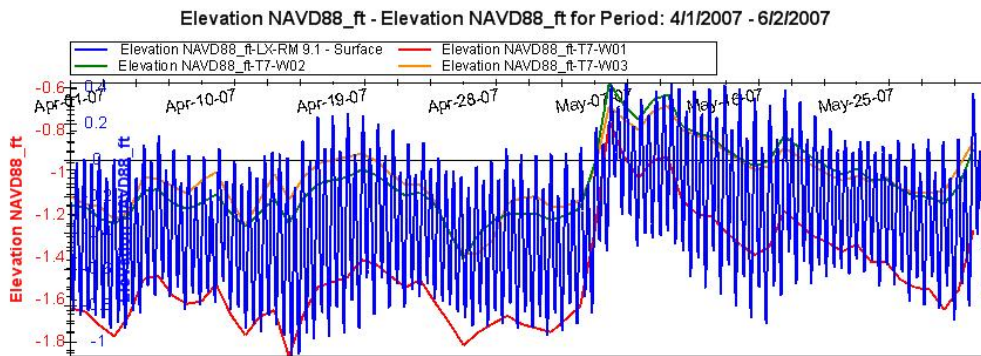


Figure 5. 15-minute river stage at RM 9.1 (blue) and average daily groundwater elevation at wells in the floodplain of Transect 7 (red, green, yellow) for a 2-month period in 2007. Note: different y-axis scales.

Additional correlation analysis (Table 4) shows a varying degree of correlation between groundwater wells and nearby surface water measurement locations, including Lainhart Dam, River Mile 9.1, Kitching Creek, Boy Scout Dock, and Coast Guard Station. These results were used to identify likely explanatory variables in the subsequent dynamic factor model (DFM). Correlation coefficients greater than 0.8 are highlighted in **bold**. Note that “correlation” refers to the Pearson product-moment correlation coefficient (r), not the coefficient of determination (r^2). Upstream transects 1 and 3 show highest correlation with surface water at Lainhart Dam, as do the upland wells on transects 7, 8, and 9. In the floodplain, wells are nearly equally well correlated with any of the surface water measurements in the tidal area of the Northwest Fork (i.e., all locations except for Lainhart). Further investigation highlights strong correlation among these surface water series, with all tidal surface water time series correlations greater than 0.94 (Table 5).

Table 4. Correlation coefficients (r) between groundwater wells and surface water measured in the Northwest Fork of the Loxahatchee River.

Well	Lainhart	RM 9.1	Kitching	Boy Scout	Coast Guard
T1W1	0.919	0.353	0.361	0.252	0.278
T3W1	0.946	0.4	0.409	0.29	0.322
T7W1	0.438	0.964	0.951	0.915	0.929
T7W2	0.405	0.877	0.88	0.833	0.843
T7W3	0.213	0.692	0.687	0.65	0.671
T7W4	0.798	0.428	0.464	0.342	0.359
T8W1	0.537	0.943	0.949	0.878	0.898
T8W2	0.584	0.723	0.747	0.675	0.685
T8W3	0.817	0.392	0.421	0.305	0.316
T9W1	0.351	0.839	0.844	0.801	0.814
T9W2	0.504	0.916	0.927	0.861	0.884
T9W3	0.688	0.641	0.668	0.541	0.563

Table 5. Correlation coefficients (r) between surface water measured in the Northwest Fork of the Loxahatchee River.

	Lainhart	RM 9.1	Kitching Creek	Boy Scout Dock	Coast Guard
Lainhart	1	0.452	0.457	0.326	0.37
RM 9.1		1	0.985	0.944	0.96
Kitching Creek			1	0.956	0.97
Boy Scout Dock				1	0.966
Coast Guard					1

Water Table Elevation

Water table elevations were highest in upriver wells (T1W1; T3W1) and downriver upland wells (T7W4; T8W3) (Fig. 6). Data from 2009 are not included in this figure (only 5 days of data), and presence of data from 2004 depends on availability and reliability as described above. In general, lowest groundwater elevation levels were seen in 2006 (highest groundwater EC values were seen in 2007, however—see below). In the tidal floodplain, average annual water table elevation was below mean sea level (referenced to NAVD88) for many wells.

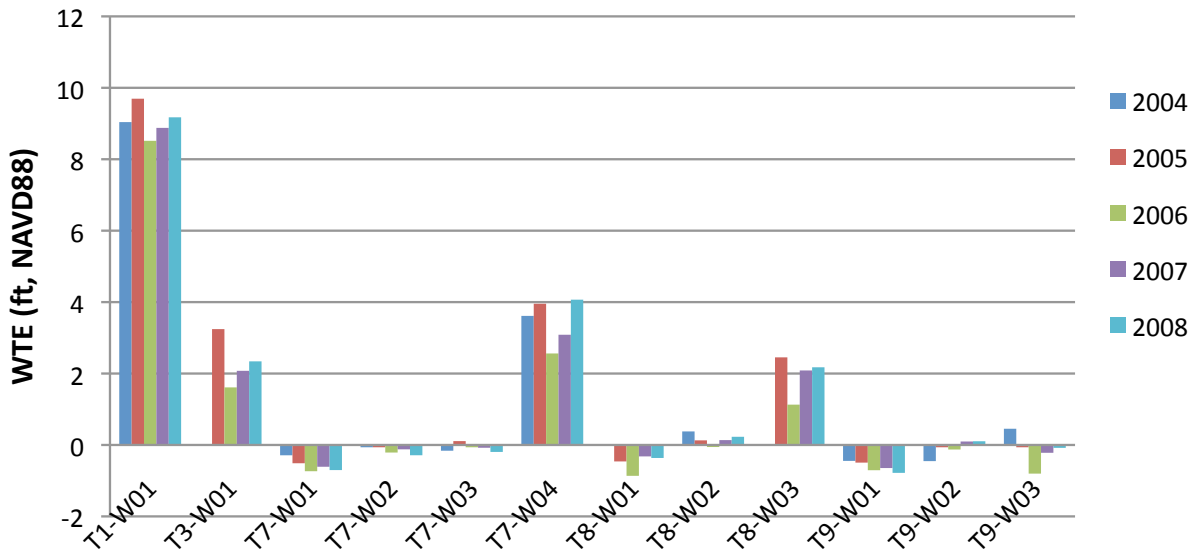


Figure 6. Annual average water table elevation (ft, NAVD88) for all 12 wells in the project.

Water table elevations in higher elevation wells, i.e. outside from the floodplain and further from the river (T1W1, T3W1, T7W4, T8W3, and T9W3) correlate well and show similar responses to the wet and dry season rainfall patterns (Fig. 7). For example, the impacts of late season rains in 2005 and dry summer in 2006 and 2007 on the water table elevations are apparent across all these wells. Groundwater elevations generally decrease from upstream (T1) to downstream (T9). One exception to this is the upland well T7W4, which maintains greater groundwater elevations than upstream well T3W1 throughout most of the period of record.

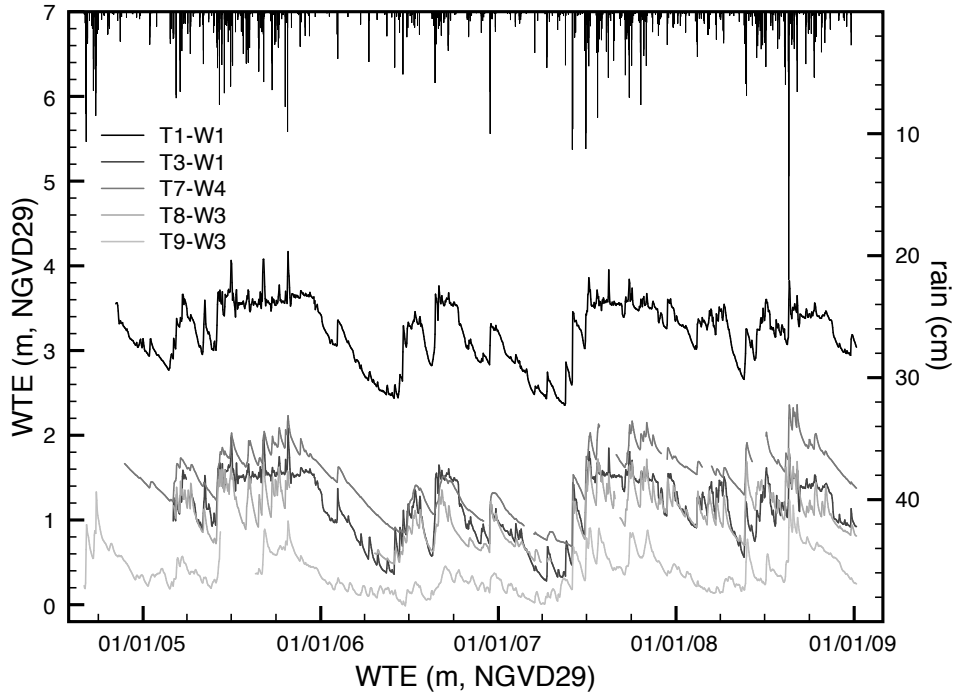


Figure 7. Average daily water table elevation (ft, NAVD88) in higher elevation wells over the period of record.

Water table elevations in lower elevation wells closer to the river are more influenced by daily tidal flooding, with elevations often below mean sea level (Fig. 8). Some seasonal wet/dry patterns are still apparent, but much less so, as their signal is damped by daily and monthly tidal fluctuations. Note high water events from September 2004 during hurricanes Frances and Jeanne. Low groundwater elevation recorded in well T8W1 (yellow line) was investigated for measurement errors, but appears to be valid.

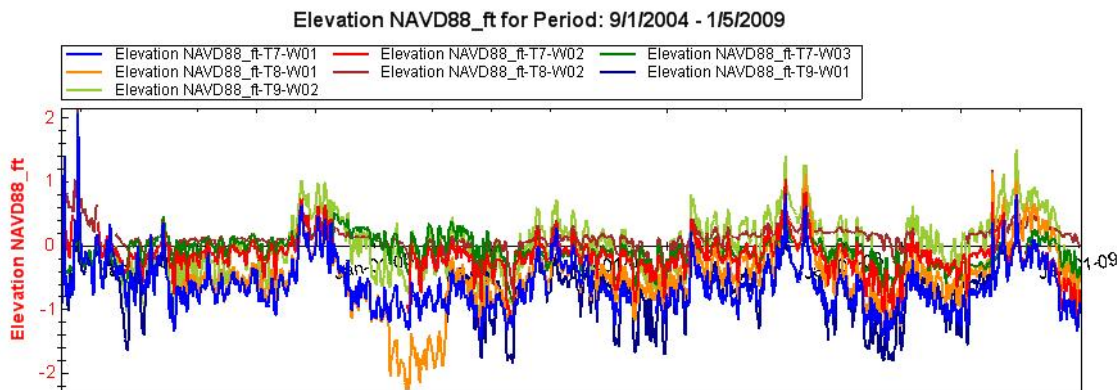


Figure 8. Average daily water table elevation (ft, NAVD88) in lower elevation wells over the period of record.

Other trends become apparent when looking across specific transects. For example, Figs. 9 and 10 show water table elevations from wells on Transects 7 and 8. On Transect 7, the general progression of increasing water table elevation with distance from the river is apparent,

with the upland well (T7W4) showing the maintenance of a high water table head (of freshwater, as discussed below) in the upland. During the dry seasons of 2006 to 2007, this freshwater head falls, nearly equalizing with the water table elevations in the floodplain, but always remaining higher. This indicates a variable flow of freshwater from the uplands towards the river, even in extremely dry seasons. The dry season of 2008 shows considerably less drawdown in this upland well. Unfortunately, data back to September 2004 were not available for well T7W4.

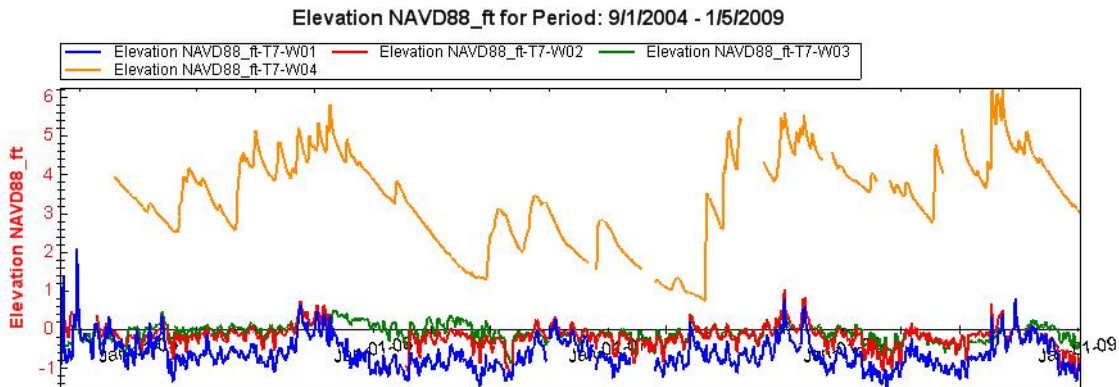


Figure 9. Average daily water table elevation (ft, NAVD88) of wells on Transect 7. Note maintenance of large freshwater head in upland well (T7W4).

The same pattern is apparent on Transect 8, with higher water table elevations maintained in well T8W3, except for the dry seasons of 2006 and 2007, when the groundwater levels in T8W2 and T8W3 meet during an extreme water table drawdown. Water table elevation in well T8W3 may fall below that of floodplain wells T8W1 and T8W2 during this time, as probe readings from this period were negative, indicating water table fell below the probe in this well (and were not useable). At Transect 9, which has the river on two sides, these patterns are not as apparent, with upland and floodplain wells sharing similar groundwater elevations (Fig. 11).

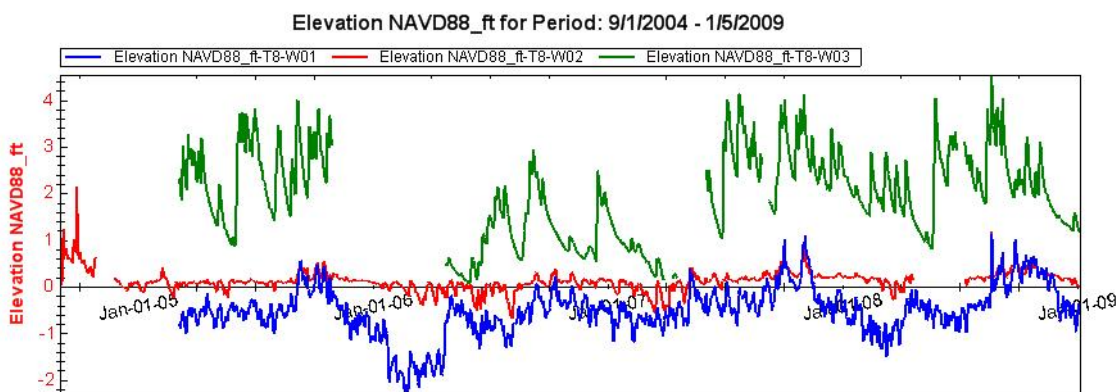


Figure 10. Average daily water table elevation (ft, NAVD88) of wells on Transect 8. Note maintenance of higher head in upland well (T8W3). Data gap in 2007 is due to water table falling below probe level.

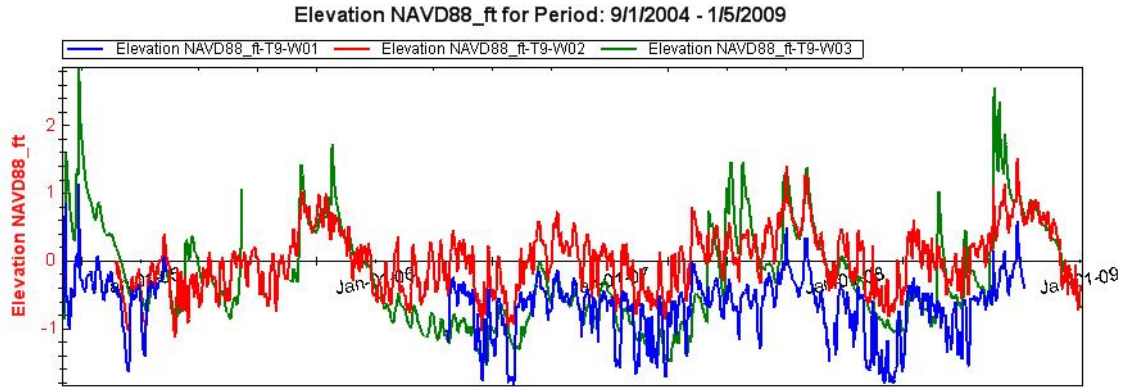


Figure 11. Average daily water table elevation (ft, NAVD88) of wells on Transect 9.

Electrical Conductivity

Trends in EC can be observed over individual tidal cycles as well as over longer seasonal and yearly time periods. In general, the EC values recorded were low upstream and increased with proximity to Jupiter Inlet and the Atlantic Ocean (Fig. 12). The global average EC at upstream well T1W1 was 0.068 S/m, with very little variation in this value between wet and dry seasons. On the other hand, the average groundwater EC at downstream well T9W2 was 2.066 S/m (over 30 times greater than that at T1W1) and varied significantly between wet and dry seasons. For comparison, the threshold identified for maintenance of bald cypress health is 2 parts per thousand (ppt) or 0.3125 S/m. The lowest average groundwater EC was observed in upland well T7W4. The extremely fresh nature of this water, combined with the maintenance of a high water table elevation in this location likely play a large role in maintaining the floodplain salinity on Transect 7 below critical threshold for bald cypress health (0.3125 S/m). This combination of fresh water and high upland WTE likely plays a role in mitigating the severity of saltwater intrusion into the floodplain throughout the watershed.

The highest annual average EC values were observed in wells T9W1 and T9W2 (by one to two orders of magnitude). Highest annual average EC values were generally observed in 2007 for all wells, even though lowest groundwater levels were seen in 2006 (see above). The notable exception to this is for wells with data available during the hurricanes of 2004. For example, average annual EC is highest for downriver floodplain well T9W1 in 2004, when high river stages associated with hurricanes likely pushed high salinity surface water into the transect. Data is not available for T9W2 during this period, but would likely show the same effect. Annual average river EC is similar to the groundwater EC measured in nearby transects. For example, Transects 1 and 7 are similar to annual average groundwater EC measured in wells at these transects (Fig. 12). However, daily average river EC far exceeds that seen in the groundwater at all wells in downriver transects (again using T7 as an example; Fig. 13).

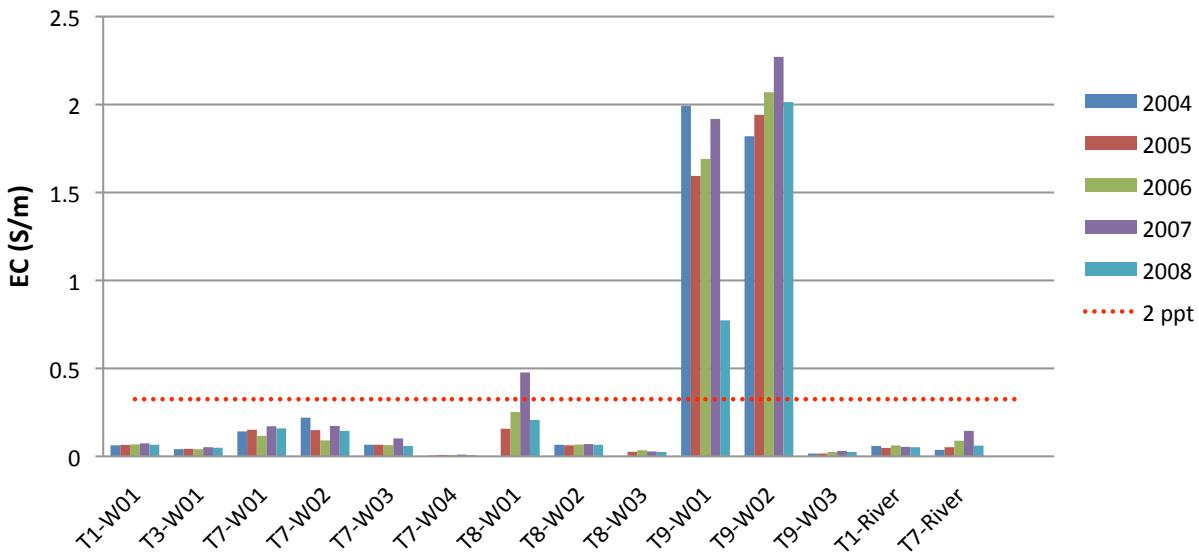


Figure 12. Annual average EC (S/m) for 12 wells in the project and river EC near Transects 1 and 7. The dotted red line indicates the 2 ppt (0.3125 S/m) salinity threshold identified for the protection of bald cypress health.

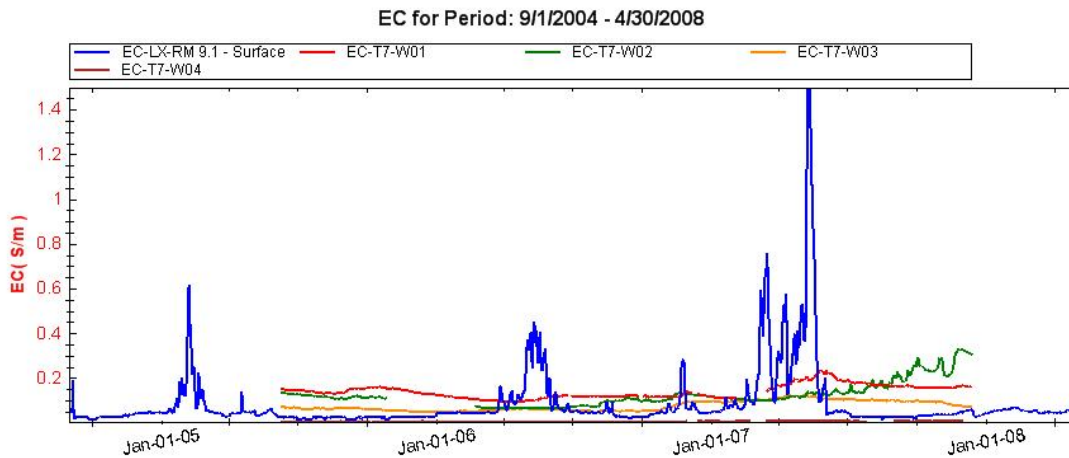


Figure 13. Daily average EC (S/m) in the river at RM 9.1 (near Transect 7) and in the 4 wells on that Transect. Note river salinity far exceeds groundwater salinity in dry seasons.

On Transects with multiple wells, observed EC was generally greatest closest to the river and decreased with distance towards the upland. On Transect 7, this trend reversed in 2007, when the EC in well T7W2 surpassed that of well T7W1 and remained significantly higher for the duration of the year before falling in 2008 (Fig. 14). On Transect 8, the well closest to the river (T8W1) experiences EC values several orders of magnitude above the wells further from the river (Fig. 15). This pattern is again complicated on Transect 9, which has the river on both sides of the Transect. Here, wells T9W1 and T9W2 have the highest EC of any wells in the project, while EC in well T9W3 is two orders of magnitude lower (Fig. 16). Though aligned in a transect, three wells on T9 are located on a small peninsula into the river and thus have a

minimum distance to the river of 70, 50, and 30 m for wells T9W1, T9W2, and T9W3, respectively. Average annual EC is usually higher in well T9W2 (Fig. 12), although the highest EC readings were observed in well T9W1. The maintenance of relatively high groundwater EC in well T9W2 may be due to prolonged ponding of saline surface water behind the small berm trails on the peninsula. The upland location of well T9W3 likely explains the maintenance of fresh groundwater in this well.

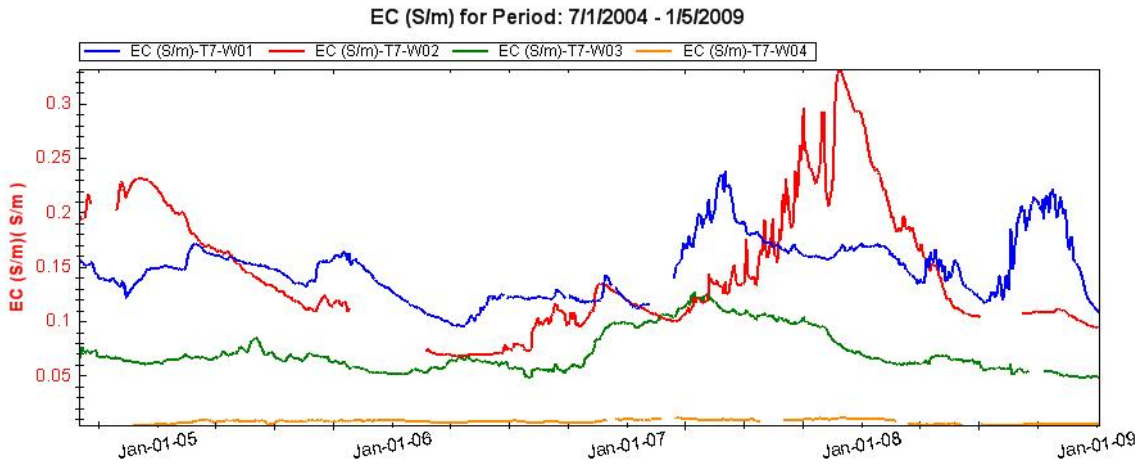


Figure 14. Average daily EC (S/m) for 4 wells on Transect 7.

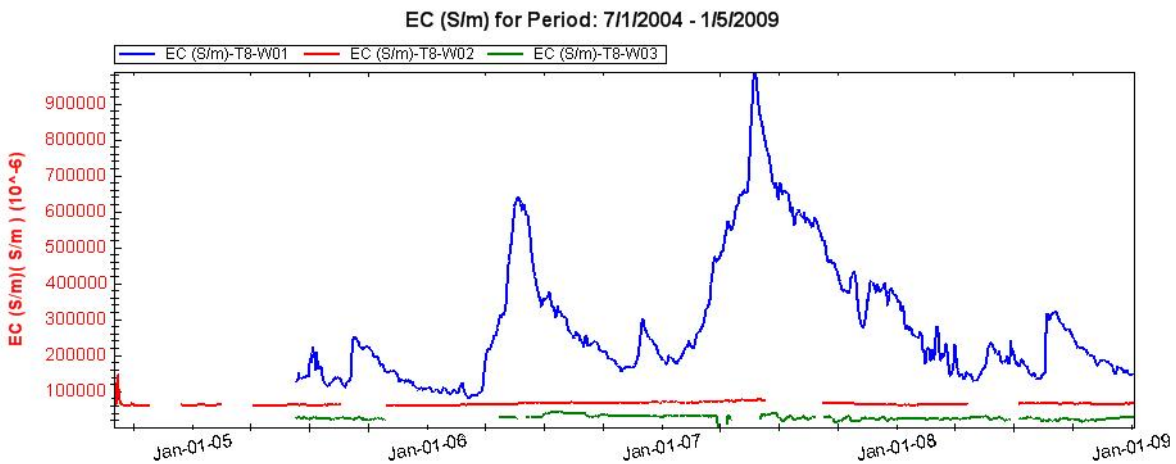


Figure 15. Average daily EC (S/m) for 3 wells on Transect 8.

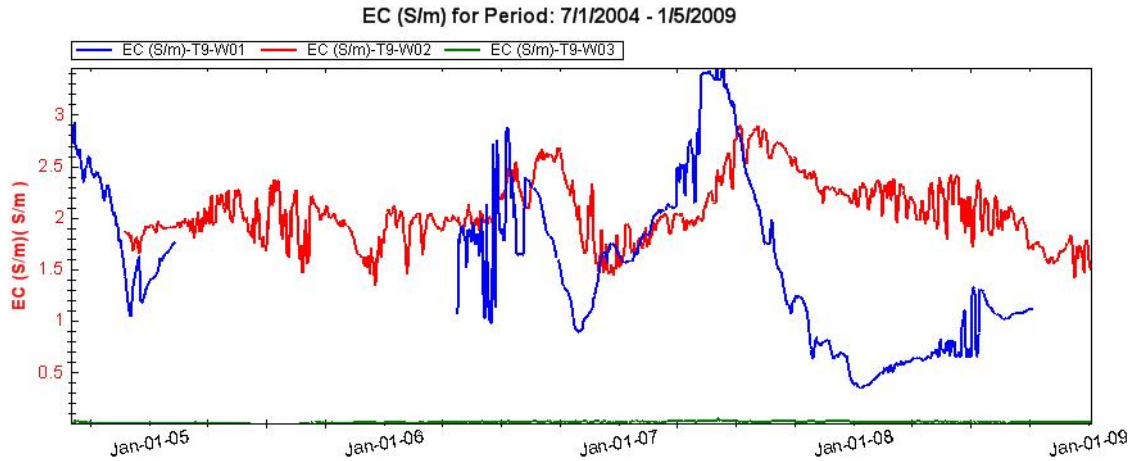


Figure 16. Average daily EC (S/m) for 3 wells on Transect 9.

Temperature

Seasonal variation in groundwater temperature was observed in all twelve groundwater wells as discussed in Task 2.2 and the previous SOW. Though important for accurate calculation of specific conductivity, groundwater temperature has not been identified as a variable of concern for the restoration of the Northwest Fork, and is not discussed here.

Wet/Dry Seasonality

Figure 17 shows the sum of rainfall recorded at the S-46 gauging station during the wet and dry seasons of 2004 – 2008 (only complete seasons were considered for sums). Wet season rainfall was higher than dry season rainfall for all years. This is in agreement with previous seasonal rainfall observations in the Loxahatchee River Basin, which have shown that two-thirds of yearly rain falls during the wet season (Dent, 1997). Significant spatial variation between rain data collected at the S-46 and JDWX stations was also found (Fig. 18), and is discussed in more detail in the following section.

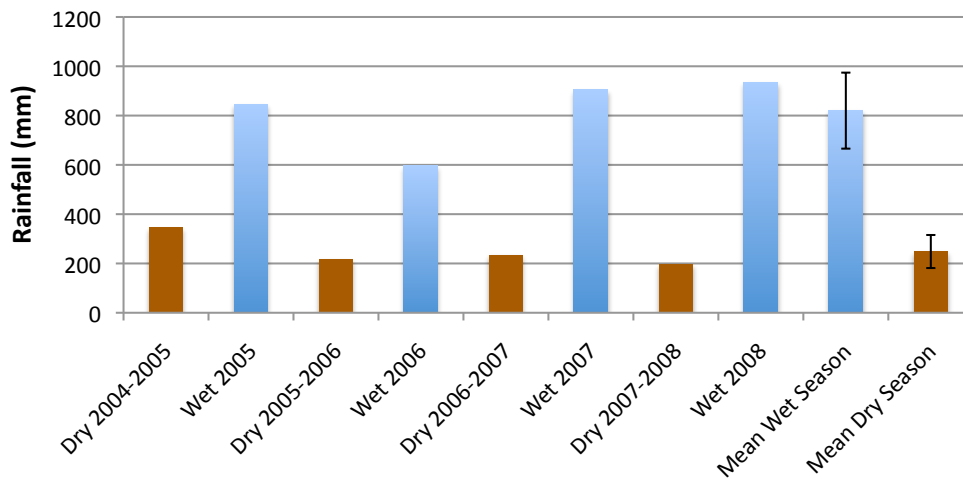


Figure 17. Seasonal rainfall totals recorded at the S-46 gauging station on the Southwest Fork of the Loxahatchee River. Error bars indicate plus/minus one standard deviation.

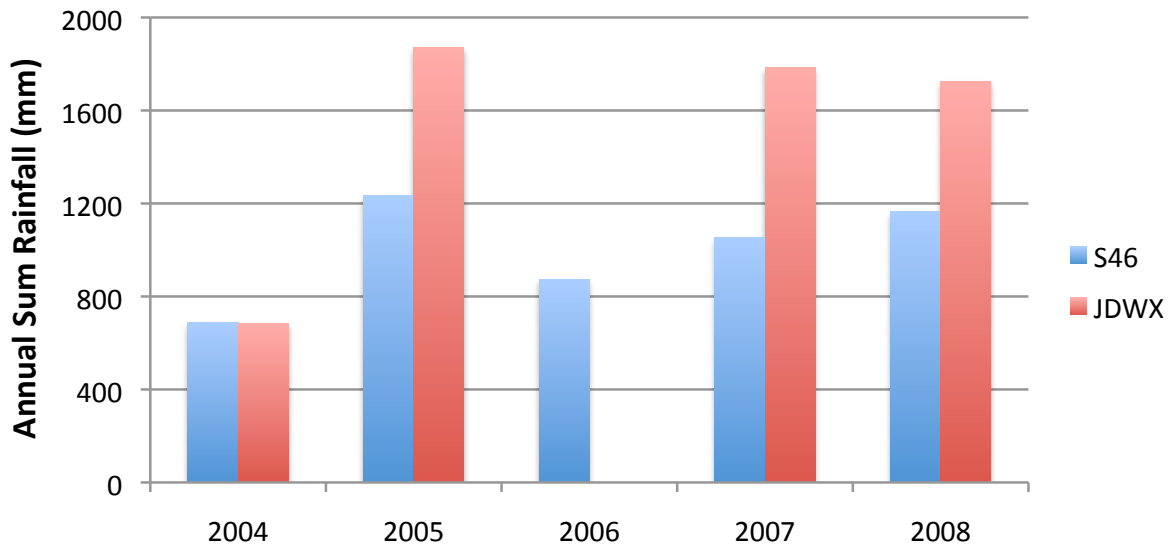


Figure 18. Annual rainfall sums for rain gauges at S-46 structure and weather station JDWX. 2006 is not shown for JDWX because of incomplete records at this station during this year.

Wet/dry season differences in average water table elevation and groundwater EC were also observed in all wells, though the magnitude of this difference was variable across the twelve wells and was small. Average wet season water table elevations were higher than dry season elevations by an average of 0.37 ft, with a range of 0.04 to 0.68 ft. The greatest seasonal differences in water table elevation were seen in wells T1W1, T3W1, and T8W3 (Fig. 19). Seasonal changes in groundwater depth impact soil moisture profiles and water availability, and can have an impact on the type of vegetation seen in the area of each well. Wet season groundwater EC was *higher* than dry season EC by an average of 0.069 S/m (range of 0.02 S/m lower to 0.44 S/m higher). The greatest seasonal differences in EC were seen in T9W1 and T9W2 (Fig. 20). A slightly *higher* dry season EC was seen in T3W1, T7W2, and T7W4, but none of these differences was significant.

Although dividing the year into wet (May – October) and dry (November – April) seasons is useful for describing the general pattern of rainfall in the Loxahatchee River Basin, it does not work well for identifying seasonal patterns in groundwater elevations or electrical conductivity. This is likely because some of the driest periods of the year are often experienced during the beginning of the “wet” season. Only after the onset of large and regular summer rains does the “wet” season really begin, and this is often delayed until July or later. Thus, after a long dry season, water table elevations may continue to drop and groundwater EC continue to rise for several months into the wet season. While summing rainfall over the wet and dry months negates this effect and provides a clear division of seasons, averaging other variables over the same time periods masks these seasonal differences. This is likely also the case for surface water, where lowest levels and highest EC values are often seen in the early months of the “wet” season.

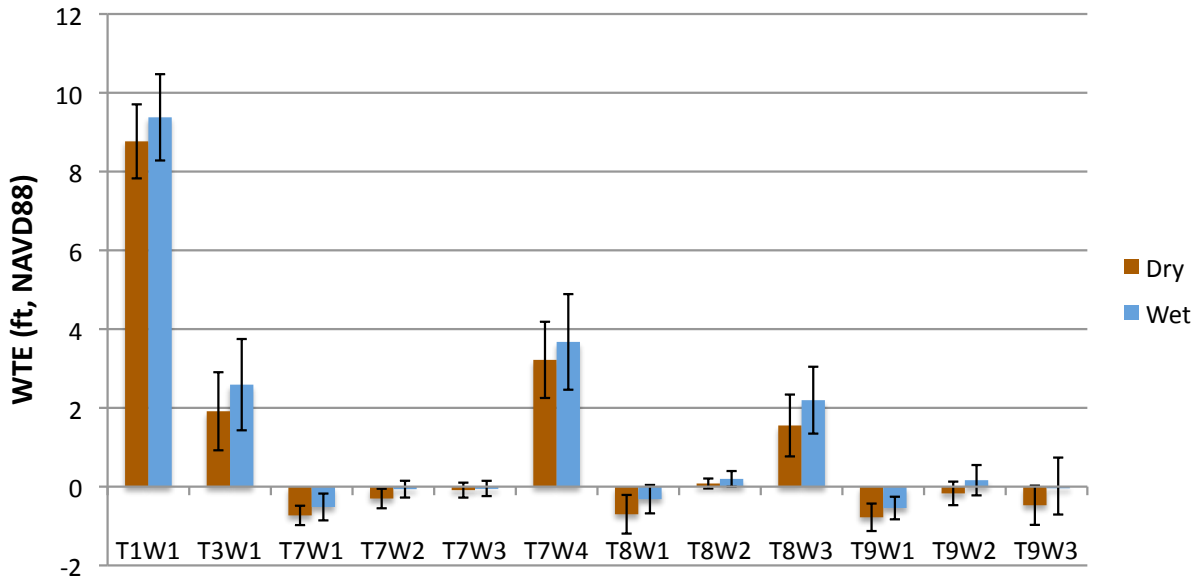


Figure 19. Average wet/dry season water table elevation (ft, NAVD88). Error bars indicate plus/minus one standard deviation.

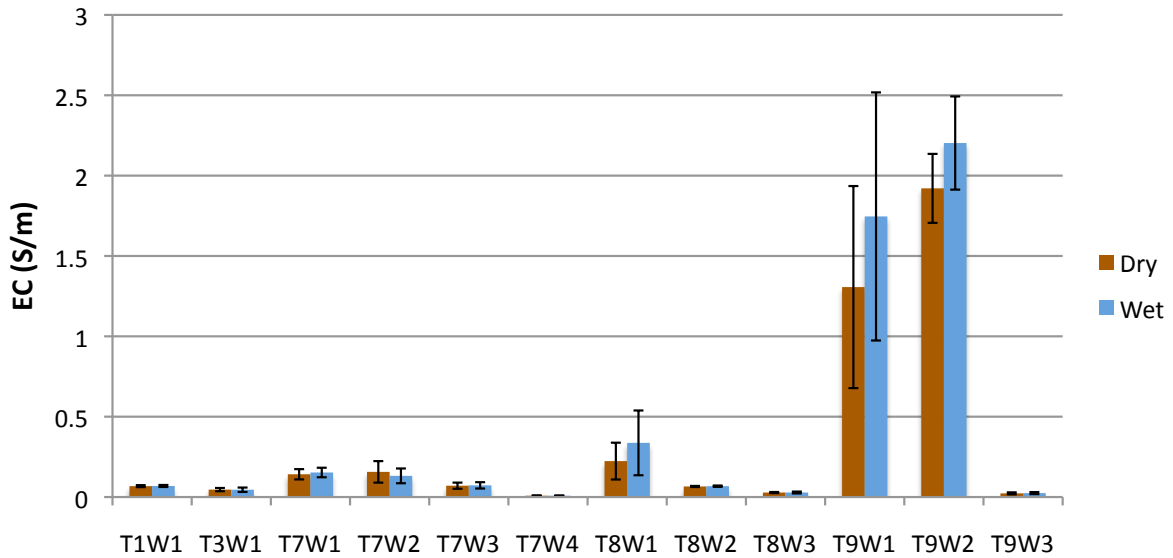


Figure 20. Average wet/dry season groundwater EC (S/m). Error bars indicate plus/minus one standard deviation.

Dynamic Factor Analysis of Water Table Elevation

Baseline DFA (no explanatory variables)

As mentioned above, DFA was performed separately for WTE and GWEC. Additionally, the analysis was advanced in two discrete steps. First, an increasing number of common trends were fit to the twelve response variables until a minimum AIC and maximum $ceff$ were achieved. Both diagonal and non-diagonal error covariance matrices were explored. With a diagonal matrix, AIC is minimized and $ceff$ maximized with six trends ($M=6$; Fig. 21a). Using a symmetric, non-diagonal matrix, AIC continues to decrease with increasing number of trends, becoming increasingly negative (Fig. 21b). This is due to the calculation of AIC which includes a term for the natural log (\ln) of the residual sum of squares (RSS). Thus, there is no inflection point in AIC using the non-diagonal matrix as the RSS term decreases below unity. Additionally, although the AIC for the non-diagonal matrix continues to decrease with added trends (Table 6), $ceff$ is worse than for the corresponding number of trends using a diagonal matrix. For these reasons a diagonal error covariance matrix was selected for all subsequent analyses.

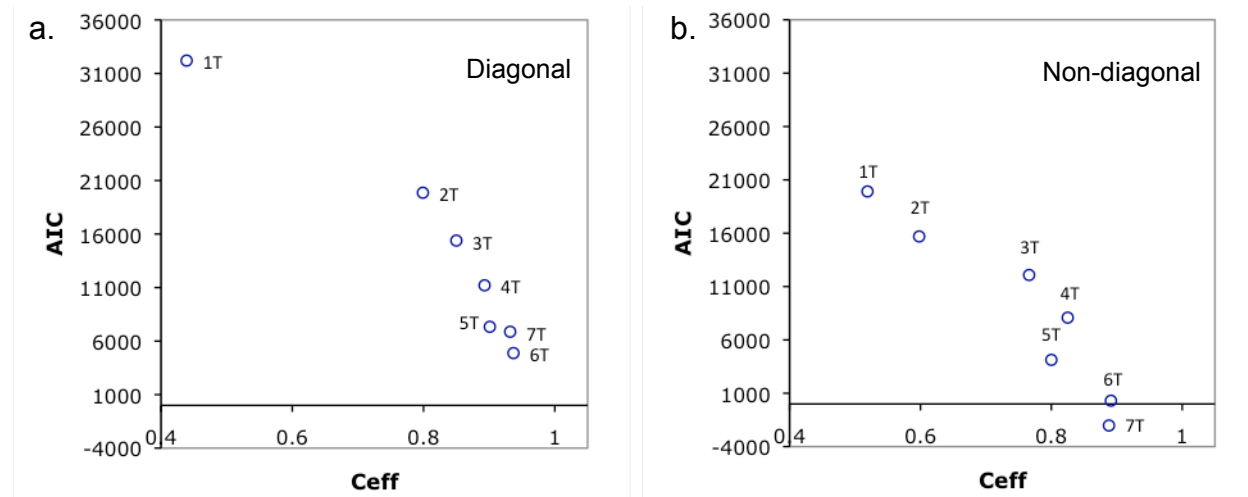


Figure 21. Akaike Information Criteria (AIC) versus Nash-Sutcliffe coefficient of efficiency ($ceff$) with increasing number of common trends ($M = 1-7$) using (a) a diagonal error covariance matrix and (b) a symmetric, non-diagonal error covariance matrix

Table 6. AIC and $ceff$ values for the DFMs with no explanatory variables and 1 – 7 common trends. Best model is represented in bold numbers.

M	Diagonal Matrix		Non-Diagonal Matrix	
	$ceff$	AIC	$ceff$	AIC
1	0.439	32,204	0.519	19,914
2	0.799	19,860	0.598	15,697
3	0.85	15,390	0.766	12,085
4	0.893	11,211	0.825	8,088
5	0.901	7,337	0.8	4,130
6	0.937	4,880	0.891	302
7	0.932	6,875	0.888	-2,021

The minimized AIC of 4,880 and maximized *ceff* of 0.937 using six common trends (Model I) were then used as targets for subsequent DFMs. That six common trends were necessary to achieve the best DFM with no explanatory variables reflects the variability of the response variables (WTE) and suggests that several latent effects influence WTE in varying ways across the watershed. It is instructive to examine these common trends and their associated factor loadings ($\gamma_{m,n}$) and canonical correlation coefficients ($\rho_{m,n}$) to explore possible explanatory variables to improve the DFM. The $\gamma_{m,n}$ for each of the six trends indicate their relative importance to each response variable in the model while high $\rho_{m,n}$ values indicate high correlation between two latent variables. Figure 22 shows $\gamma_{m,n}$ for each of the six trends, indicates which wells are most affected by each of the trends, and suggests that 1st, 3rd, and 4th trends are likely most important to the overall model.

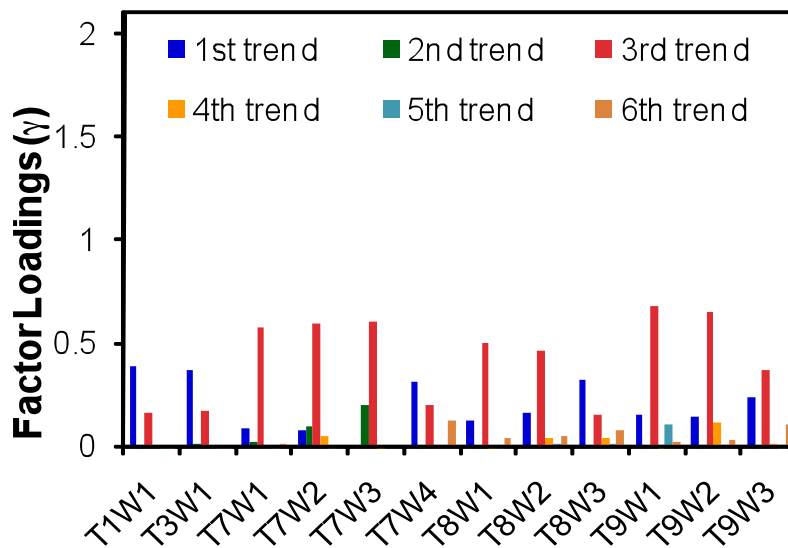


Figure 22. Factor loadings for the model with six trends and no explanatory variables. The importance of each trend to the model can be seen individually for each input time series (in this case, WTE).

The three trends with the highest $\gamma_{m,n}$ values and their associated $\rho_{m,n}$ values are shown in Figure 23a-c. Though only describing latent (unknown) variability at this point, these trends are useful for developing ideas about how WTE elevation varies in the Loxahatchee River floodplain and where to look for the most useful explanatory variables. For example, the trend in Figure 23a is very highly correlated with all five upriver and downriver upland wells (T1W1, T3W1, T7W4, T8W3, and T9W3), but relatively unimportant to the seven floodplain wells (T7W1, T7W2, T7W3, T8W1, T8W2, T9W1, and T9W2). The opposite is true for the trend in Figure 23b, which is most highly correlated with floodplain wells. The trend in Figure 23c is only highly correlated with two of the twelve wells, both on T8, and the correlations are in opposite directions. This indicates a latent trend specific to these wells and could be an indicator of anomalous data or some other environmental factor that only affects these wells. In this case, the sharp drop in 2006 seen in this common trend is coincident in time with the drop in WTE observed in well T8W1, which was investigated for measurement errors, as mentioned above, but found to be valid. As evidenced by $\gamma_{m,n}$ and $\rho_{m,n}$ values, the model requires this common trend to achieve a good match of this part of the input time series.

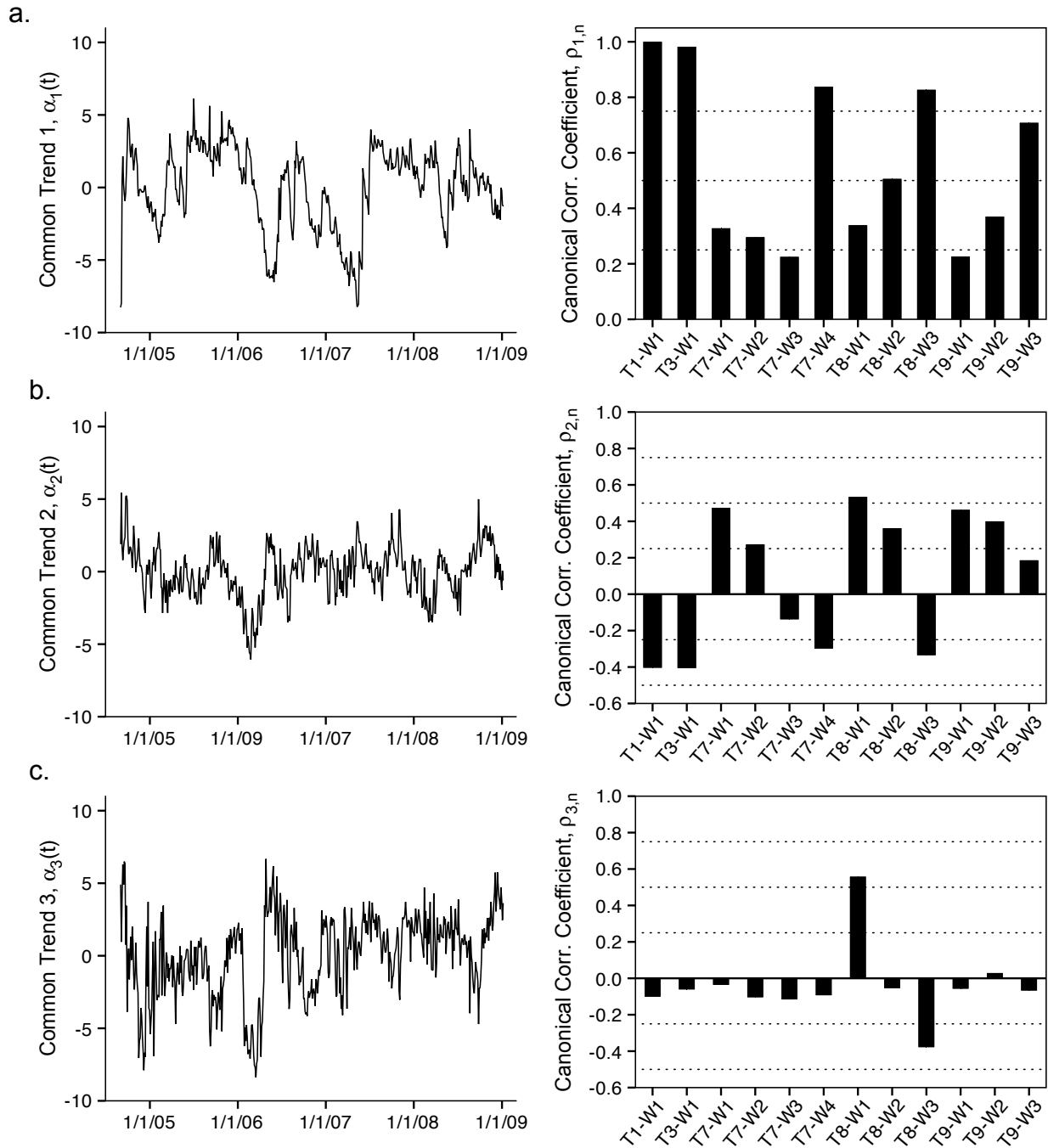


Figure 23. The three most important trends to Model I (left) and their associated canonical correlation coefficients (right). Panel (a) shows high correlation to upland and upstream wells; (b) is most associated with floodplain wells; (c) has low correlations except for wells T8W1 and T8W3.

DFA with explanatory variables

The next step was to reduce the number of common trends required to achieve an adequate fit of WTE (and to minimize the factor loadings of any remaining trends) by adding appropriate explanatory variables. As mentioned above, candidate explanatory variables included surface water elevations (SWE) at five locations in the Northwest Fork, regional groundwater

elevations (WTE_R) in eight regional wells, and net recharge (NR) from two rain gauges and one ET monitoring station in the Loxahatchee River watershed. When two or more candidate explanatory variables were collinear or multi-collinear (resulting in VIFs>5), the explanatory variable resulting in the best overall model fit was selected. For SWE time series, river stage at Lainhart Dam and RM 9.1 provided the best benefit to the model and were not collinear. For WTE_R time series, USGS well M1001 most improved the model.

The model was also improved by using both net recharge series (NR_S46 and NR_JDWX) and did not exceed the VIF threshold. Though these two rain gauges are only seven miles (11.2 km) apart, and roughly equidistant from the shore in flat terrain, their cumulative rainfall totals were different by more than 2,000 mm. Pearson correlation (r) between the rainfall time series was also low ($r = 0.43$). Thus, when the series were used to calculate net recharge (Fig 24), each series had distinct information, and the use of both series improved the model. Since both rainfall series had passed QA/QC procedures from the SFWMD, both were deemed reliable. The use of both series highlighted the effects of the high spatial variability of rainfall in the region. Additionally, the effects of this variable rainfall on model results were explored by developing DFMs using only one of the series and their average and comparing the results to the DFM using both series. While the average NR series comes closer to “closing the loop” hydrologically, it performs poorly in the DFM (see results below).

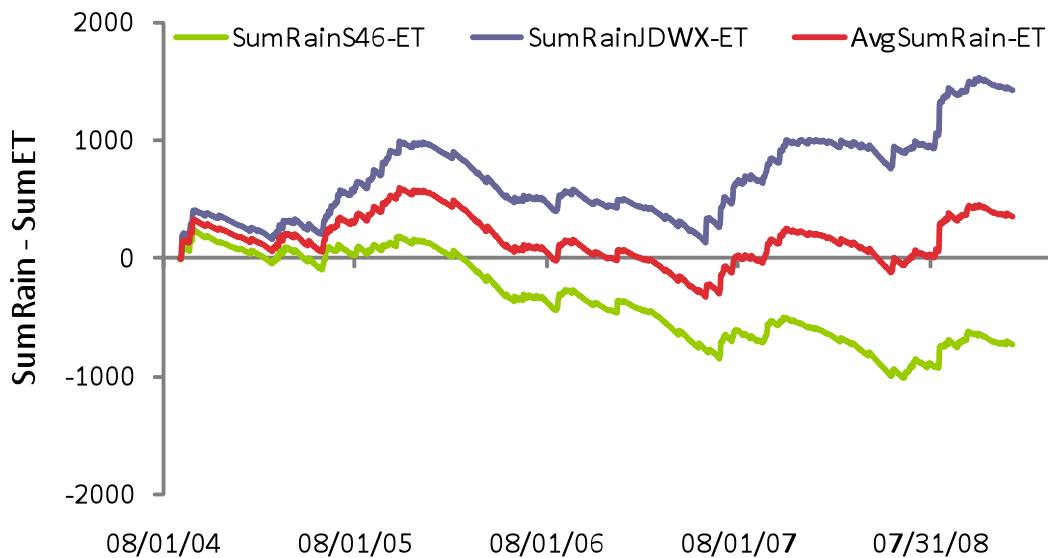


Figure 24. Net Recharge (NR; cumulative rainfall – cumulative ET) for the two rainfall time series used in the DFM. Note that NR_S46 shows a steady drying pattern over the ~4-year period, while NR_JDWX shows a wetting trend.

Finally, the best DFM used five explanatory variables: SWE at Lainhart Dam and RM 9.1; WTE_R at USGS well M1001; and both net recharge series NR_S46 and NR_JDWX. Using these explanatory variables, it was possible to reduce the number of required common trends from six to three ($M=3$), thus reducing the unexplained variability in the model. This model (Model II) yielded an AIC value of 2,998 (lower than the 4,880 target from Model I) and a *ceff*

value of 0.91 across the twelve wells (compared with the target of 0.937). AIC was found to be more sensitive to changes in number of trends and explanatory variables, and thus models that meet the AIC target and had $ceff > 0.9$ were deemed to be adequate. For example, reducing this model to $M=2$ using the same explanatory variables increased AIC to 8,117 (which no longer meets the $M=6$ target), but reduced $ceff$ only slightly to 0.89.

Alternate DFMs were investigated to help illustrate the importance of the explanatory variables (X). Figure 25 shows AIC versus $ceff$ for Model I (0 X), Model II (5X), and other selected DFMs. This figure shows that the best model performance (Model II) is only slightly reduced by removing the regional groundwater well (WTE_R), indicating the relatively low importance of this variable in explaining variability in WTE. Additionally, the target AIC (4,880) can be achieved using one of the net recharge series (NR_S46) or both rains (NR_JDWX and NR_S46), but can *not* be achieved using the other series or the average of the two series (NR_JDWX or Average NR). For comparison, results from a DFM with $M=3$ and just the two NR series (2X) is also shown. This DFM has a much higher AIC, but achieves a similar $ceff$, highlighting the relative insensitivity of this diagnostic.

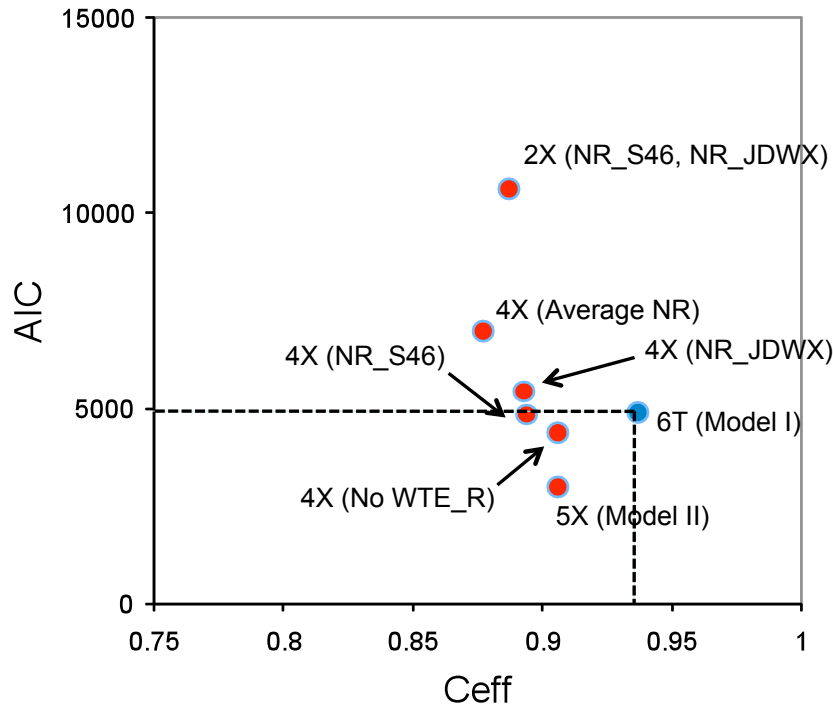


Figure 25. AIC versus $ceff$ for Models I, II, and several alternate DFMs.

Table 7 summarizes the results obtained from Model II ($M=3, K=5$). Significant regression parameters (t -value > 2) are shown in bold. WTE in the 12 wells in the Loxahatchee River had variable relationships to the common trends from Model II, but canonical correlations were reduced from Model I, indicating a reduced dependence of the DFM on these latent series. The trends in Model II had zero “high” and four “moderate” correlations with response variables, compared to four “high” and seven “moderate” correlations in Model I.

Table 7. Constant level parameters (μ_n), canonical correlation coefficients ($\rho_{m,n}$), factor loadings ($\gamma_{m,n}$), regression coefficients ($\beta_{k,n}$), and coefficients of efficiency (C_{eff}) from Model II (3 trends, 5 explanatory variables). Significant regression parameters in bold.

S_n	μ_n	Canonical Correlations			Factor loadings			Regression coefficients ($\beta_{k,n}$)					$C_{eff,n}$	
		$\rho_{1,n}$	$\rho_{2,n}$	$\rho_{3,n}$	$\gamma_{1,n}$	$\gamma_{2,n}$	$\gamma_{3,n}$	$SWE_{RK23.3}$	$SWE_{RK14.6}$	$R_{net,S46}$	$R_{net,JDWX}$	WTE_{RM1001}		
T1-W1	-0.44	0.61	0.10	-0.30	0.08	0.02	0.00	0.53	-0.01	0.73	0.10	0.22	1.00	
T3-W1	-0.26	0.52	0.14	-0.31	0.05	0.02	0.00	0.58	0.01	0.56	0.13	0.19	0.97	
T7-W1	-0.10	0.19	0.23	0.02	0.00	-0.01	0.04	-0.07	0.92	0.23	0.05	0.16	0.94	
T7-W2	0.58	0.16	0.35	0.26	0.00	0.02	0.18	0.02	0.62	0.71	0.74	-0.05	0.90	
T7-W3	0.22	-0.08	0.09	-0.04	-0.01	-0.02	0.20	0.12	0.47	1.05	1.00	-0.12	0.83	
T7-W4	1.20	0.27	0.43	-0.38	0.00	0.10	-0.01	0.10	-0.01	0.09	0.77	0.24	1.00	
T8-W1	-0.14	0.05	0.30	0.27	0.00	-0.01	0.03	0.19	0.74	-0.26	0.00	0.12	0.78	
T8-W2	0.01	0.45	0.36	0.04	0.03	0.01	0.12	-0.08	0.43	0.54	0.72	0.19	0.80	
T8-W3	0.90	0.35	0.55	-0.14	0.02	0.10	0.00	0.21	-0.09	0.3	0.65	0.2	0.88	
T9-W1	0.50	0.16	0.31	0.29	0.00	0.00	0.23	-0.12	0.58	0.92	1.03	0.06	0.97	
T9-W2	0.09	0.02	0.30	0.24	0.01	0.00	0.16	0.06	0.70	0.49	0.84	0.01	0.98	
T9-W3	1.06	0.35	0.54	-0.16	-0.01	0.07	0.03	0.12	0.27	0.03	0.70	0.16	0.86	
													Overall	0.91

The spatially distributed effects of the explanatory variables and common trends on Model II are compared in Fig. 26. Regression parameters ($\beta_{k,n}$; Figs. 26a-e) represent the relative importance of each explanatory variable to each response time series, with black bars indicating significant regression parameters by t-test. In general, inclusion of explanatory variables in Model II reduced factor loadings (Fig. 26f) over those in Model I (overall average $|\gamma_n|$ for the six trends in Model I was 0.13 ± 0.16 compared to 0.05 ± 0.04 in Model II), suggesting that the patterns observed in the Loxahatchee River floodplain wells may be adequately described using only the selected explanatory variables (see following section).

Visualizing the spatial distribution of the importance of each explanatory variable in the floodplain can be useful when assessing river management options. For example, Fig. 26a shows that the Lainhart Dam surface water time series ($SWE_{RK23.3}$) was most important in describing variability in wells T1-W1 and T3-W1, but had reduced impact downriver. As the major management tool in the Northwest Fork, river stage (i.e., flow) at Lainhart Dam had only limited impact in maintaining WTE downstream of T3. Similarly, Fig. 26b demonstrates the strong importance of tidal surface water ($SWE_{RK14.6}$) in lower elevation wells further downstream. This variable was most important for explaining WTE variability on downstream transects (T7, T8, and T9) and was strongest for those wells closest to the river, decreasing with distance from the river—for example, from T7-W1 (strongly significant, with $\beta=0.92$) to T7-W4 (insignificant, with $\beta=0.01$). This explanatory variable, and by extension the response variables that it influences most, is most susceptible to sea level rise caused by climate change, which is beyond the scope of local management.

Figs. 26c-d show regression parameters for the two net recharge series ($R_{net,S46}$ and $R_{net,JDWX}$). Though the importance of these two series is distributed across the twelve wells in the floodplain, a geographic pattern is apparent. Wells T1-W1 and T3-W1 are closer to the rainfall gauging station at the S-46 structure (3.2 and 3.9 km, respectively) than the JDWX gauging station (9.7 and 7.2 km, respectively). These wells are more strongly affected by $R_{net,S46}$, (significant, with β values of 0.73 and 0.56, respectively), than by $R_{net,JDWX}$

(insignificant β values of 0.10 and 0.13). The importance of the two net recharge series are split fairly equally over the remainder of the wells (average $\beta_{R_{net, S46}}$: 0.46 ± 0.34 ; average $\beta_{R_{net, JDWX}}$: 0.65 ± 0.35), with $\beta_{R_{net, JDWX}}$ being slightly more important in describing the downstream wells. The importance of capturing this spatially distributed rainfall is reinforced when building a DFM using just one of the R_{net} series or the average of the two, which yielded poorer results ($4859 \leq AIC \leq 6998$; $0.88 \leq C_{eff} \leq 0.89$).

Figs. 26c-d show regression parameters for the two net recharge series ($R_{net, S46}$ and $R_{net, JDWX}$). Though the importance of these two series is distributed across the twelve wells in the floodplain, a geographic pattern is apparent. Wells T1-W1 and T3-W1 are closer to the rainfall gauging station at the S-46 structure (3.2 and 3.9 km, respectively) than the JDWX gauging station (9.7 and 7.2 km, respectively). These wells are more strongly affected by $R_{net, S46}$,

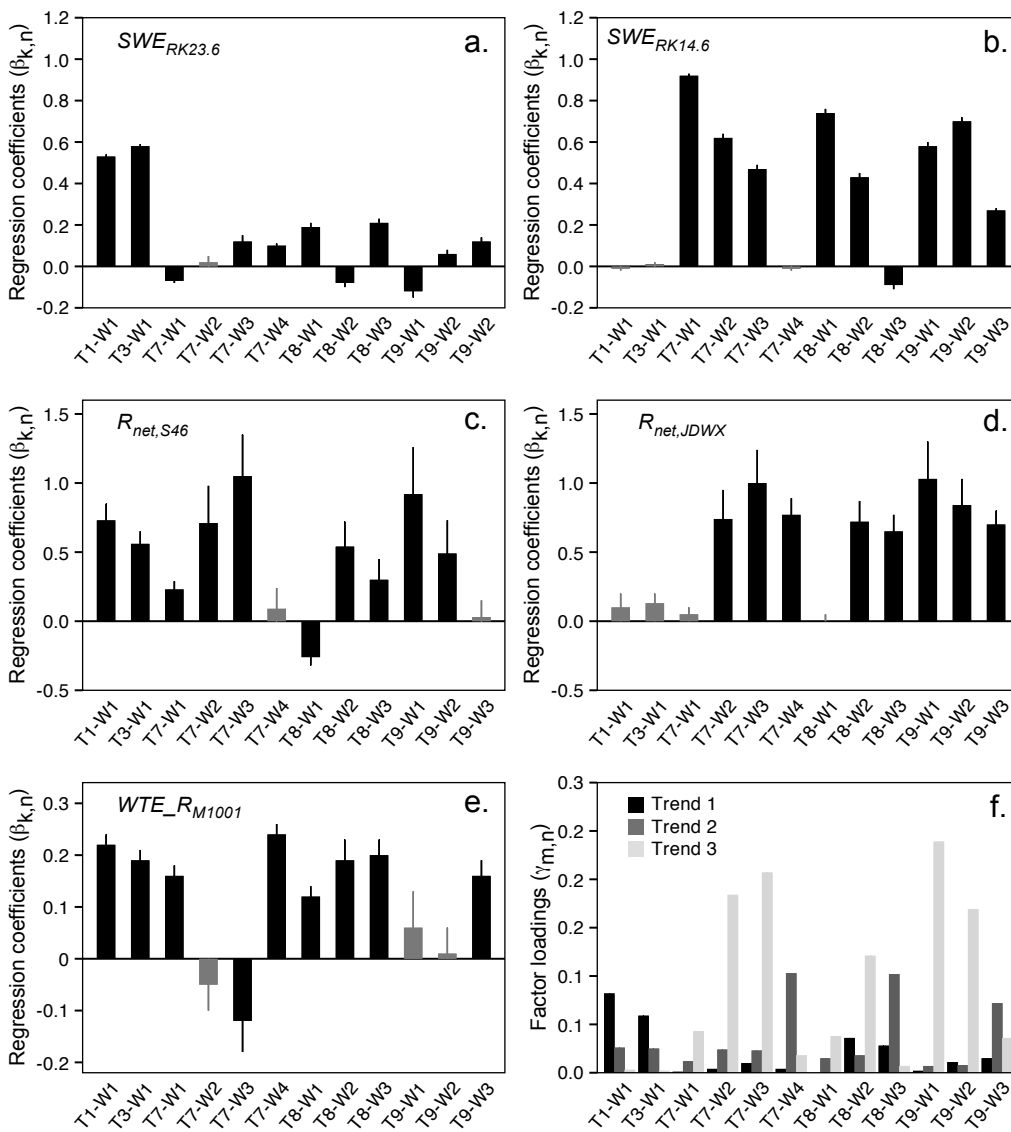


Figure 26. Regression parameters and factor loadings for Model II ($M=3, K=5$). Regression parameters (a-e) are shown with their standard errors, with black bars indicating significance.

(significant, with β values of 0.73 and 0.56, respectively), than by $R_{net,JDWX}$ (insignificant β values of 0.10 and 0.13). The importance of the two net recharge series are split fairly equally over the remainder of the wells (average $\beta_{R_{net, S46}}$: 0.46 ± 0.34 ; average $\beta_{R_{net, JDWX}}$: 0.65 ± 0.35), with $\beta_{R_{net, JDWX}}$ being slightly more important in describing the downstream wells. The importance of capturing this spatially distributed rainfall is reinforced when building a DFM using just one of the R_{net} series or the average of the two, which yielded poorer results ($4859 \leq AIC \leq 6998$; $0.88 \leq C_{eff} \leq 0.89$).

Fig. 26e shows that highest β values for WTE_R were associated with upstream wells (T1-W1, T3-W1) and downstream, high elevation wells (T7-W4, T8-W3, and T9-W3) wells, whose time series closely resembled regional groundwater circulation. Though the importance of regional groundwater elevation (WTE_R_{trend}) increased with well elevation, it was significant for nine of the twelve wells. A lowered regional groundwater table has been identified as a cause of reduced hydroperiod and increased saltwater intrusion in the Loxahatchee River (SFWMD, 2002), and the dependence of floodplain WTE on regional groundwater is substantiated by these results. It is interesting to note that, although the regional groundwater trend and SWE at Lainhart Dam are correlated ($r^2 = 0.71$), including both explanatory variables in Model II allows us to decompose the general effect of the regional groundwater circulation from the more local effect of SWE at Lainhart Dam shown in Fig. 26a.

The remaining three trends in Model II and their associated $\rho_{m,n}$ values are given in Figure 27. These common trends represent the remaining unexplained (latent) variability among the WTE series. Common trend 1 has a high starting value, likely helping the DFM fit measured high water events associated with the hurricanes of 2004, which may not be sufficiently described by explanatory variables, especially if measurement errors occurred during these extreme events. This trend is most important to wells T1-W1 and T3-W1, which were also most strongly affected by SWE at Lainhart Dam. WTE in all wells are generally positively correlated with both common trends 1 and 2, but have low correlations (average $\rho_{1,n}$ value: 0.25 ± 0.21 ; average $\rho_{2,n}$ value: 0.31 ± 0.15). Common trend 3 is weaker and less consistent, with positive correlations for most floodplain wells and negative correlation for most upland wells, all of which were either “minor” or “low.”

Model fits for upstream (T1W1 and T3W1) and downstream, upland (T7W4, T8W3, and T9W3) wells are given in Figure 28. Model fits are good ($0.86 < c_{eff} < 1.0$, visual inspection). Model fits for floodplain wells (T7W1, T7W2, T7W3, T8W1, T8W2, T9W1, and T9W2) are given in Figure 29. Model fits for these wells are also good ($0.78 < c_{eff} < 0.98$, visual inspection). Note that most upland wells lack data from the beginning of the time series, so model results help paint a more complete picture of WTE in these wells during the hurricanes of 2004. Overall model fits can also be evaluated by inspecting the observed versus predicted values compared with the 1:1 line (the basis for c_{eff} ; Fig. 30).

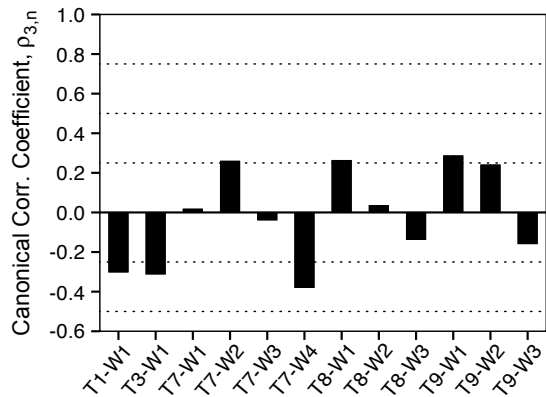
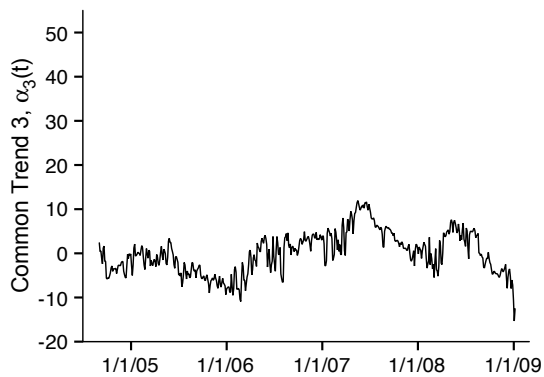
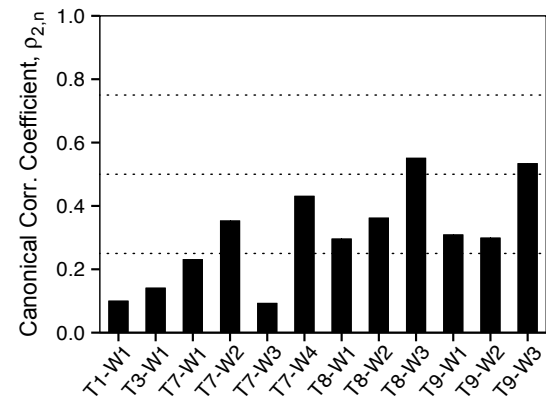
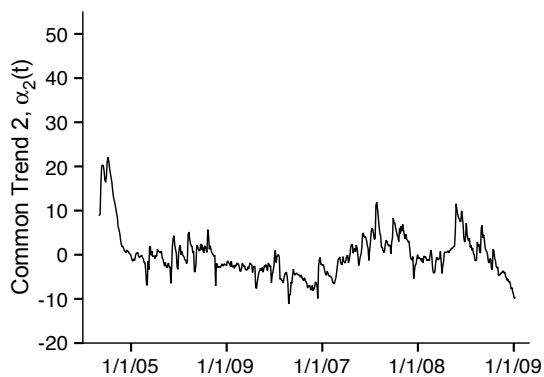
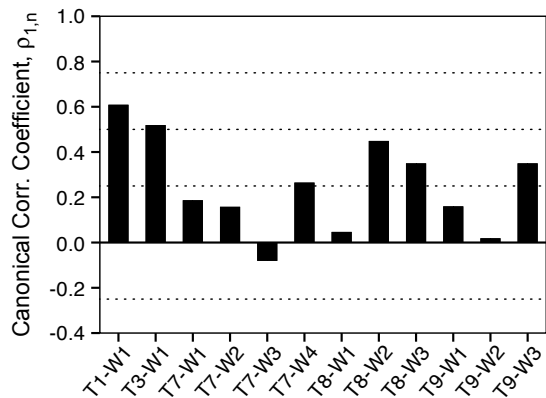
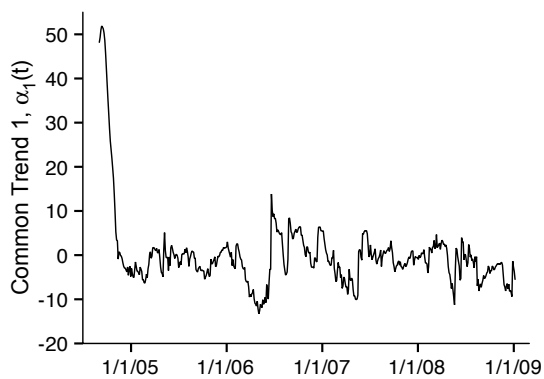


Figure 27. Common trends and associated $\rho_{m,n}$ values for Model II.

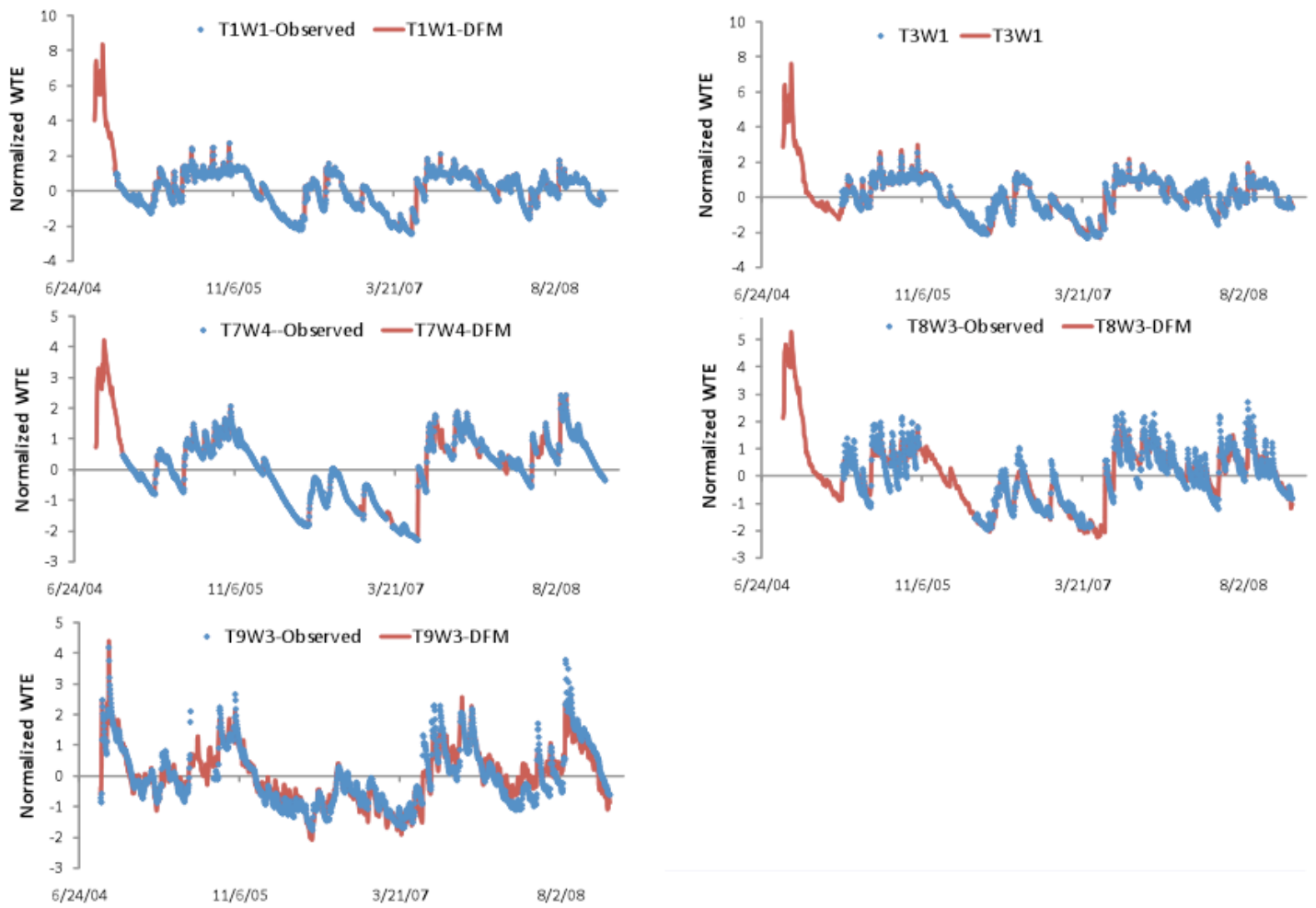


Figure 28. Observed and modeled time series for upland wells. C_{eff} ranges from 0.86 to 1.0.

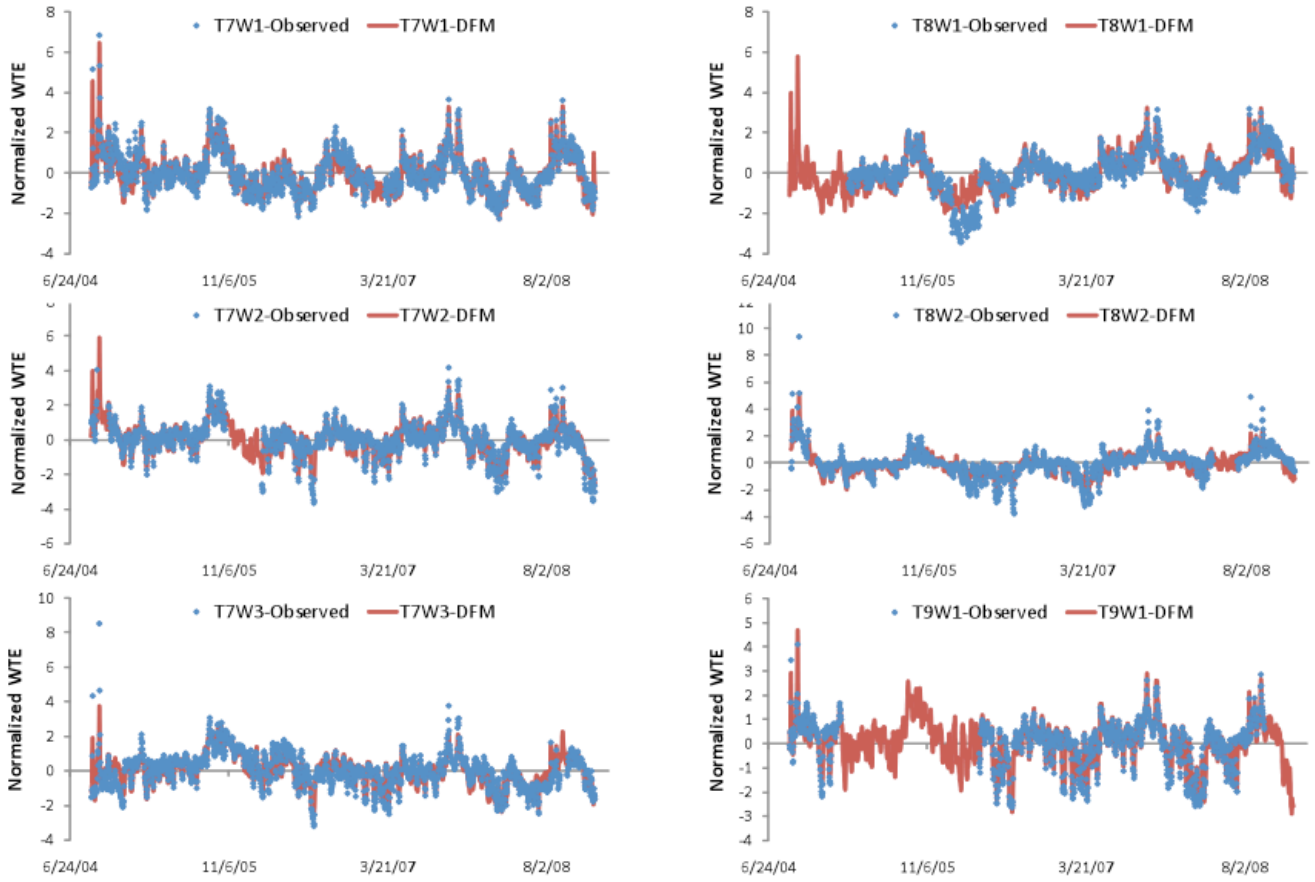


Figure 29. Observed and modeled time series for floodplain wells. C_{eff} ranges from 0.78 to 0.98.

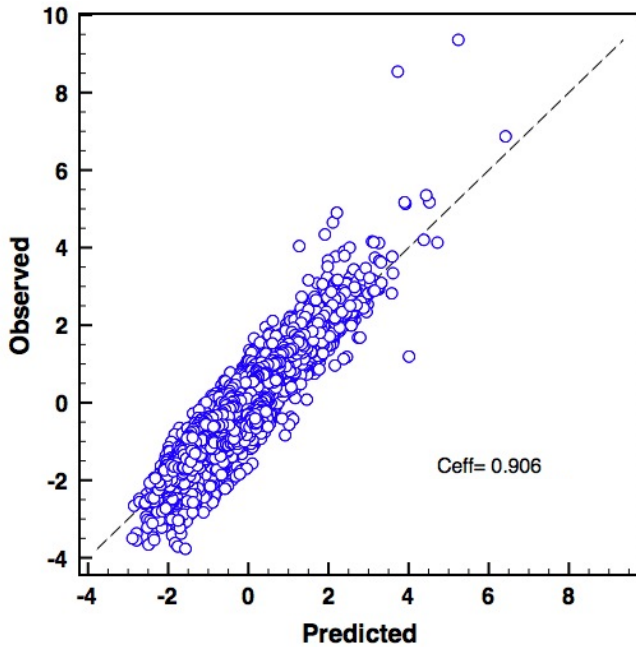


Figure 30. Observed versus predicted normalized WTE and the 1:1 line.

Multilinear regression model (DFA with no common trends)

Finally, common trends were removed from the model to assess the validity of a DFM using only explanatory variables. In this model (Model III), the five explanatory variables identified in the DFA were used to create a multi-linear model of the response variables. As expected, C_{eff} values for Model III were somewhat reduced from Model II (overall $C_{eff} = 0.81$, $0.59 < C_{eff} < 0.94$; compared to $C_{eff} = 0.91$, $0.78 < C_{eff} < 1.0$ for Model II), but are still be adequate for most wells (Table 8). Model III does a good job predicting WTE in higher elevation wells farthest from the river (e.g., Fig. 9a) and in lower elevation wells close to the river (e.g., Fig. 9b), and a fair job for middle distance and elevation wells (e.g., Fig. 9c).

Table 8. Constant level parameters (μ_n), model parameters, and coefficients of efficiency (C_{eff}) from Model III (no trends, 5 explanatory variables). Significant model parameters in bold.

S_n	μ_n	Model parameters					C_{eff}
		$SWE_{RK23.3}$	$SWE_{RK14.6}$	WTE_{RM1001}	$R_{net,S46}$	$R_{net,JDWX}$	
T1-W1	0.00	0.69	-0.09	0.41	0.07	-0.02	0.91
T3-W1	0.00	0.70	-0.06	0.35	0.08	0.00	0.94
T7-W1	0.00	-0.07	0.95	0.09	0.08	-0.05	0.93
T7-W2	0.00	0.07	0.86	0.09	-0.05	-0.31	0.76
T7-W3	0.00	0.13	0.65	-0.32	0.42	0.30	0.59
T7-W4	0.00	0.18	0.03	0.68	0.07	0.23	0.91
T8-W1	0.00	0.18	0.78	0.07	-0.38	-0.09	0.80
T8-W2	0.00	0.06	0.55	0.35	-0.12	0.01	0.68
T8-W3	0.00	0.34	-0.04	0.69	-0.05	-0.04	0.81
T9-W1	0.00	-0.12	0.87	0.10	-0.06	-0.11	0.81
T9-W2	0.00	0.12	0.87	-0.04	-0.17	0.15	0.86
T9-W3	0.00	0.14	0.38	0.50	-0.01	0.05	0.77
Overall							0.81

Closer to the edges of the system, explanatory variables act as boundary conditions (e.g., regional WTE at the farthest landward end of transects and SWE acting at the river) and their effects can be seen directly in the WTE series. In middle distance and middle elevation wells, the interaction of surface water and groundwater is most complex and non-linear, which is not as well captured by a linear combination model. Despite these limitations, overall performance of Model III is adequate to describe variations in WTE in the Loxahatchee River floodplain and may be useful for assessment of Loxahatchee River restoration scenarios, especially considering the wide range of climatic conditions captured in the study.

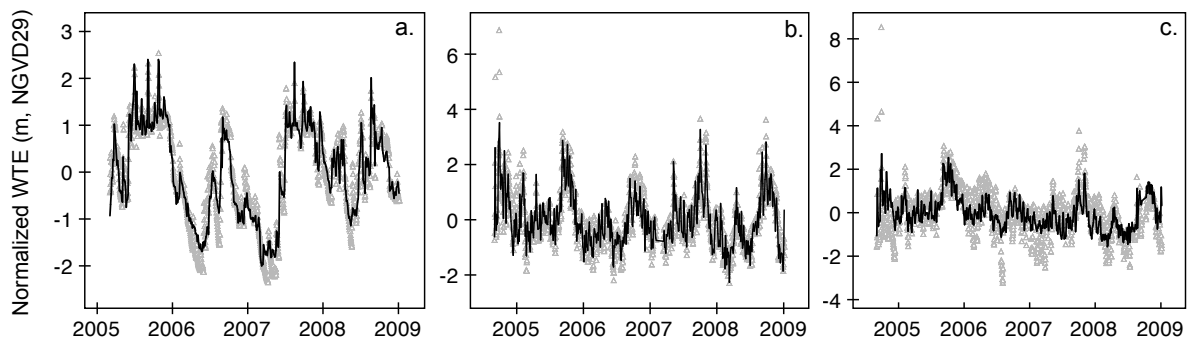


Figure 31. Figure 32. Observed (symbols) and modeled (lines) normalized WTE for (a) well T3-W1; (b) well (T7-W1); and (c) well T7-W3 obtained from Model III using 5 explanatory variables and no trends.

Dynamic Factor Analysis of Groundwater Electrical Conductivity

Baseline DFA (no explanatory variables)

Next, DFA was performed for groundwater electrical conductivity (GWEC). First, an increasing number of common trends were fit to the twelve response variables until a minimum AIC and maximum *ceff* were achieved. With a diagonal matrix, AIC continues to decrease and *ceff* to increase with up to nine trends ($M=9$; Fig. 32), where an inflection point in *ceff*, but not AIC, was found. A non-diagonal matrix yielded similar results, with an inflection in *ceff* at $M=8$ and no inflection in AIC.

The fact that eight or more common trends were necessary to achieve the best DFM reflects the high variability of the GWEC series and again suggests that multiple latent effects influence GWEC across the watershed. As with the DFA for WTE, although AIC continues to decrease with added trends with both matrices (Table 9), *ceff* is worse with the non-diagonal than for the corresponding number of trends using a diagonal matrix. Thus, though less clear than with the DFA for WTE, this analysis indicates the best DFM using twelve response variables, no explanatory variables, and a diagonal error matrix would require nine common trends (Model I-a; Table 10).

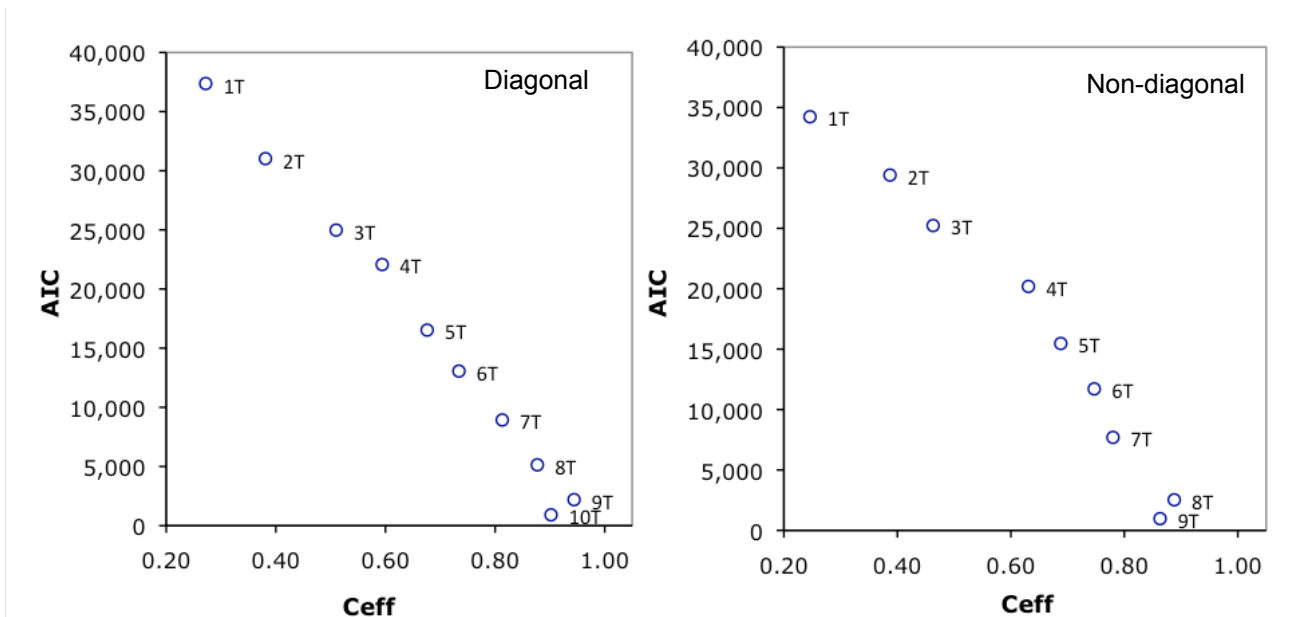


Figure 33. Akaike Information Criteria (AIC) versus Nash-Sutcliffe coefficient of efficiency (*ceff*) with diagonal (left) and non-diagonal error matrices for the baseline DFM using twelve response variables.

Table 9. AIC and *ceff* values for the GWEC DFMs with twelve response variables and no explanatory variables and 1 – 10 common trends. The best DFM (diagonal matrix; $M=9$; $ceff=0.944$; AIC = 2198) is in bold.

<i>M</i>	Diagonal Matrix		Non-Diagonal Matrix	
	<i>ceff</i>	AIC	<i>ceff</i>	AIC
1	0.272	37,371	0.246	34,233
2	0.381	31,025	0.387	29,406
3	0.510	24,983	0.463	25,231
4	0.594	22,071	0.631	20,191
5	0.676	16,531	0.688	15,469
6	0.734	13,063	0.747	11,712
7	0.813	8,934	0.780	7,701
8	0.877	5,138	0.888	2,534
9	0.944	2,198	0.863	974
10	0.902	914		

Initial examination of the nine common trends required to maximize $ceff$ and their associated factor loadings ($\gamma_{m,n}$) and canonical correlation coefficients ($\rho_{m,n}$) yielded few clues to possible explanatory variables to improve the DFM. The three common trends with the largest average $|\rho_{m,n}|$ values are shown in figure 33. None of the common trends share a consistently positive or negative correlation with all twelve GWEC series. Moreover, positive and negative correlations are often split across wells on the same transect (i.e., common trend 1 is negatively correlated with GWEC in wells T7W1 and T7W2, but positively correlated with GWEC in wells T7W3 and T7W4; Fig. 33a).

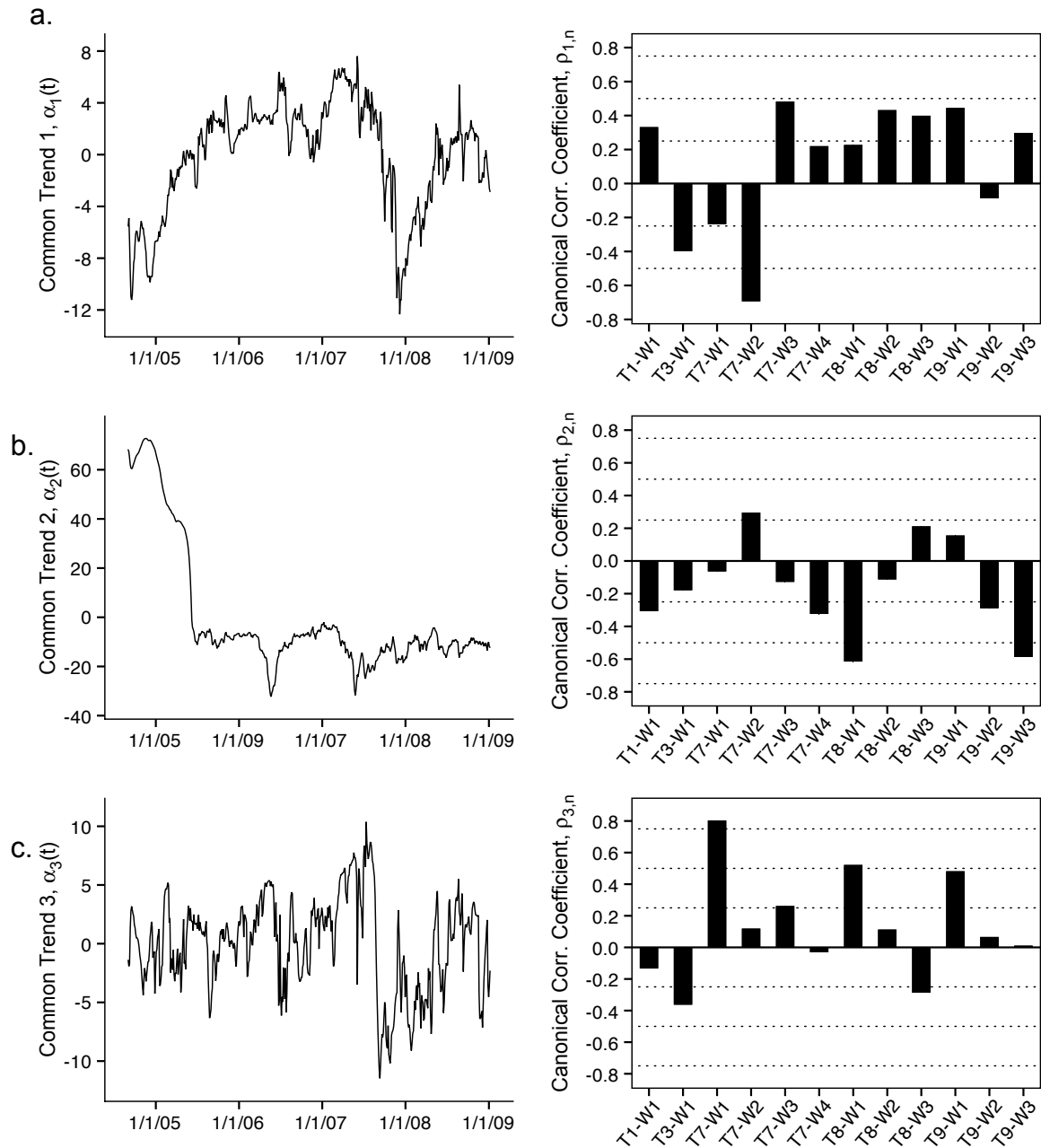


Figure 34. The three most important trends to Model I-a (left) and their associated canonical correlation coefficients (right). Patterns of shared variation among GWEC in the twelve wells are unclear.

Alternate Baseline DFAs

Adding various suites of explanatory variables to remove unexplained variability from Model I-a allowed for the removal of some common trends (net recharge series were the most important explanatory variables identified), but due to the relatively unenlightening results of Model I-a, several alternate DFMs were evaluated first before settling on the best candidate explanatory variables.

When looking at the variability in GWEC in the twelve wells in the Northwest Fork, some series exhibit relatively minor EC variation. For example, GWEC in wells T1W1, T3W1, T7W4, T8W3, and T9W3 all exhibit changes only in the range below 0.01 S/m (0.06 ppt). When compared with GWEC variation in the remaining seven wells, these five time series may be considered more or less as straight lines of very low magnitude (black lines in Fig. 34). The goal of this analysis is to take into account how groundwater EC is affected by other hydrological variables in the watershed. However, normalizing small variations to make them useful for the DFA scales up these small changes, which from a physical point of view may not be relevant (they are far below the 0.3125 S/m [2 ppt] threshold, for example).

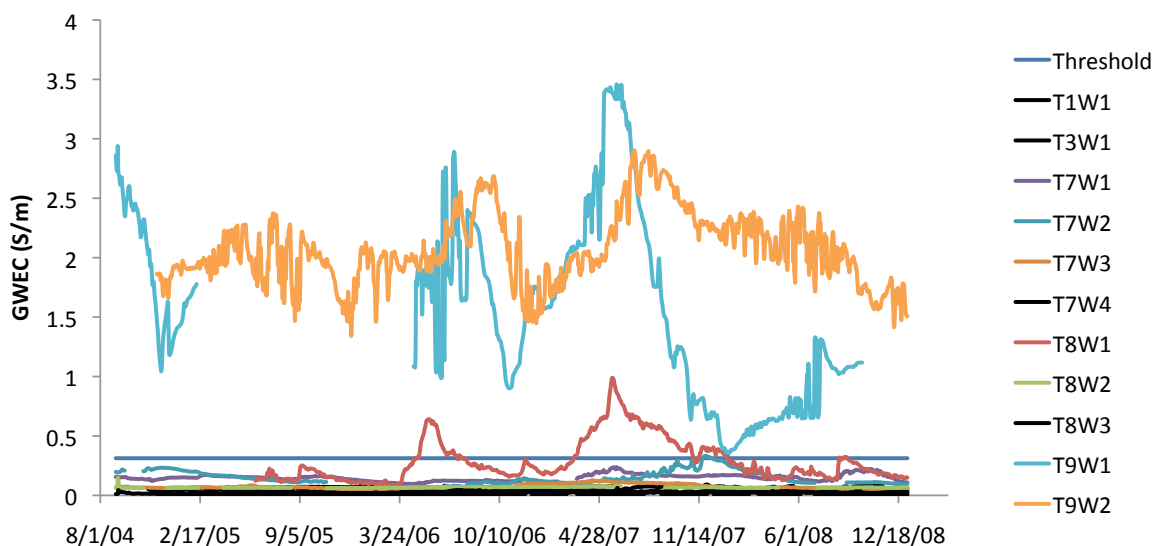


Figure 35. GWEC in the twelve wells in the Loxahatchee River. Low magnitude and low variation wells (T1W1, T3W1, T7W4, T8W3, and T9W3) shown in black.

Thus, an additional baseline DFA was performed using only seven response variables (T7W1, T7W2, T7W3, T8W1, T8W2, T9W1, and T9W2; Model I-b). Though removed from the calculations of common trends and explanatory variables, these series are not removed from the study; but could be added to the final DFM as constant values (i.e., a level parameter) with factor loadings equal to zero. Since commonalities among input time series were GWEC time series were difficult to identify in Model I-a, an third baseline DFA was explored using aggregated weekly averages of GWEC (Model I-c).

Results from the exploratory model with seven response variables ($Y=7$; Model I-b) are shown in figure 35a. Again an increasing number of common trends were fit to the seven response

variables with the goal of indentifying a minimum AIC and maximum $ceff$. With a diagonal error matrix, AIC continues to decrease and $ceff$ to increase with increasing trends, with no inflection point identified (shown for $M=1-7$; Fig. 35). Results for the weekly average GWEC baseline DFA (Model I-c) are shown in figure 35b, with similar results.

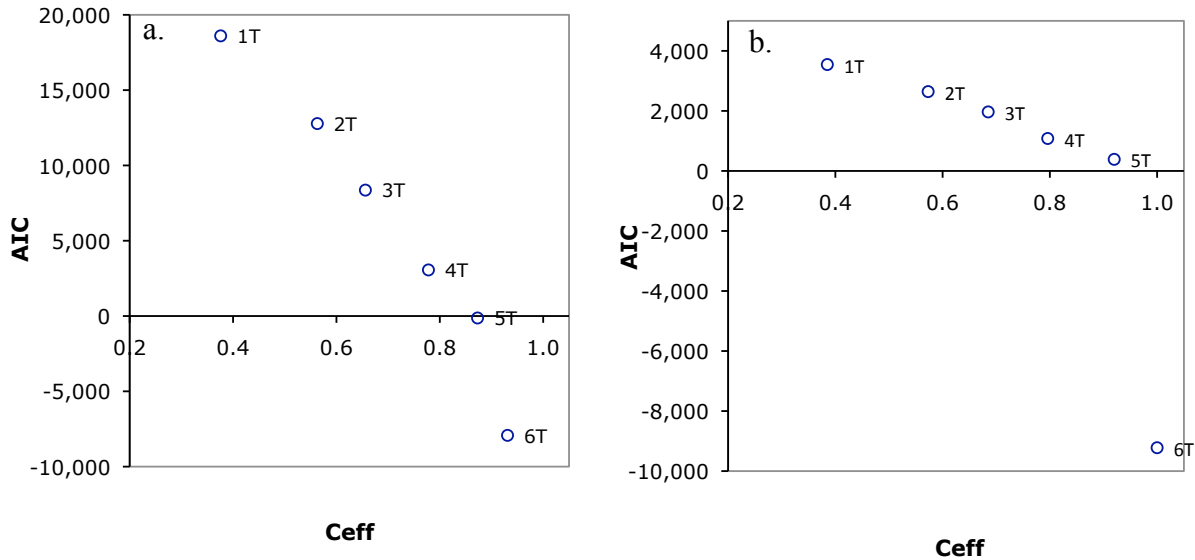


Figure 36. Akaike Information Criteria (AIC) versus Nash-Sutcliffe coefficient of efficiency ($ceff$) for Model I-b (seven response variables; left) and Model I-c weekly GWEC (seven response variables; right). Both used diagonal error covariance matrices.

Though this phenomenon complicates the interpretation of DFA results, it can be explained by examining the definition of the AIC. The AIC is computed as:

$$AIC = 2k - 2\ln(L) \quad [4]$$

where k is the number of DFM parameters and L is the maximized value of the likelihood function for the estimated model (i.e., an estimation of the sum of squared errors between observed and predicted values, RSS). When an additional trend is added to the DFM, the model uses twelve (or seven) additional factor loadings plus a level parameter. Thus, the AIC increases linearly, since k is higher. On the other hand, if the inclusion of the extra trend helps to better predict the response time series, than AIC may also be reduced because the RSS is lower.

Due to this “balancing act,” the AIC is generally a useful indicator of model performance and parsimony, but only if the improvement in predictions is comparable to the penalization due to the extra parameters. In the case of dynamic factor modeling of GWEC, it appears that the AIC is more sensitive to reductions in RSS than to increases in k . Although it may result in only a small improvement of the model performance (measured with $ceff$), adding an extra trend may considerably increase the likelihood function (decrease RSS). By contrast, the extra parameters imply a penalization with lower order of magnitude. For example, if the change in

the likelihood functions is of the order of 1,000 and the change in the number of parameters is of the order of 10, than the AIC may be insensitive to the number of parameters. This would yield considerable reductions in AIC with small corresponding changes in *ceff*. This may be particularly true for long data sets like those analyzed here.

Where no inflection point in AIC can be identified, we propose using the *ceff* and visual inspection as a measure of a model’s goodness-of-fit. Though choice of a threshold *ceff* is necessarily arbitrary, it is common to choose an "appropriate" model based on its predictive ability (goodness-of-fit). For the subsequent analysis and identification of explanatory variables, the baseline DFA using weekly aggregated GWEC (Model I-c) was used and an arbitrary *ceff* of 0.8 was selected as the key model performance criterion. To achieve $ceff \geq 0.8$, Model I-c required the use of four common trends to model the seven response variables (though it just barely met this criteria with four trends and a *ceff* = 0.80; five trends improved the fit, with *ceff* = 0.92). The objective of the subsequent DFA with explanatory variables was thus to reduce below four the number of common trends required to achieve $ceff \geq 0.8$.

DFA with explanatory variables

Next, appropriate explanatory variables were added to reduce the number of common trends required to achieve an adequate fit of GWEC (and to minimize the factor loadings of any remaining trends). As mentioned above, candidate explanatory variables collected in the Loxahatchee River watershed included surface water elevations (SWE) at six locations in the Northwest Fork; surface water EC (SWEC) at five locations (including three stations with top and bottom EC for a total of eight SWEC series); one common trend representing the eight regional wells used in the DFA of WTE (WTE_R; the common trend did a good job of representing variation in WTE_R among the nine wells [*ceff*=0.83]); and two net recharge (NR) series (Table 10).

Table 10. Candidate explanatory variables used in the DFA of groundwater electrical conductivity.

Variable	# of Series	Description
SWE	6	Surface water elevation (m NGVD29) from monitoring stations (Lainhart Dam, RM 9.1, Kitching Creek up/downstream, Boy Scout Dock, and Coast Guard Station) in the Loxahatchee River
SWEC	8	Surface water electrical conductivity (S/m) from monitoring stations (Indiantown Road, RM 9.1 [top/bottom], Kitching Creek Outlet, Boy Scout Dock [top/bottom], and Coast Guard Station [top/bottom]) in the Loxahatchee River
NR	2	Cumulative net recharge (cumulative rainfall – cumulative ET, mm) from weather stations at the S-46 structure and in Jonathan Dickinson State Park (NR_S46 and NR_JDWX) in the Loxahatchee River watershed.
WTE_R	1	Common trend of WTE_R from the nine USGS wells explored in the DFA of WTE.

Several additional explanatory variables were also explored to better represent the dynamics of GWEC in the floodplain of the Loxahatchee River. For example, SWE at Lainhart Dam did not improve the model of GWEC, likely because the effects of freshwater flow on GWEC are delayed and occur over longer time periods. Since a model using linear combinations of environmental variables cannot account for this effect, a “cumulative flow debt” (CFD) was calculated on a weekly basis (to match the weekly aggregated GWEC series). To calculate

CFD, average daily flow ($\text{m}^3 \text{s}^{-1}$) at Lainhart dam was used to calculate cumulative weekly flow ($\text{m}^3 \text{week}^{-1}$). Next, a weekly critical flow volume was subtracted from this total, and the results were cumulated over the course of the four-year period. For example, in the first week of January 2005, $462,067 \text{ m}^3$ of water flowed over Lainhart dam. With a critical flow volume of $604,807 \text{ m}^3$ (based on a flow rate of $1 \text{ m}^3 \text{ s}^{-1}$ or 35 cfs), this resulted in a “flow debt” of $142,740 \text{ m}^3$ for the week. These flow debts (sometimes positive, sometimes negative) were then cumulated over the entire period of record. The analysis was performed with critical flow volumes of 1, 1.5, 1.95, 2.5, and $3 \text{ m}^3 \text{ s}^{-1}$ (equivalent to 35, 53, 69, 88, and 106 cfs), based in part on flow rates from the MFL and Restoration Plan for the Northwest Fork.

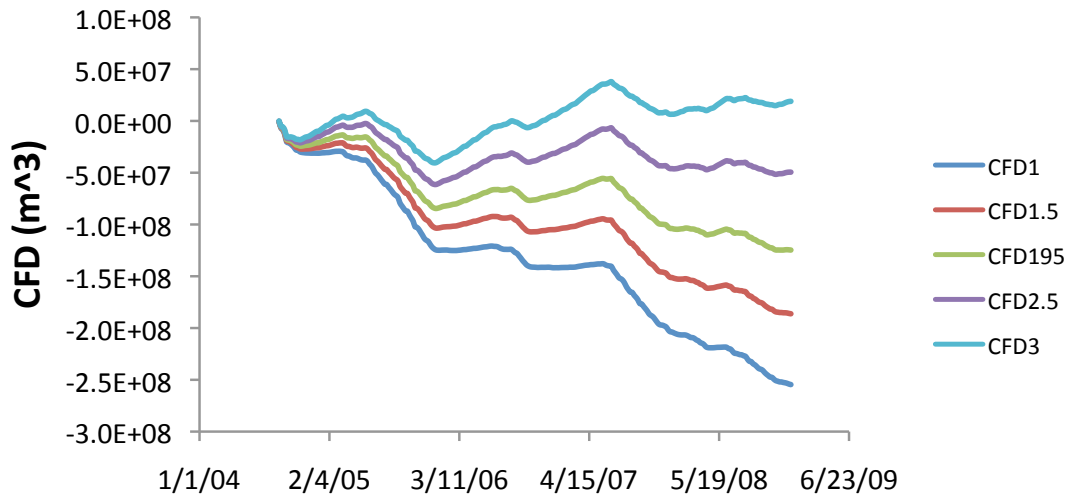


Figure 37. Calculated cumulative flow debt (CFD) for five critical flow levels ($1 - 3 \text{ m}^3 \text{ s}^{-1}$)

Next, a similar technique was applied to SWEC series to create “cumulative salt surplus” (CSS) series, since changes in SWEC also appeared to be reflected in a delayed and extended manner in GWEC. To calculate CSS for each SWEC series, the four-year average EC value for each series was subtracted from each weekly average EC value. These values were then cumulated over the study period. For example, for the SWEC station at RM9.1 (top), average EC during the first week of January 2005 was 0.047 S/m and the global average was 0.084 S/m, resulting in a CSS of -0.037. These salt surpluses (sometimes positive, sometimes negative) were then cumulated over the entire period of record. The analysis was performed with the SWEC series at RM9.1 (top), Boy Scout Dock (top), Kitching Creek outlet, and Coast Guard Station (top) (Fig. 37).

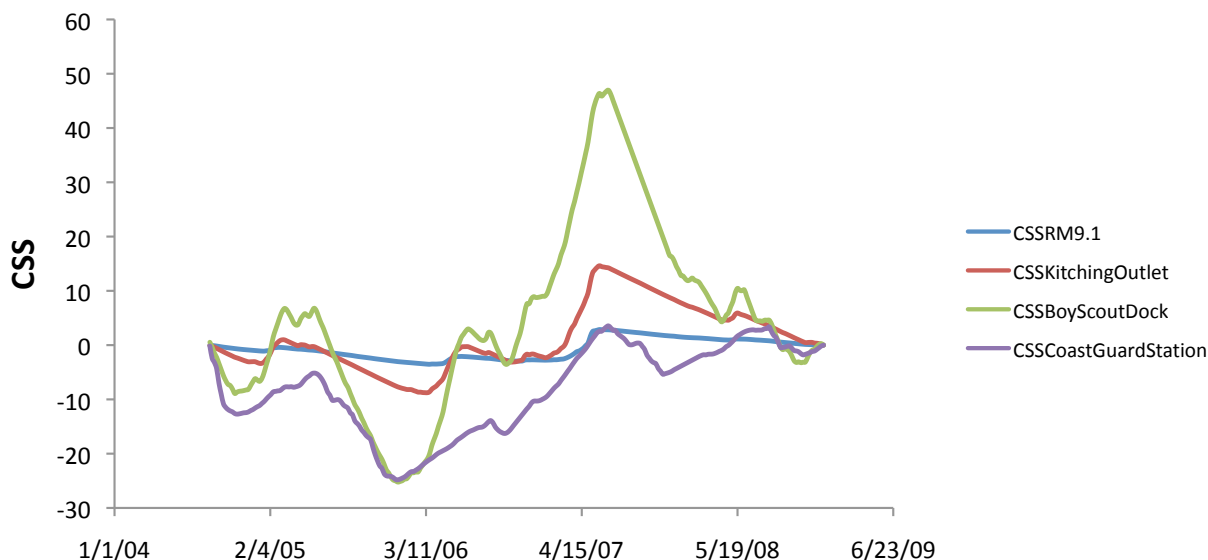


Figure 38. Calculated cumulative salt surplus (CSS) for four SWEC stations.

Approximately 100 combinations of common trends and explanatory variables were explored in Brodgar. Finally the best DFM was achieved using three explanatory variables: net recharge (NR_S46), cumulative flow debt with a critical flow of $2.5 \text{ m}^3 \text{ s}^{-1}$ (88 cfs; CFD_2.5), and cumulative salt surplus from the outlet at Kitching Creek (CSS_Kitch.). Other CFD and CSS series were collinear and thus could not be included in the DFM, however the DFM was most improved with this particular suite of variables. In this DFA, using both net recharge series did not improve the model and NR_S46 performed better than NR_JDWX or the average of the two series. Using these explanatory variables, it was possible to reduce the number of required common trends from four to three ($M=3$), thus slightly reducing the unexplained variability in the model. This model (Model II) yielded an AIC value of 827 and a *ceff* value of 0.85 across the twelve wells (performing better than the 1,082 AIC target and *ceff* value of 0.80 for the four-trend Model I-c).

Table 11 summarizes the results obtained from Model II ($M=3$, 3 explanatory variables). These results include the factor loadings ($\gamma_{m,n}$) and canonical correlation ($\rho_{m,n}$) for each trend; regression parameters ($\beta_{k,n}$) for each explanatory; and the constant level factor (μ_n) and *ceff* for each of the wells. Significant regression parameters ($t\text{-value}>2$) are shown in bold. GWEC in the seven wells used in this analysis have variable relationships to the common trends, but factor loadings are relatively small. Average (absolute value) γ_n value: 0.07 ± 0.07 for trend 1; 0.06 ± 0.06 for trend 2; and 0.05 ± 0.05 for trend 3. Inclusion of explanatory variables reduced these factor loadings over those in Model I-c (average γ_n value over all four trends in Model I-c: 0.11 ± 0.08).

Table 11. Output results from DFA with explanatory variables (Model II).

s_n	μ_n	$\gamma_{1,n}$	$\rho_{1,n}$	$\gamma_{2,n}$	$\rho_{2,n}$	$\gamma_{3,n}$	$\rho_{3,n}$	$\beta_{CFD\ 2.5}$	$\beta_{CSS\ Kitch.}$	$\beta_{NR\ S46}$	$ceff_n$
T7W1	0.04	0.23	0.844	0.03	-0.01	0.01	-0.24	0.35	1.05	-0.08	1.00
T7W2	-0.35	-0.03	0.058	-0.08	-0.46	0.05	-0.46	0.95	0.84	-0.6	0.84
T7W3	0.09	0.04	0.037	0.01	0.01	0.15	0.48	0.07	0.17	0.28	1.00
T8W1	0.34	0.05	0.171	0.19	0.52	0.01	0.34	0.29	1.69	-0.36	1.00
T8W2	0.26	0.03	0.058	0.05	0.30	0.04	0.49	-0.62	-0.09	0.47	0.58
T9W1	0.38	0.03	0.15	0.08	0.05	-0.04	0.24	0.14	0.25	1.13	0.90
T9W2	0.13	-0.12	-0.208	0.02	0.28	-0.07	0.04	0.44	1.11	-0.03	0.61

The effects of the common trends and regression parameters on Model II can be compared in Figure 38. Regression parameters represent the importance of the corresponding explanatory variable on each response variable. Factor loadings (Fig. 38d) are small compared to regression parameters (Fig. 38a-c), suggesting that the patterns observed in the Loxahatchee River wells may be adequately described using only explanatory variables. Regression parameters for the calculated variables cumulative flow debt (CFD) and cumulative salt surplus (CSS) were far greater than for all other explanatory variables used initially (e.g., SWEC, SWE, etc.). Incorporating these cumulative “memory” variables was important for improving the DFM and may be explored further.

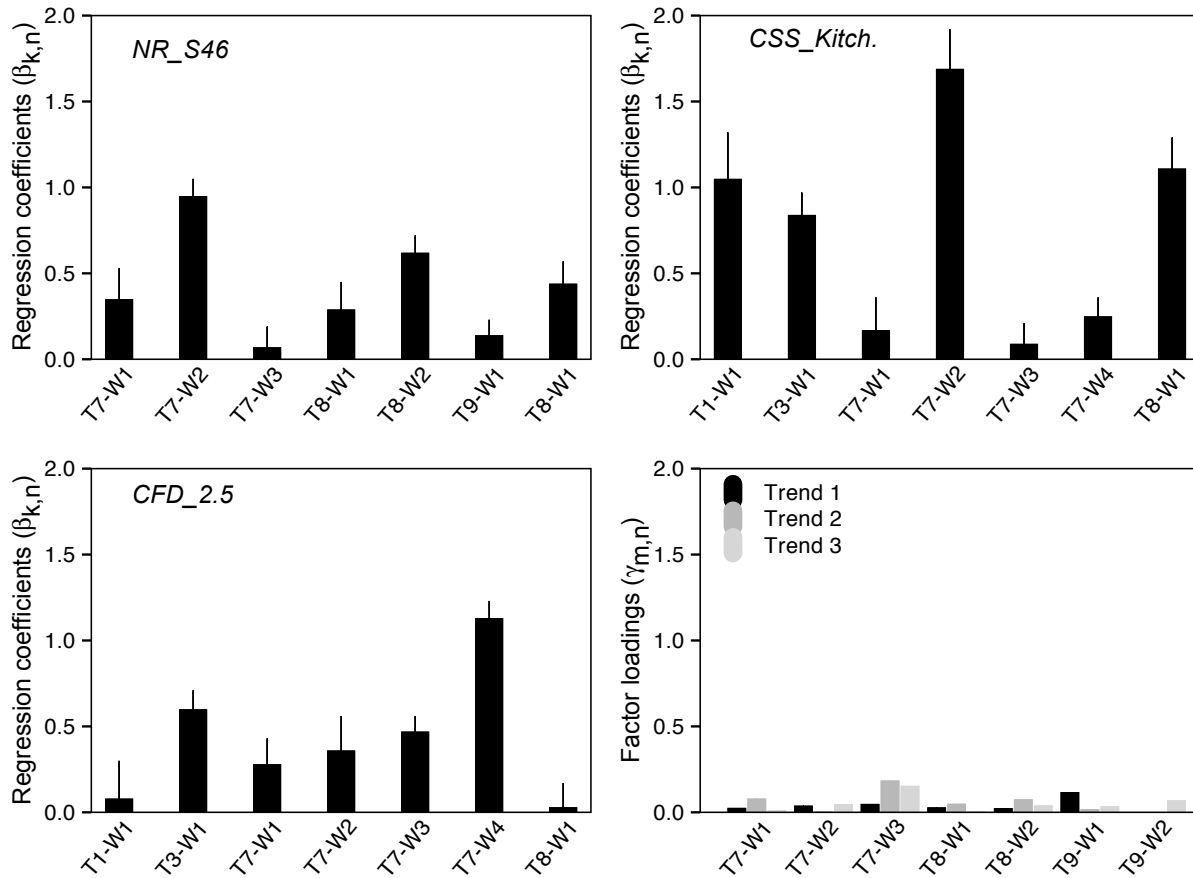


Figure 39. Regression parameters and factor loadings for Model II ($M=3$, 3 explanatory variables). Regression parameters are shown with their standard errors.

The remaining three trends and their associated $\rho_{m,n}$ values are given in Figure 39. These trends represent the remaining unexplained (latent) variability among the GWEC series. Trend 1 is only important to GWEC in well T7-W1, and describes GWEC variation specific to this well. Trends 2 and 3 are more broadly correlated with the seven wells, but no clear associations between trends and well are apparent. As with Model I-c, none of the common trends share a consistently positive or negative correlation with all twelve GWEC series. Again, positive and negative correlations are often split across wells on the same transect (i.e., common trend 3 is negatively correlated with GWEC in wells T7W2, but positively correlated with GWEC in wells T7W3; Fig. 39c). Model fits for GWEC are given in Figure 40. Model fits are good to excellent ($0.58 < c_{eff} < 1.0$, visual inspection).

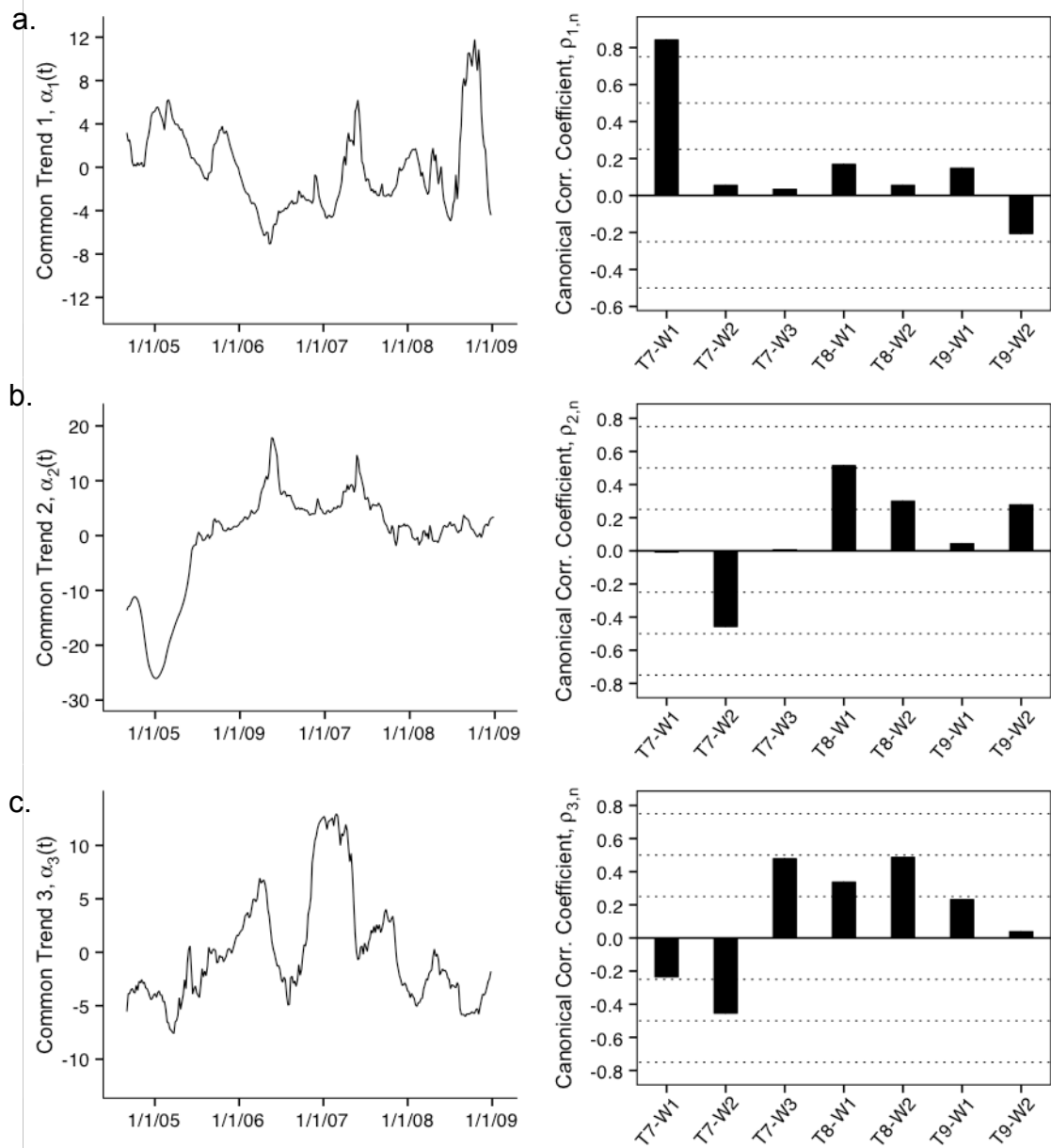


Figure 40. Common trends and associated $\rho_{m,n}$ values for Model II.

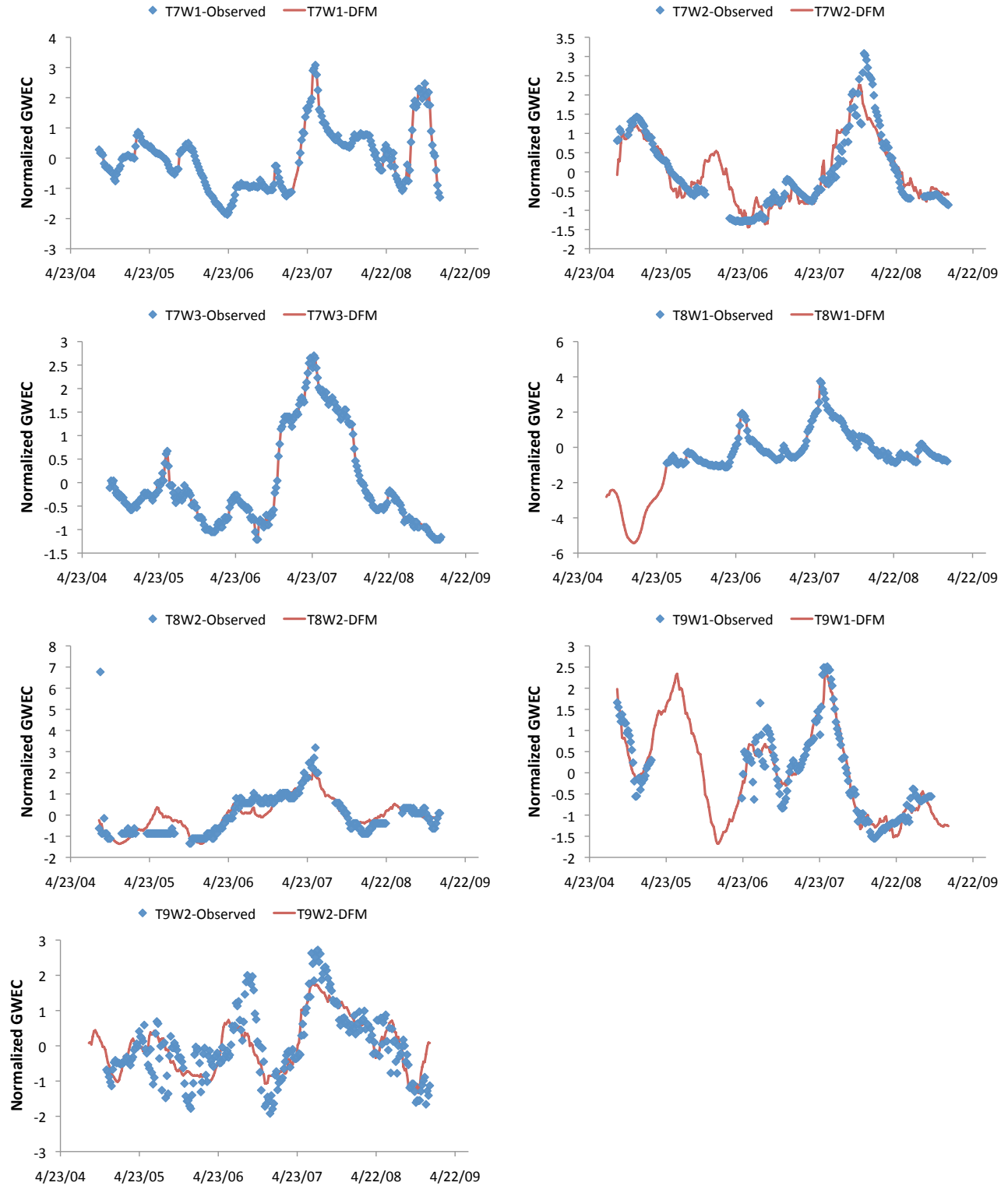


Figure 41. Observed and modeled time series for floodplain wells. C_{eff} ranges from 0.58 to 1.0.

Multilinear regression model (DFA with no common trends)

Finally, common trends were removed from the model to assess the validity of a DFM using only explanatory variables. In this model (Model III), level parameters (μ_n) and regression coefficients ($\beta_{m,n}$) from the three explanatory variables were used to create a multi-linear model of the response variables, but common trends were excluded. As expected, *ceff* values were reduced, with an overall *ceff* value of 0.20 (range $-0.51 < ceff < 0.43$) compared to 0.85 (range $0.58 < ceff < 1.0$) for Model II. Visual inspection of the “best” and “worst” model fits from Model III indicate that the model without trends may not adequately describe the response variables (Fig. 41). For comparison, correlation coefficients for Model III were slightly higher than *ceff* values: average r^2 of 0.44 (range 0.36 – 0.59).

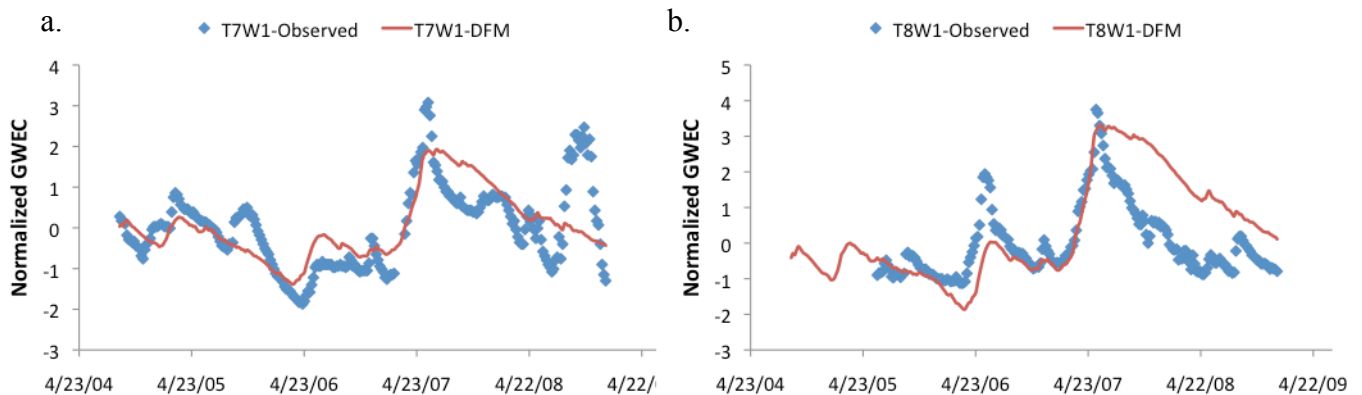


Figure 42. Observed versus predicted normalized GWEC for the model with no common trends (Model III). Panel (a) shows the best fit ($ceff = 0.431$, $r^2 = 0.45$); (b) shows the worst ($ceff = -0.51$; $r^2 = 0.44$).

Conclusions

Detailed hydrological multivariate time series, obtained in and around the Loxahatchee River watershed in south Florida, were studied and modeled using dynamic factor analysis (DFA). The analysis was successfully applied to understand the hydrological processes in this area, which has been affected by reduced hydroperiod and increased saltwater intrusion. The technique proved to be a powerful tool for the study of interactions among 30 long-term, non-stationary hydrological time series (twelve water table elevation [WTE] series and eighteen candidate explanatory variables).

Upstream and tidal surface water elevations (SWE), regional groundwater circulation (WTE_R), and cumulative net recharge (R_{net}) were found to be the most important factors responsible for groundwater profiles in the floodplain wetlands of the Loxahatchee River, and the analysis quantified the spatial distribution of the importance of each explanatory variable to WTE in the different wells. Upstream SWE at Lainhart Dam is the primary managed hydrological input in the Loxahatchee River (Kaplan et al., 2009), and was important for describing variability in wells T1-W1 and T3-W1, but had limited impact in maintaining WTE downstream of T3. Although SWE at Lainhart Dam has been shown to largely dictate downstream surface water salinity (SFWMD, 2006), its role in explaining WTE variation is limited to the upstream, riverine river reaches. Tidal SWE at river kilometer RK 14.6 was important for explaining observed WTE variability for downstream, lower elevation wells and is susceptible to sea level rise caused by climate change, which is beyond the scope of local management.

WTE_R was significant for nine of the twelve wells, corroborating the noted dependence of floodplain WTE on regional groundwater (SFWMD, 2002). The best DFM used two R_{net} series, with wells T1-W1 and T3-W1 gaining the most benefit from the R_{net} series calculated using rain from the nearby (to these wells) S-46 structure. The importance of the R_{net} series from the JDWX gauging station were split fairly equally over the remainder of the wells. Using the average of the two series (a common technique in small watersheds) yielded inferior results. This highlights the importance of using the best available rainfall data for hydrological modeling, whether it be empirical or mechanistic, and stresses the need to move to more advanced rainfall measurement techniques, including Next Generation Radar (NexRad).

The DFM resulting from the DFA (Model II) had good results (overall $C_{eff} = 0.91$, $0.78 \leq C_{eff} \leq 1.0$, visual inspection) and is useful for filling in data gaps during the study period and identifying the relative importance and relationships between hydrological variables of interest. The reduced model with no common trends (Model III) did a fair to good job (overall $C_{eff} = 0.81$, $0.59 \leq C_{eff} \leq 0.94$), and is likely adequate for describing variations in WTE in the Loxahatchee River floodplain. This empirical model may be deemed useful for assessment of the effects of Loxahatchee River restoration and management scenarios on WTE dynamics. Next, we aim to apply these methods to improve our understanding of the important shared trends and explanatory variables controlling groundwater salinity, soil moisture, and porewater salinity in the Loxahatchee River floodplain.

Application of DFA to identify common trends and important explanatory variables affecting

groundwater electrical conductivity (GWEC) was more difficult. Baseline DFMs required eight or more trends to adequately describe the twelve response variables. Results were improved by focusing only on the seven GWEC series with the highest magnitudes and variability and aggregating time series to weekly values, though these series still required four common trends to achieve adequate model fits ($ceff \geq 0.8$).

The original suite of explanatory variables successfully applied to WTE did not improve model performance when applied to GWEC. When compared with changes in surface water and meteorological data, changes in GWEC occurred in a more delayed and extended manner. Thus, two calculated variables, cumulative flow debt (CFD) and cumulative salt surplus (CSS), were used to some benefit in the model. The final model (Model II) used three common trends and three explanatory variables (net recharge from calculated with rain from the S46 structure, cumulative flow debt using a critical flow of $2.5 \text{ m}^3 \text{ s}^{-1}$, and cumulative salt surplus calculated from the SWEC series at the outlet of Kitching Creek. Other CFD and CSS series were collinear and thus could not be included in the DFM.

The Dynamic Factor Model (DFM) resulting from the DFA for GWEC (Model II) had good results (coefficient of efficiency 0.58–1.0, visual inspection), however the reduced model with no trends (Model III) did not perform as well and may not be adequate for describing variations in GWEC in the Loxahatchee River floodplain.

References

- Akaike, H., 1974. A new look at the Statistical Model Identification. IEEE Trans. Automat. Control 19, 716–723.
- Brodgar 2.5.7 (2000). Software Package for Multivariate Analysis and Multivariate Time Series Analysis. Aberdeen: Highland Statistics Ltd.
- Dempster AP, N.M. Laird, and D.B. Rubin. 1977. Maximum likelihood from incomplete data via the EM Algorithm. J. Royal Stat. Soc. Ser. B 39: 1-38.
- Dent, R.C. 1997. Rainfall observations in the Loxahatchee River Watershed. Loxahatchee River District, Jupiter, Florida.
- Geweke, J.F. 1977. The dynamic factor analysis of economic time series models. p. 365-382. In D.J. Aigner, and A.S. Goldberger (eds.) Latent variables in socio-economic models. North-Holland: Amsterdam; 365–382.
- Harvey, A.C. 1989. Forecasting, structural time series models and the Kalman filter. Cambridge University Press: New York.
- Kaplan, D. R. Muñoz-Carpena, A. Mortl, Y.C. Li. 2007. Humedad y salinidad del suelo en un pantano de ciprés calvo (*Taxodium distichum*) impactado por intrusión de agua salina. In: J.V. Giráldez Cervera and F.J. Jiménez Hornero (eds.). Estudios de la Zona No Saturada del Suelo Vol. VIII. pp. 257-266. Cordoba (Spain). ISBN: 84-690-7893-8
- Knighton, A.D., K. Mills, and C.D. Woodroffe. 1991. Tidal creek extension and salt water intrusion in northern Australia. Geology 19: 831–834.
- Lütkepohl, H. 1991. Introduction to multiple time series analysis. Springer-Verlag: Berlin.
- Mitsch, W.J., and J.G. Gosselink. 2000. Wetlands. John Wiley & Sons, Inc. New York, New York.
- Molenaar, P. C.M. 1985. A dynamic factor model for the analysis of multivariate time series. Psychometrika 50, no. 2: 181–202.
- Mortl, A. 2006. Monitoring Soil Moisture and Soil Water Salinity in the Loxahatchee Floodplain. Masters Thesis. University of Florida.
- Muñoz-Carpena, R., A. Ritter, and Y.C. Li. 2005. Dynamic factor analysis of groundwater quality trends in an agricultural area adjacent to Everglades National Park. J. Contam. Hydrol. 80: 49-70.
- Muñoz-Carpena, R., D. Kaplan and F.J. Gonzalez. 2008. Groundwater Data Processing and Analysis for the Loxahatchee River Basin. Final Project Report to the South Florida Water Management District-Coastal Ecosystems Division, SFWMD Identifier:

4500020860. August 2008. University of Florida: Gainesville
- Nash, J.E., and J.V. Sutcliffe. 1970. River flow forecasting through conceptual models. Part 1- A discussion of Principles. *J. Hydrol.* 10: 282-290.
- R Development Core Team (2007). *R: A language and environment for statistical computing.* Statistical Computing, Vienna, Austria. ISBN 3-900051-07-0.
- Ritter, A. C.M. Regalado and R. Muñoz-Carpena. 2009. Temporal common trends of topsoil water dynamics in a humid subtropical forest watershed. *Vadose Zone J.* 8(2):437-449.
- Ritter, A., and R. Muñoz-Carpena. 2006. Dynamic factor modeling of ground and surface water levels in an agricultural area adjacent to Everglades National Park. *J. Hydrol.* 317: 340-354.
- Ritter, A., R. Muñoz-Carpena, D.D. Bosch, B.Schaffer, and T.L. Potter. 2007. Agricultural land use and hydrology affect variability of shallow groundwater nitrate concentration in South Florida. *Hydrol. Process.* 21: 2464-2473.
- Roberts, R E., M.Y. Hedgepeth and T.R. Alexander. Vegetational responses to saltwater intrusion along the Northwest Fork of the Loxahatchee River within Jonathan Dickinson State Park. *Florida Scientist.* 71(4): 383-397.
- Sbarra, David A, and Emilio Ferrer. 2006. The structure and process of emotional experience following nonmarital relationship dissolution: dynamic factor analyses of love, anger, and sadness. *Emotion (Washington, D.C.)* 6, no. 2 (May): 224-238.
- SFWMD. 2002. Technical Criteria to Support Development of Minimum Flow and Levels for the Loxahatchee River and Estuary. Water Supply Department, Water Resources Management, South Florida Water Management District, West Palm Beach, Florida, November 2002 final draft.
- SFWMD. 2005. Draft Evaluation of Restoration Alternatives for the Northwest Fork of the Loxahatchee River. Coastal Ecosystems Division, South Florida Water Management District, West Palm Beach, Florida, March 2005, draft.
- Shumway, R.H., and D.S. Stoffer. 1982. An approach to time series smoothing and forecasting using the EM algorithm. *J. Time Ser. Anal.* 3: 253-264.
- South Florida Water Management District (SFWMD). 2006. Evaluation of Restoration Alternatives for the Norwest Fork of the Loxahatchee River. Palm Beach, Florida.
- Treasure Coast Regional Planning Council (TCRPC), 1995. Strategic Regional Policy Plan for the Treasure Coast Region. Rule 29K-5.002, Florida Administrative Code. Stuart, FL. 422 p.

- Tulp, Ingrid, Loes J. Bolle, and Adriaan D. Rijnsdorp. 2008. Signals from the shallows: In search of common patterns in long-term trends in Dutch estuarine and coastal fish. *Journal of Sea Research* 60, no. 1-2: 54-73.
- U.S. Geological Survey (USGS), 2001. Sea-level and Climate. USGS Fact Sheet 002-00. <http://pubs.usgs.gov/fs/fs2-00/>.
- Wanless, H.R., Parkinson, R.W., and Tedesco, L.P., 1994, Sea level control on stability of Everglades wetlands, in Davis, S.M., and Ogden, J. C., editors, *Everglades: the ecosystem and its restoration*: Delray Beach, Florida, St. Lucie Press, p. 199-224
- Wu, L.S.-Y., J.S. Pai, and J.R.M. Hosking. 1996. An algorithm for estimating parameters of state-space models. *Stat. Prob. Letters* 28: 99–106.
- Zuur, A.F., and G.J. Pierce. 2004. Common trends in Northeast Atlantic squid time series. *J. Sea Res.* 52: 57-72.
- Zuur, A.F., E.N. Ieno, and G.M. Smith. 2007. *Analysing Ecological Data*. Springer. 680 p.
- Zuur, A.F., R.J. Fryer, I.T. Jolliffe, R. Dekker, and J.J. Beukema. 2003b. Estimating common trends in multivariate time series using dynamic factor analysis. *Environmetrics* 14: 665-685.
- Zuur, A.F., Tuck, I.D., Bailey, N., 2003a. Dynamic factor analysis to estimate common trends in fisheries time series. *Can. J. Fish. Aquat. Sci.* 60, 542–552.

LIST OF APPENDICES

Appendix I. Daily Time Series Graphs

Appendix III-A – Daily time series of Water Table Elevation (ft, NAVD88)

Appendix III-B – Daily time series of groundwater temperature (°C)

Appendix III-C – Daily time series of groundwater EC (S/m)

Appendix II. Global and Wet/Dry Season Statistics Tables

Appendix IV-A – Global Statistics

Appendix IV-B – Wet/Dry Season Statistics

Appendix I. Daily Time Series Graphs

Timelines of average daily water table elevation, water table depth (below benchmark), temperature, and EC are given below. Figures 1 – 12 show average daily water table elevation (in ft, NAVD88); figures 13 – 24 show average daily water table depth below benchmark (in feet); figures 25 – 36 show average daily groundwater temperature (in degrees Celsius); and figures 37 – 48 show average daily EC (in S/m). **Note: scale on y-axis of individual daily time series graphs is variable.**

Appendix I-A – Daily time series of Water Table Elevation (ft, NAVD88)

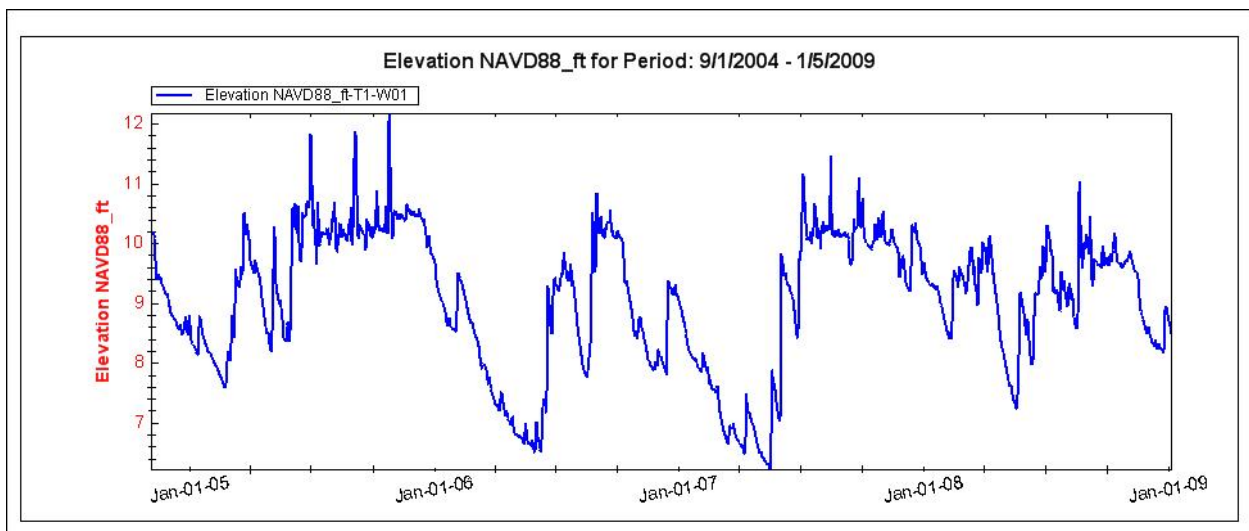


Figure 1. Average daily water table elevation at well 1 on Transect 1.

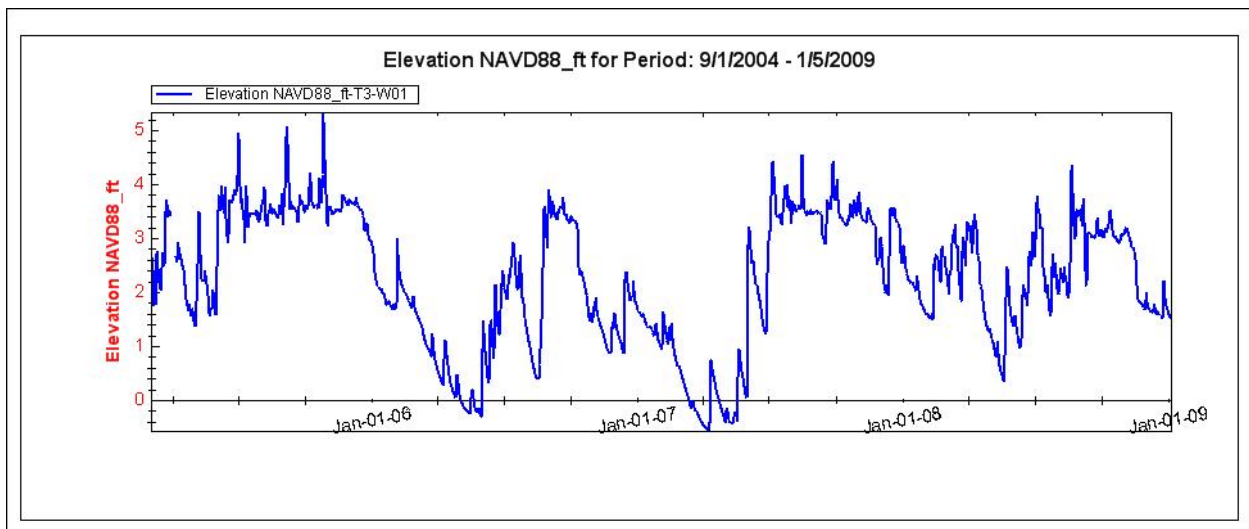


Figure 2. Average daily water table elevation at well 1 on Transect 3.

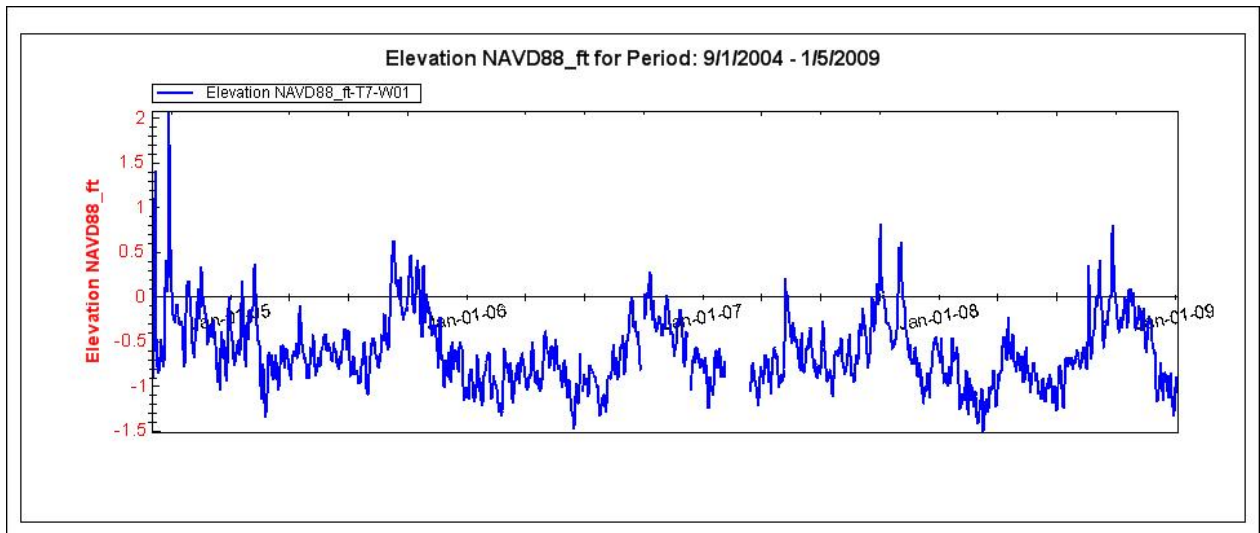


Figure 3. Average daily water table elevation at well 1 on Transect 7.

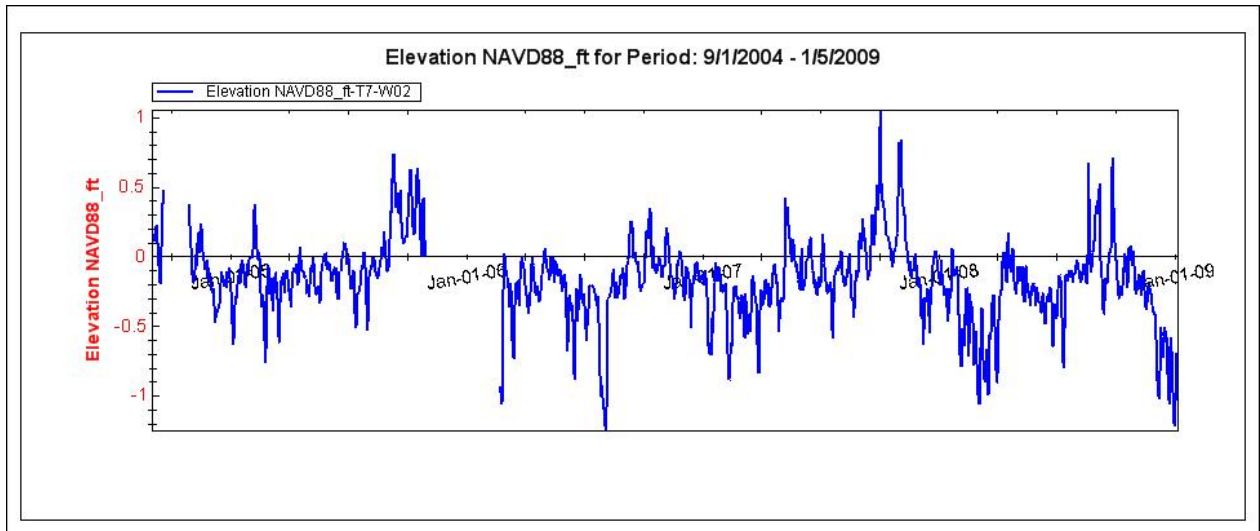


Figure 4. Average daily water table elevation at well 2 on Transect 7.

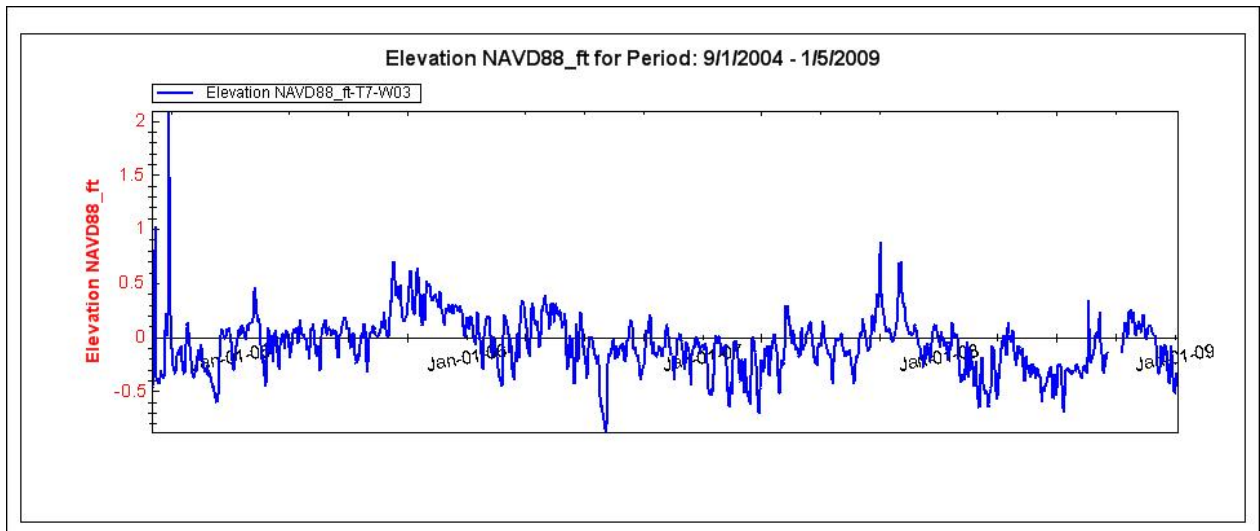


Figure 5. Average daily water table elevation at well 3 on Transect 7.

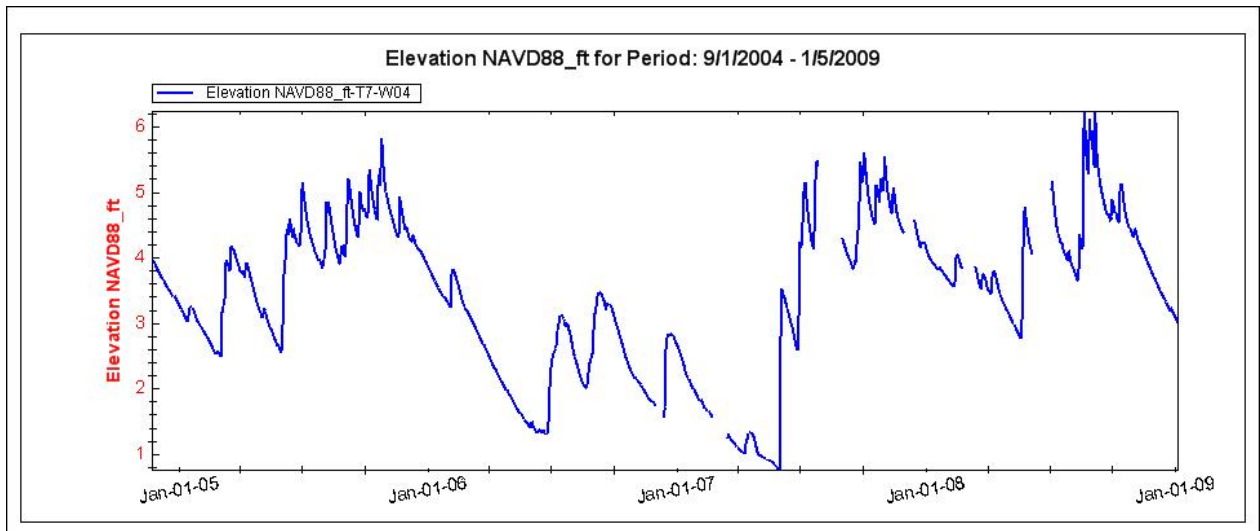


Figure 6. Average daily water table elevation at well 4 on Transect 7.

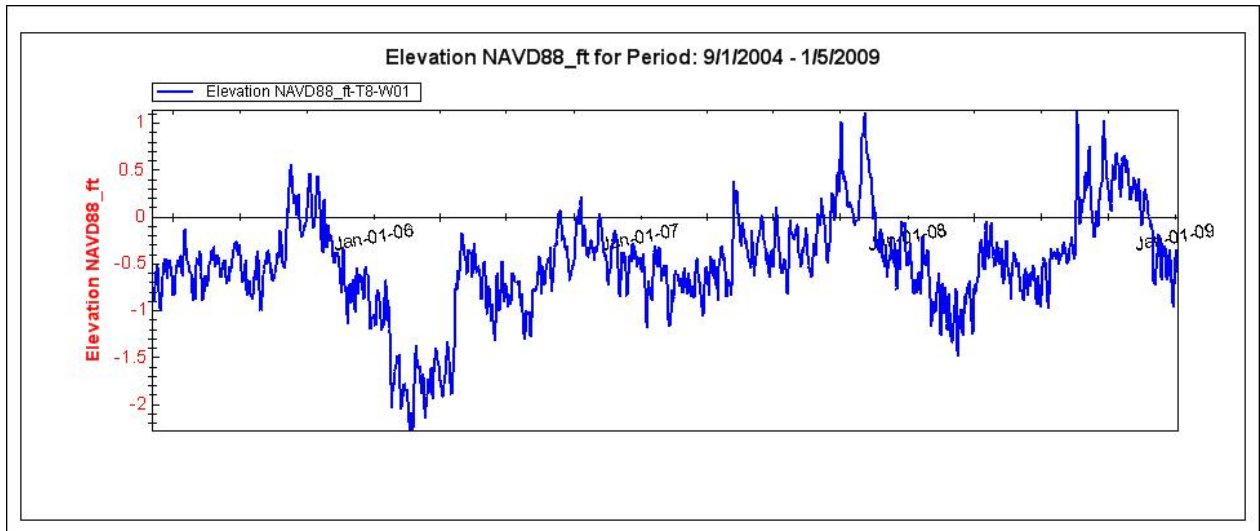


Figure 7. Average daily water table elevation at well 1 on Transect 8.

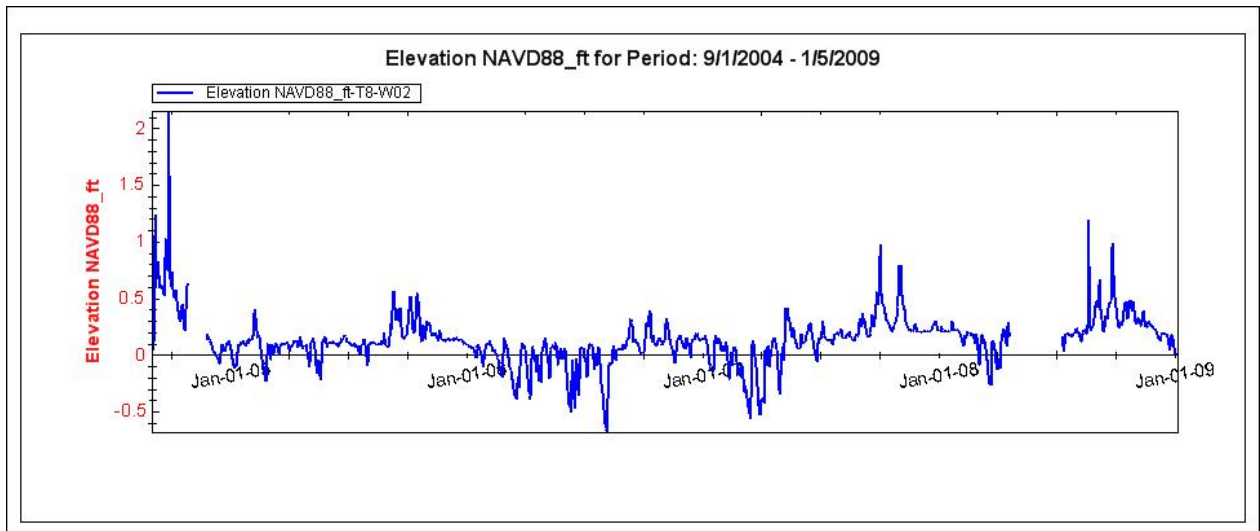


Figure 8. Average daily water table elevation at well 2 on Transect 8.

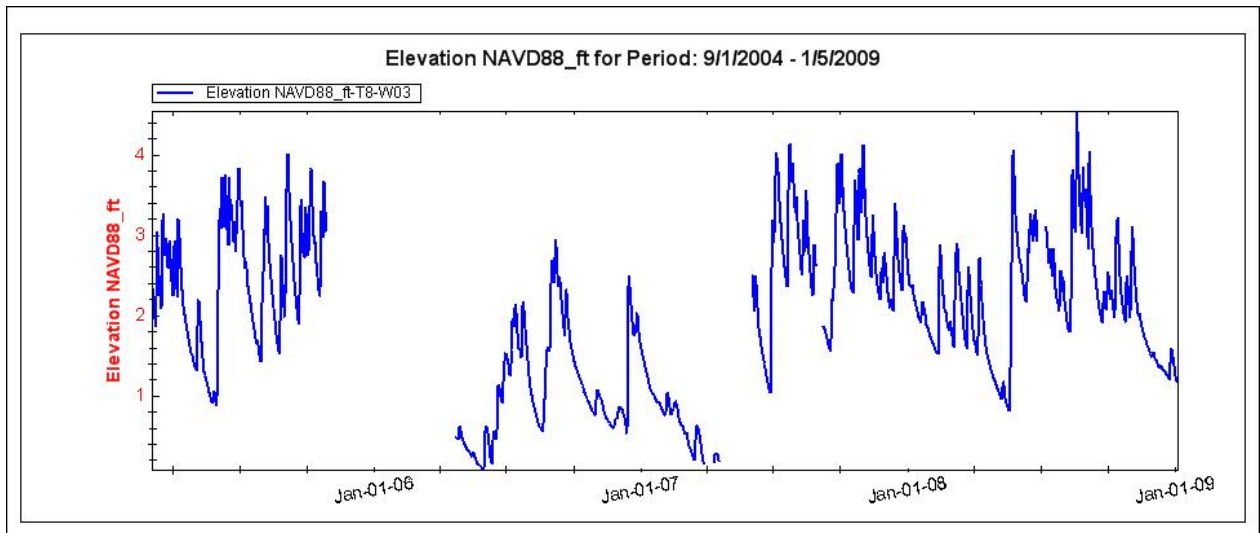


Figure 9. Average daily water table elevation at well 3 on Transect 8.

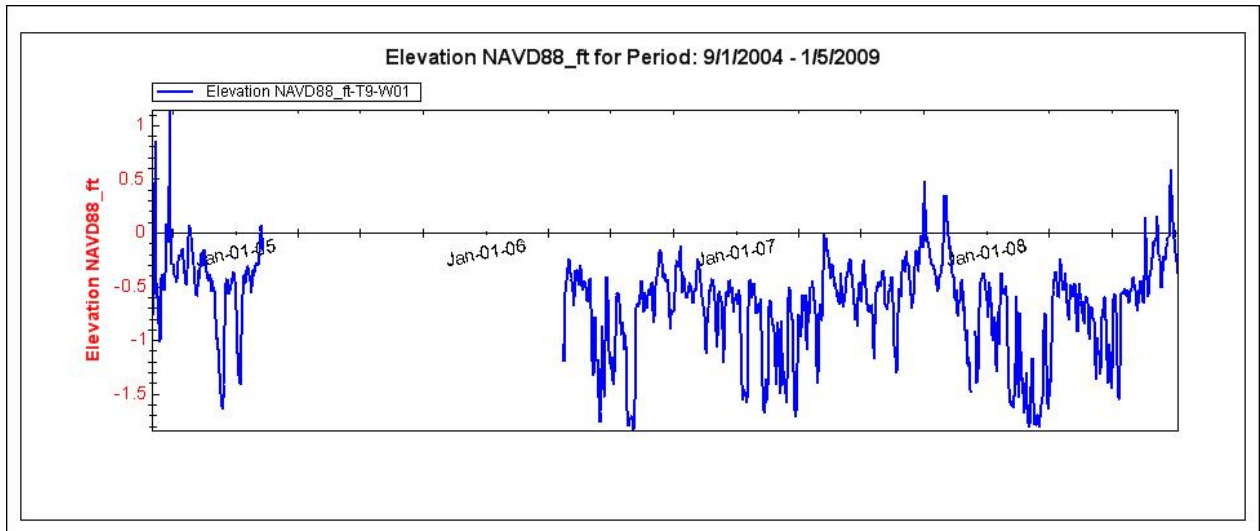


Figure 10. Average daily water table elevation at well 1 on Transect 9.

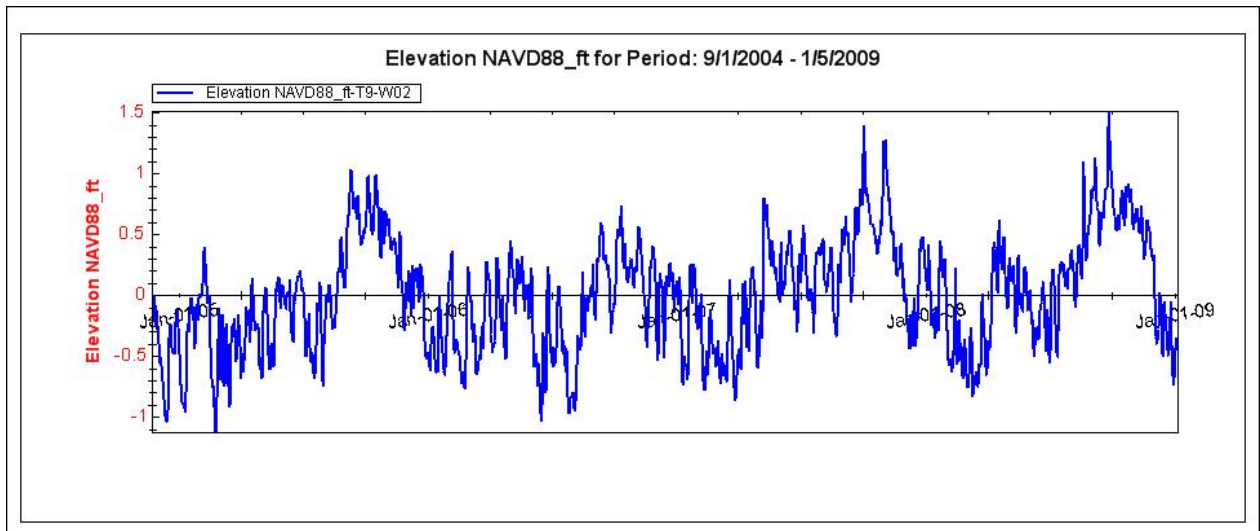


Figure 11. Average daily water table elevation at well 2 on Transect 9.

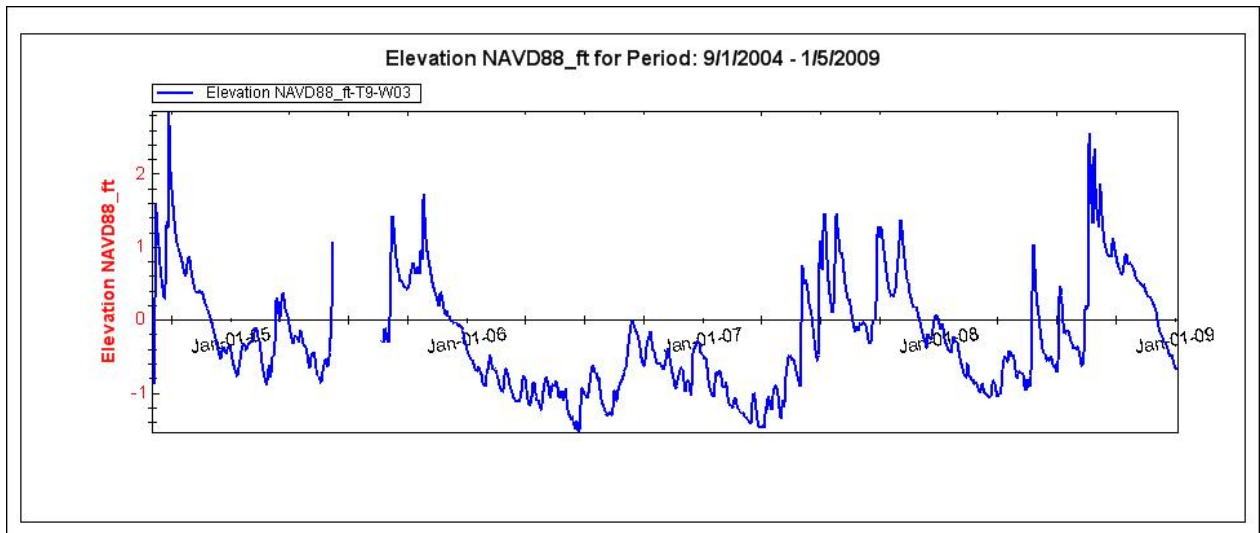


Figure 12. Average daily water table elevation at well 3 on Transect 9.

Appendix I-B – Daily time series of groundwater temperature (°C)

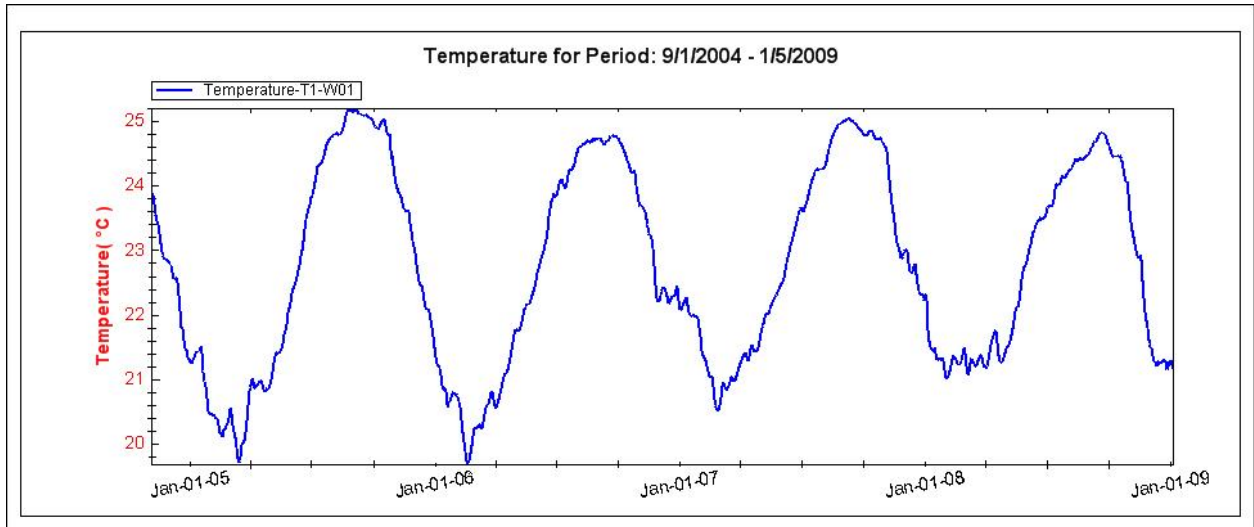


Figure 13. Average daily groundwater temperature at well 1 on Transect 1.

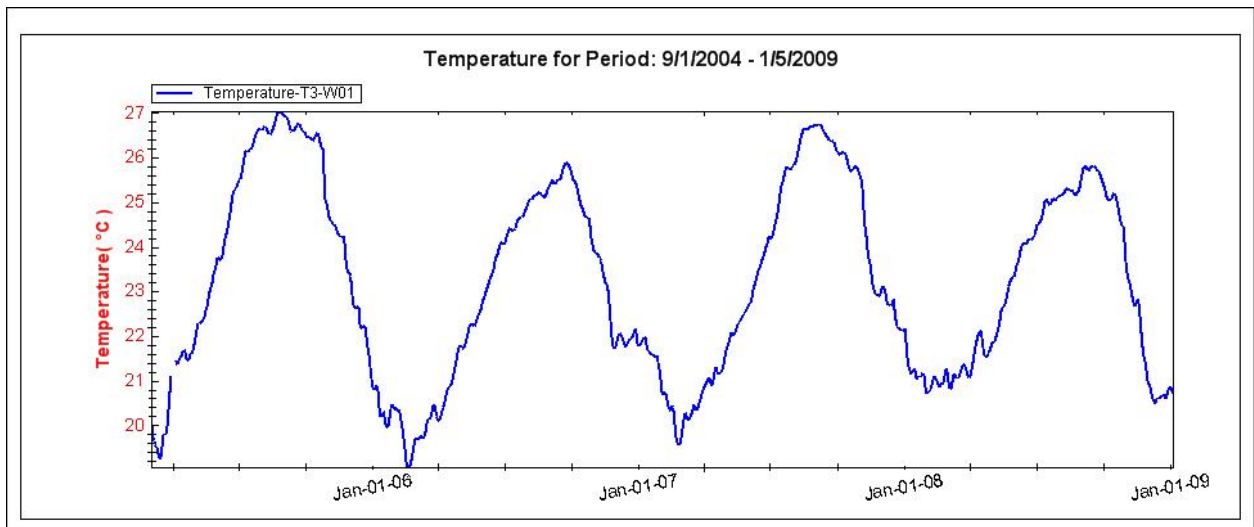


Figure 14. Average daily groundwater temperature at well 1 on Transect 3.

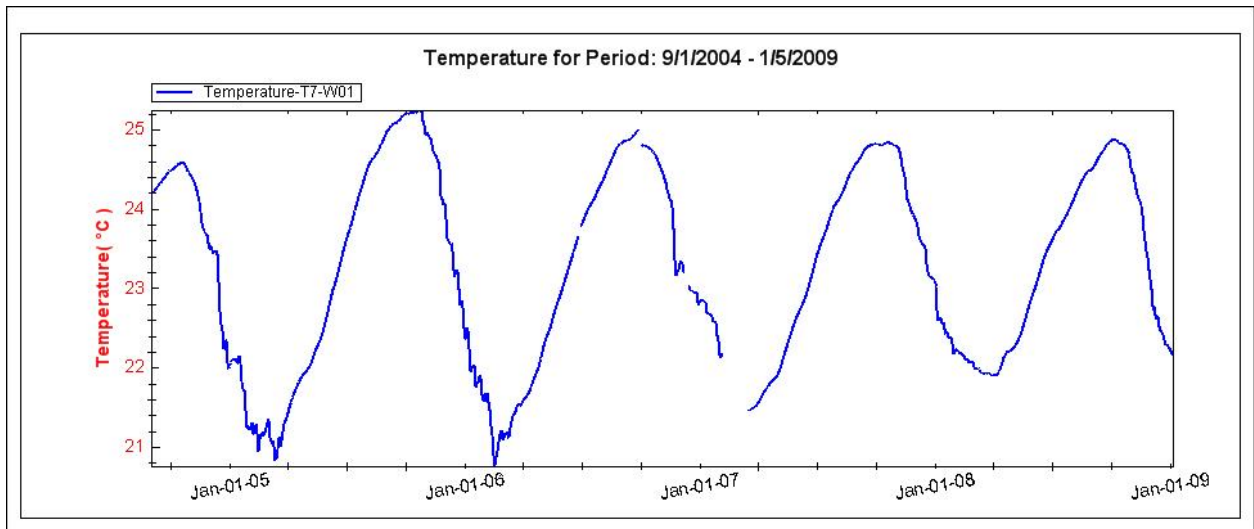


Figure 15. Average daily groundwater temperature at well 1 on Transect 7.

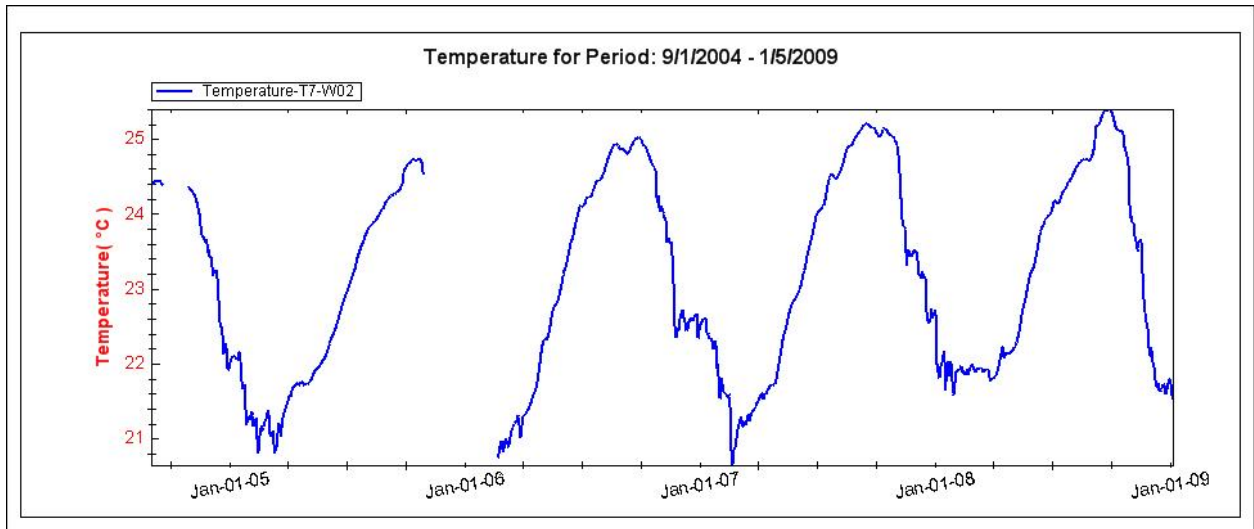


Figure 16. Average daily groundwater temperature at well 2 on Transect 7.

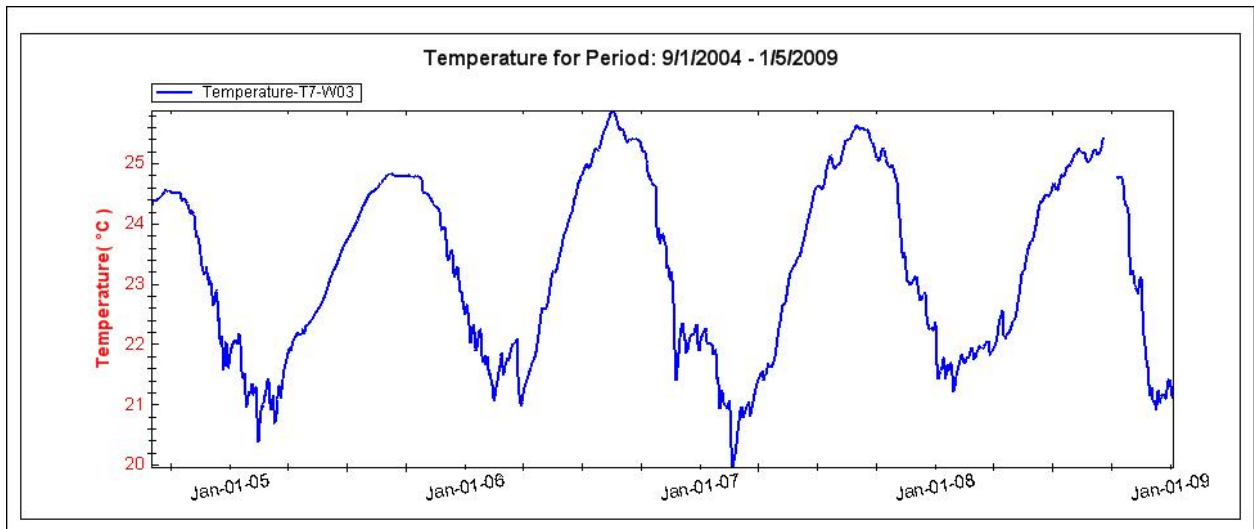


Figure 17. Average daily groundwater temperature at well 3 on Transect 7.

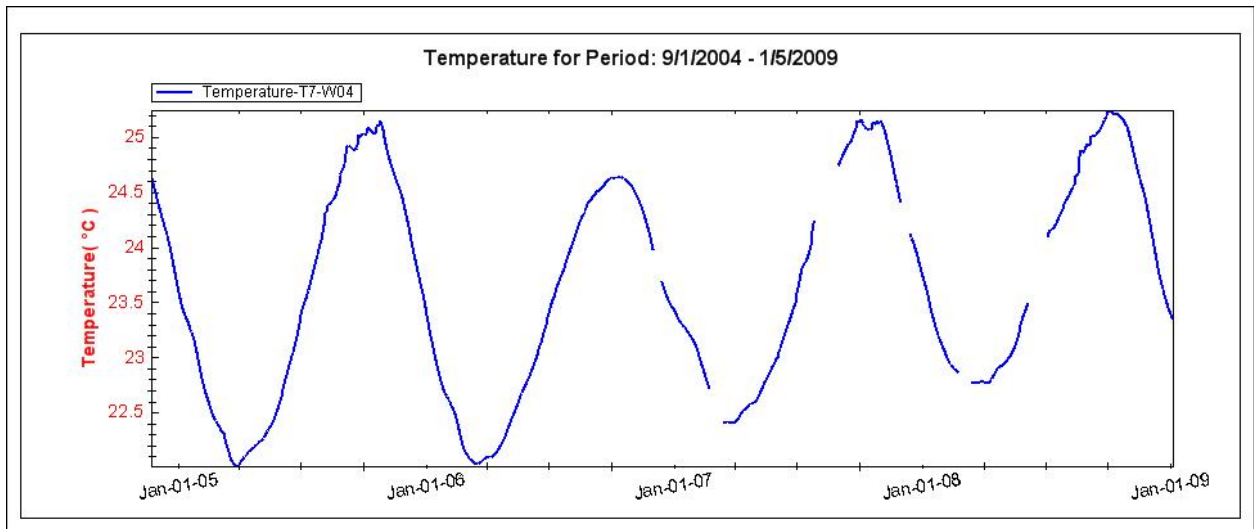


Figure 18. Average daily groundwater temperature at well 4 on Transect 7.

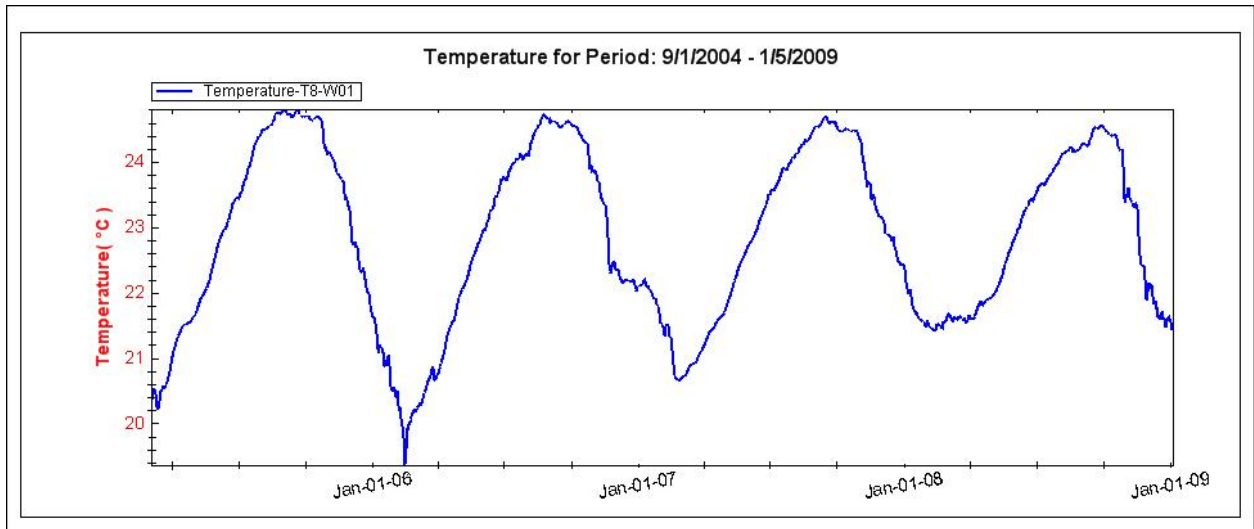


Figure 19. Average daily groundwater temperature at well 1 on Transect 8.

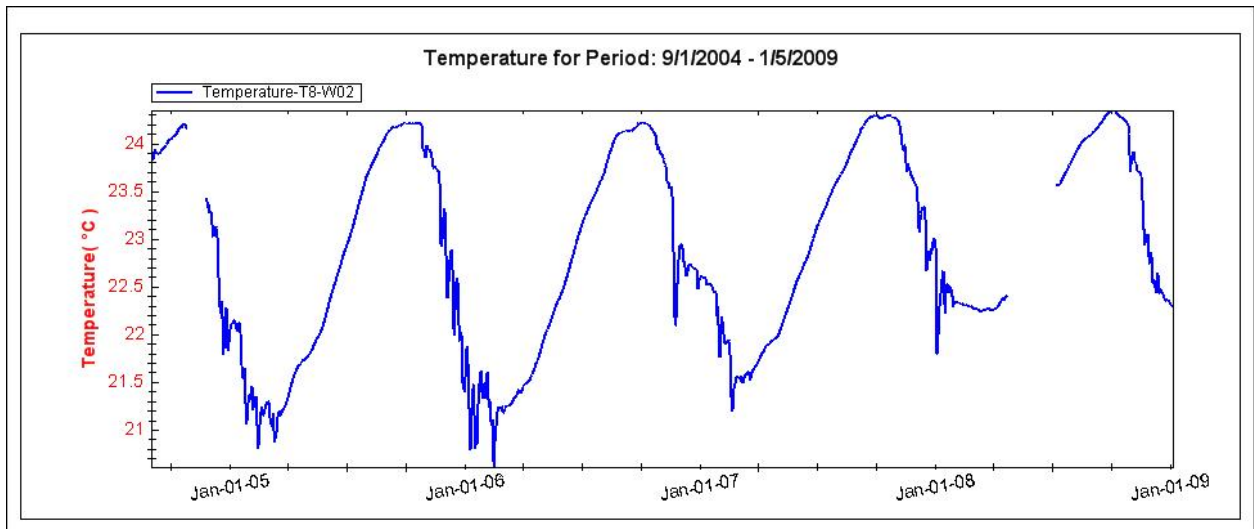


Figure 20. Average daily groundwater temperature at well 2 on Transect 8.

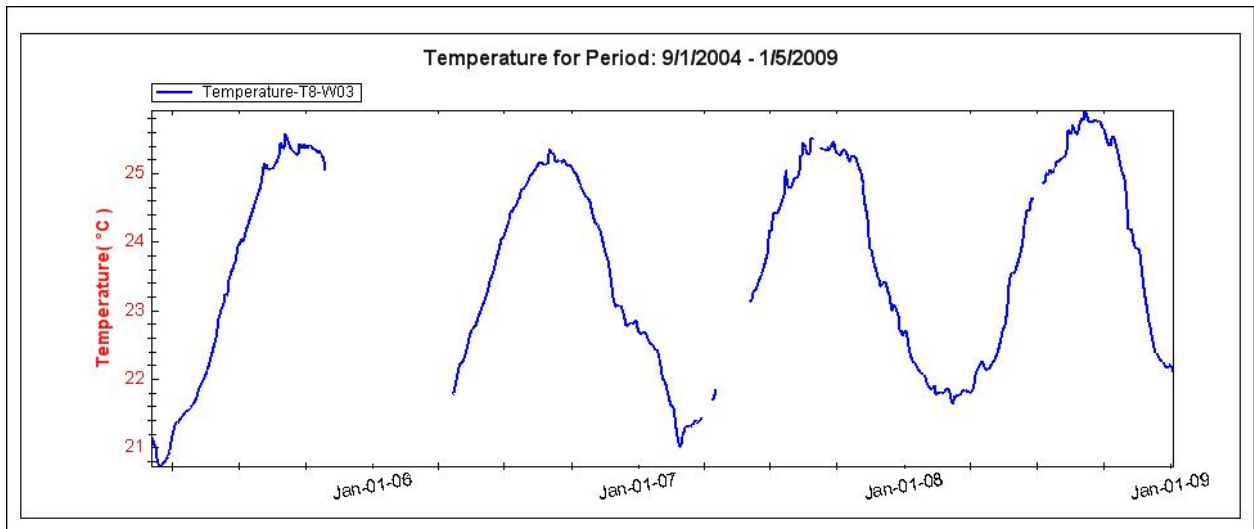


Figure 21. Average daily groundwater temperature at well 3 on Transect 8.

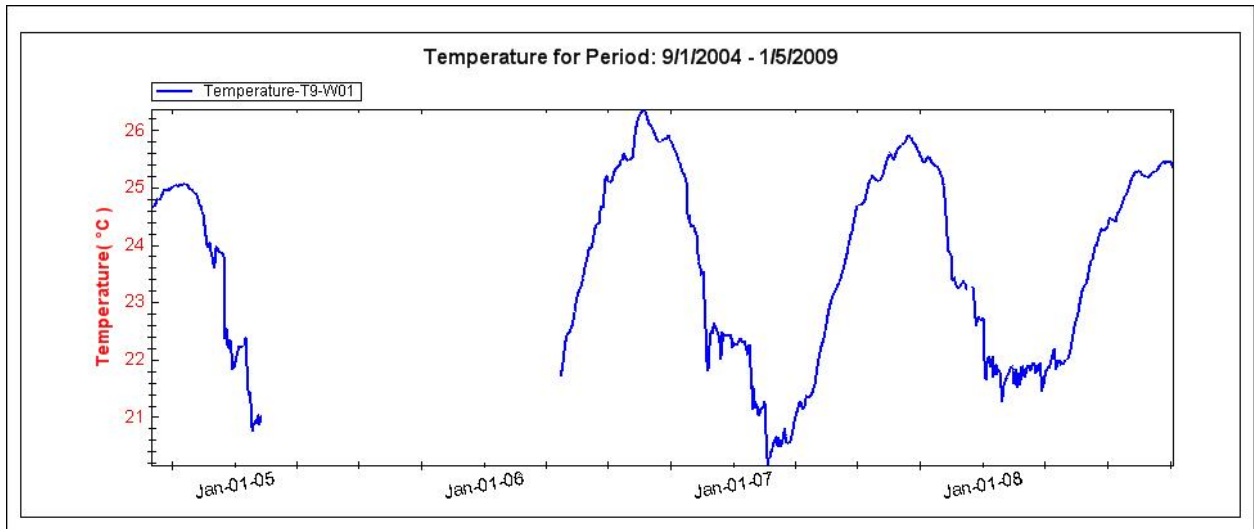


Figure 22. Average daily groundwater temperature at well 1 on Transect 9.

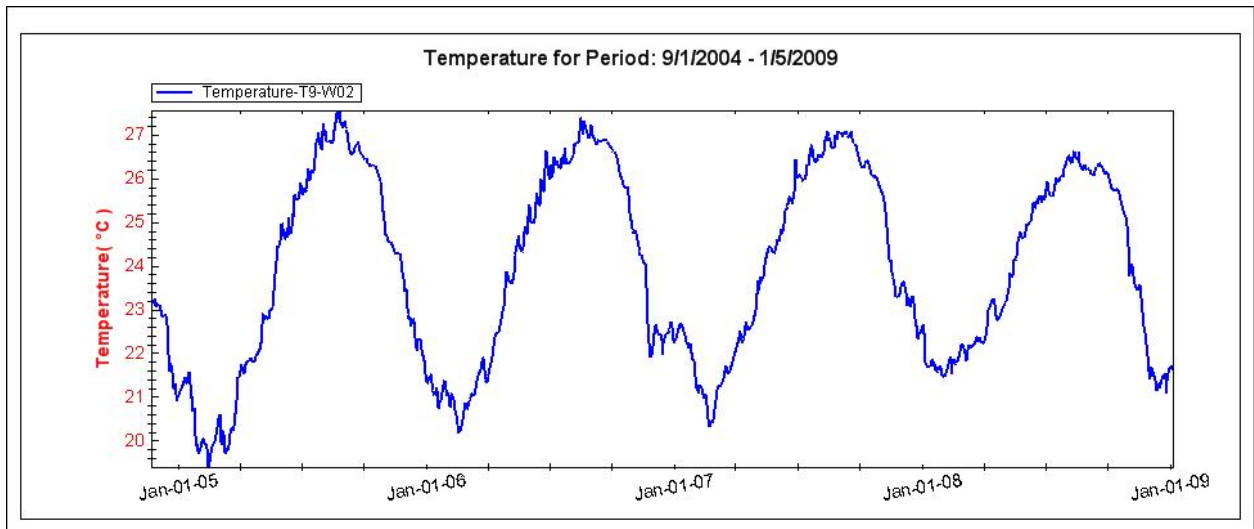


Figure 23. Average daily groundwater temperature at well 2 on Transect 9.

Appendix I-C – Daily time series of groundwater EC (S/m)

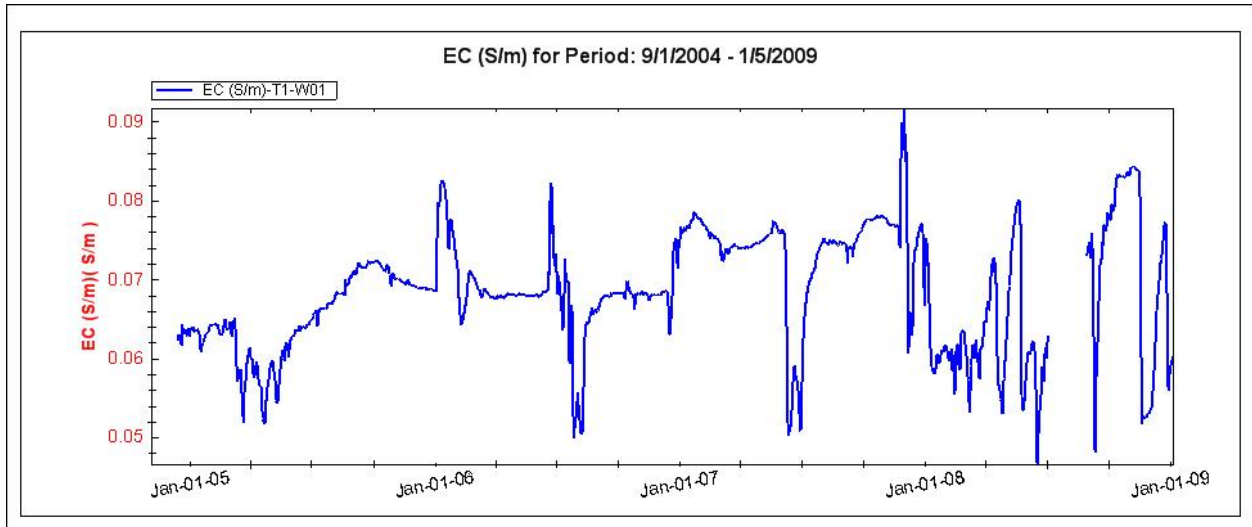


Figure 25. Average daily groundwater EC at well 1 on Transect 1.

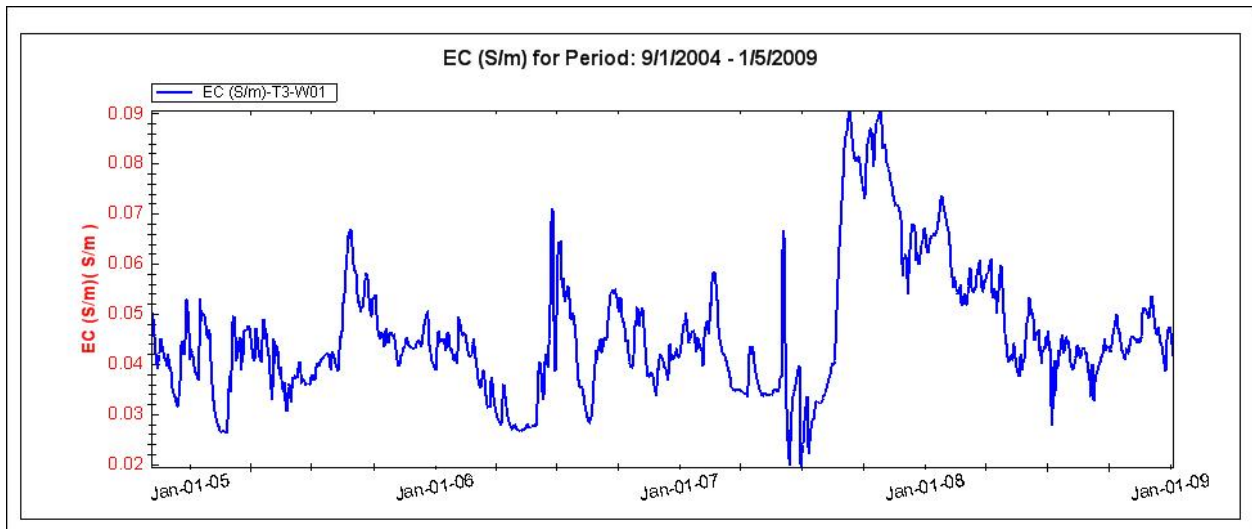


Figure 26. Average daily groundwater EC at well 1 on Transect 3.

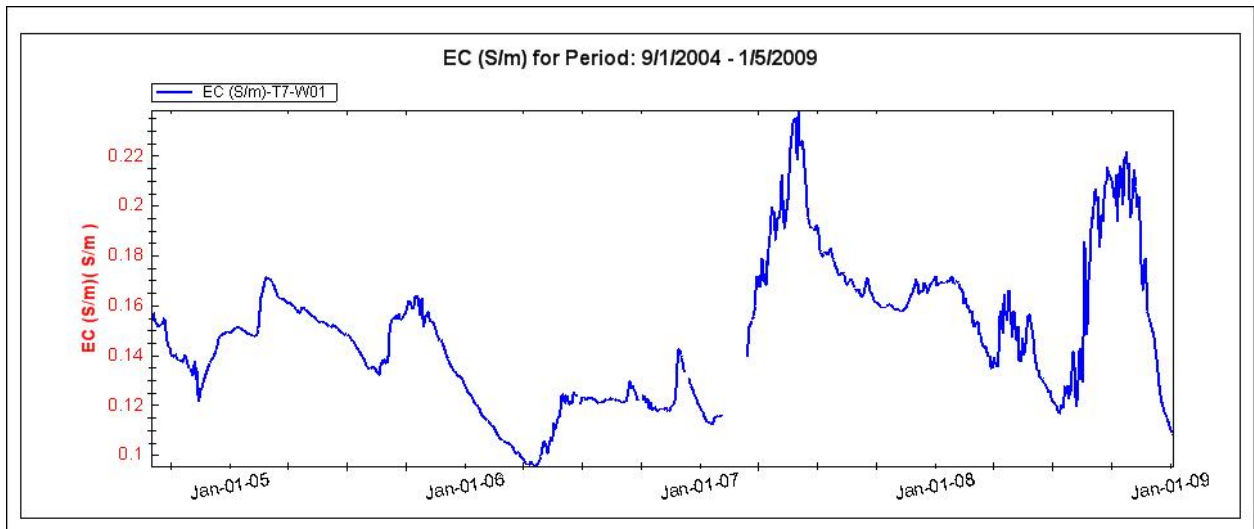


Figure 27. Average daily groundwater EC at well 1 on Transect 7.

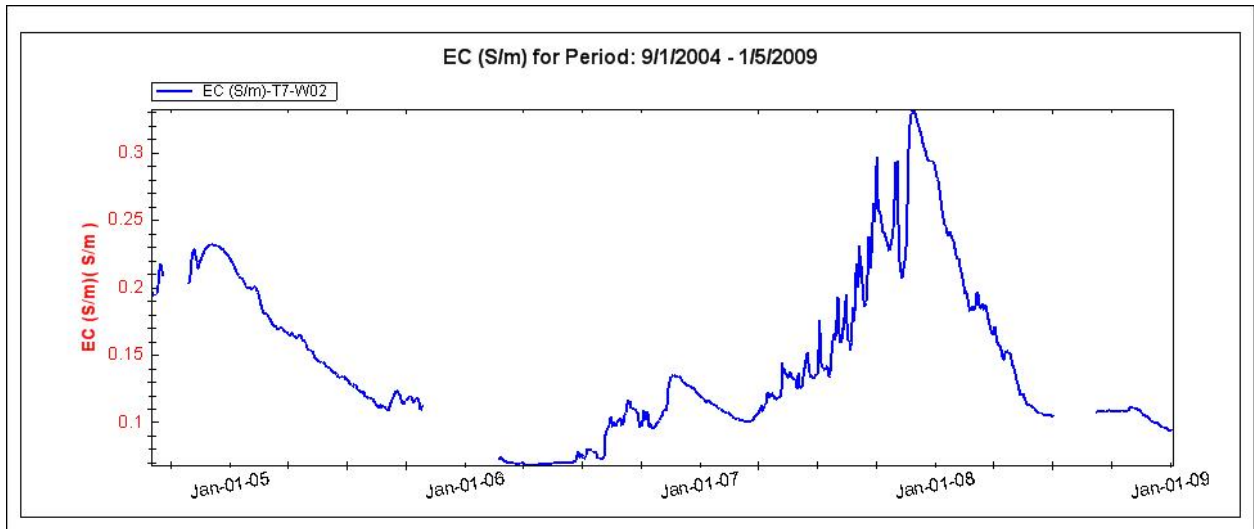


Figure 28. Average daily groundwater EC at well 2 on Transect 7.

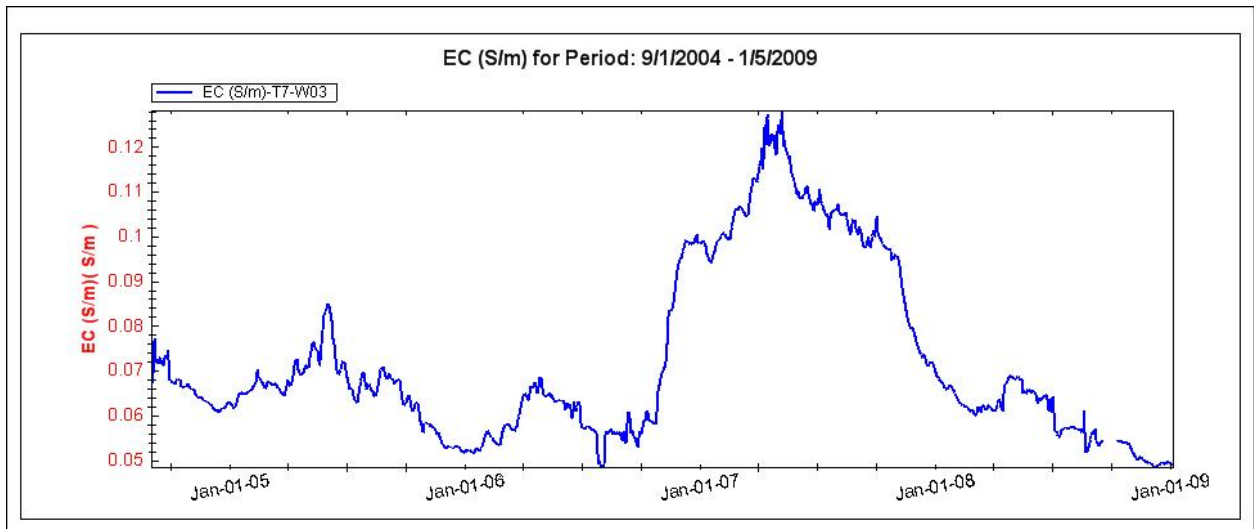


Figure 29. Average daily groundwater EC at well 3 on Transect 7.

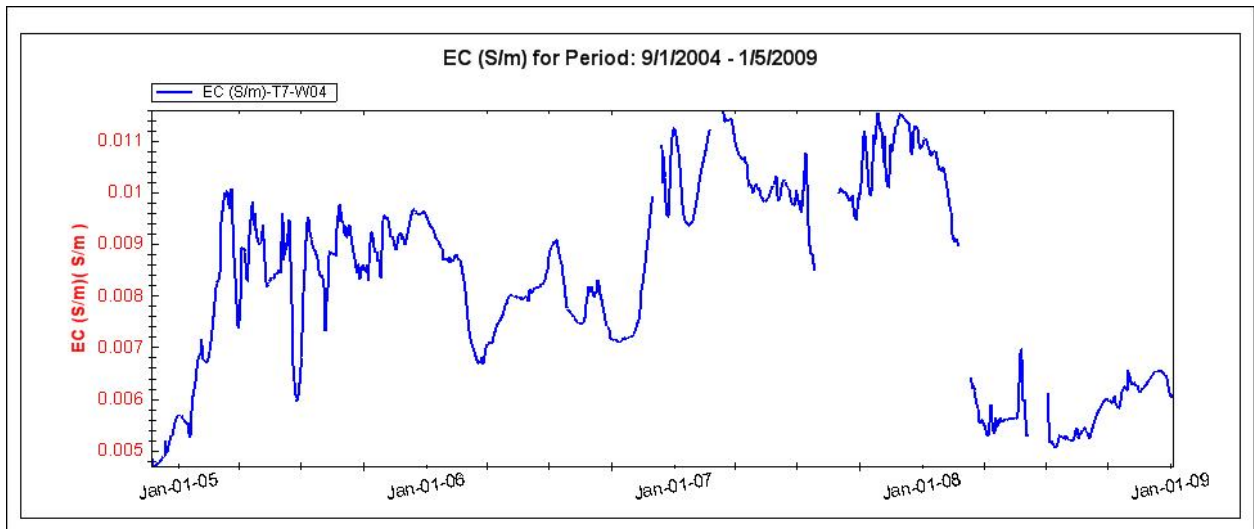


Figure 30. Average daily groundwater EC at well 4 on Transect 7.

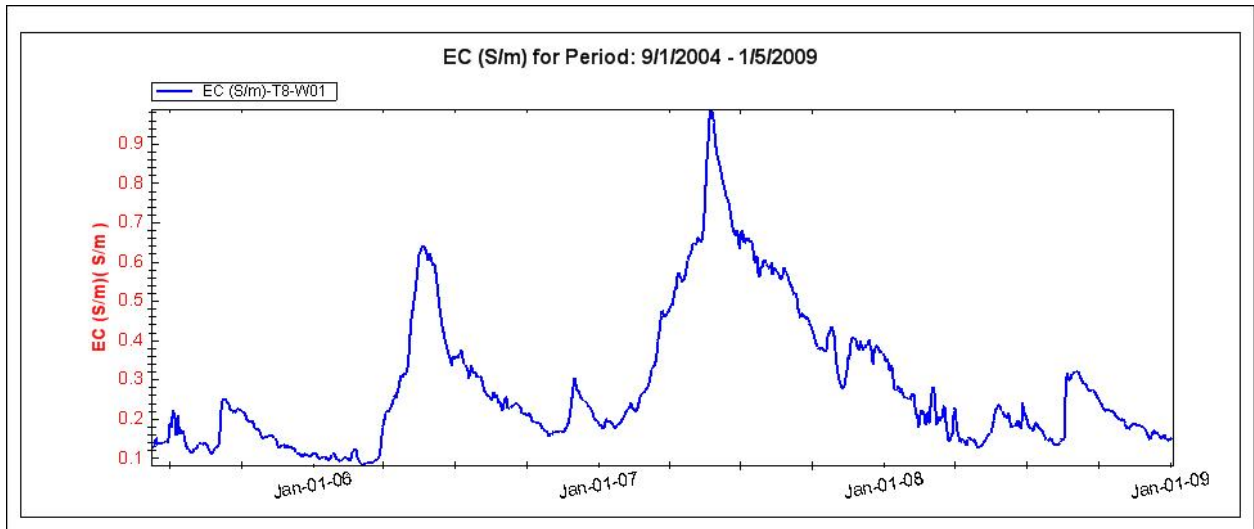


Figure 31. Average daily groundwater EC at well 1 on Transect 8.

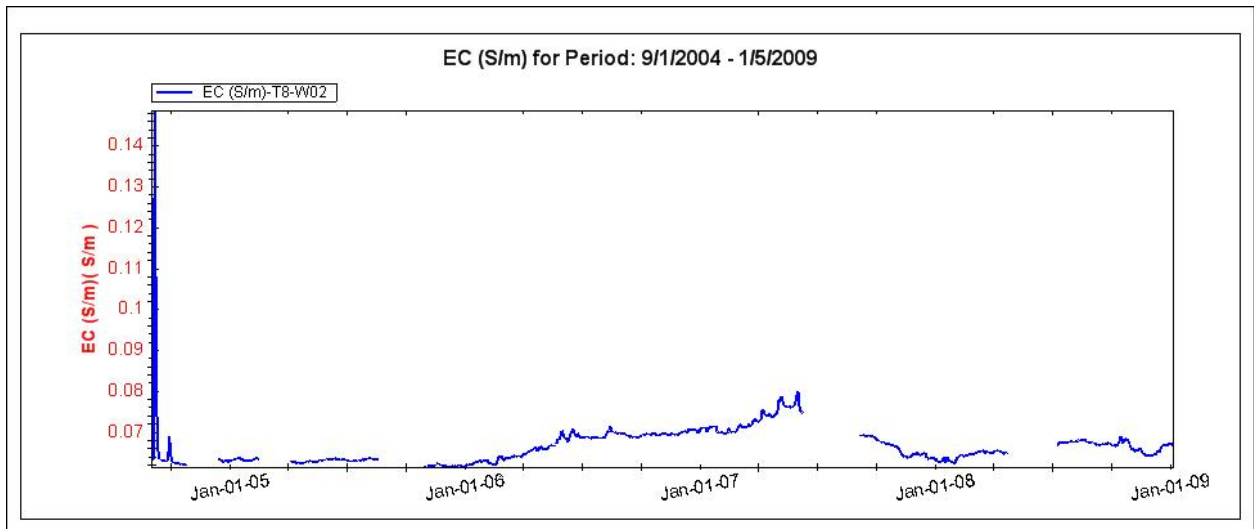


Figure 32. Average daily groundwater EC at well 2 on Transect 8.

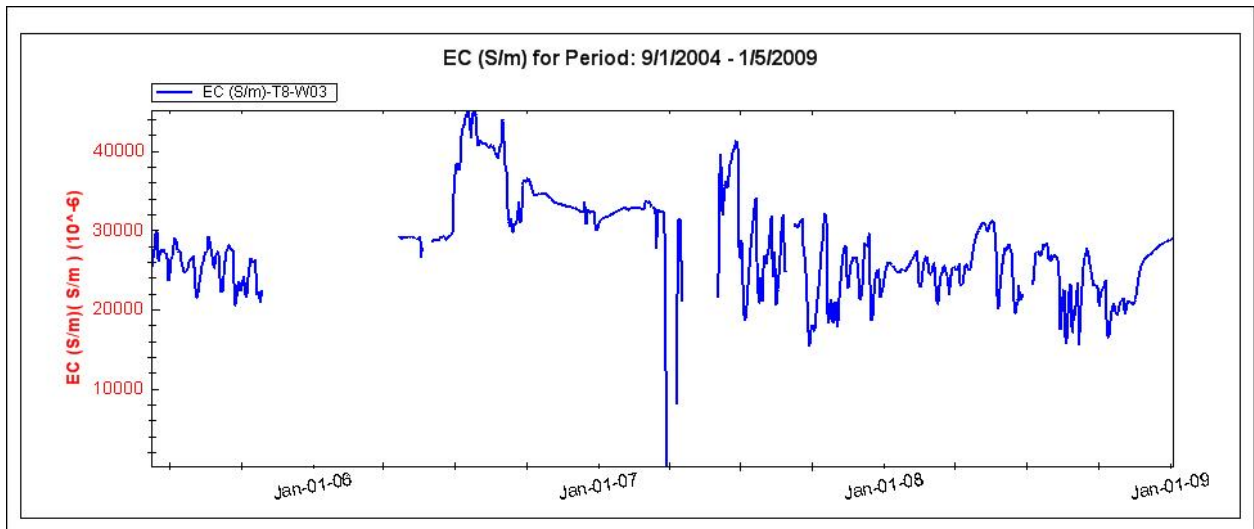


Figure 33. Average daily groundwater EC at well 3 on Transect 8.

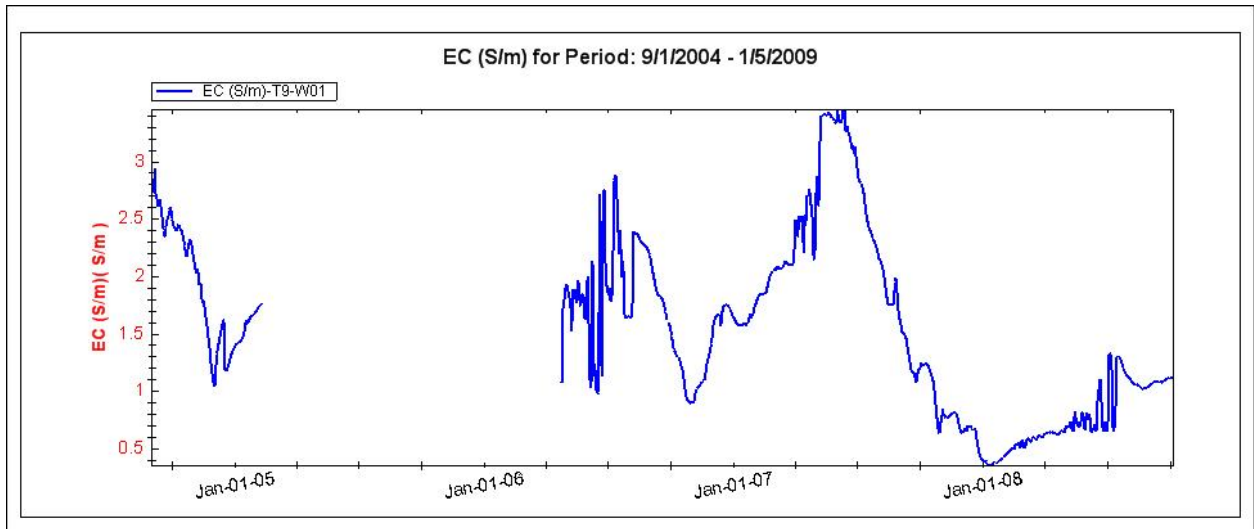


Figure 34. Average daily groundwater EC at well 1 on Transect 9.

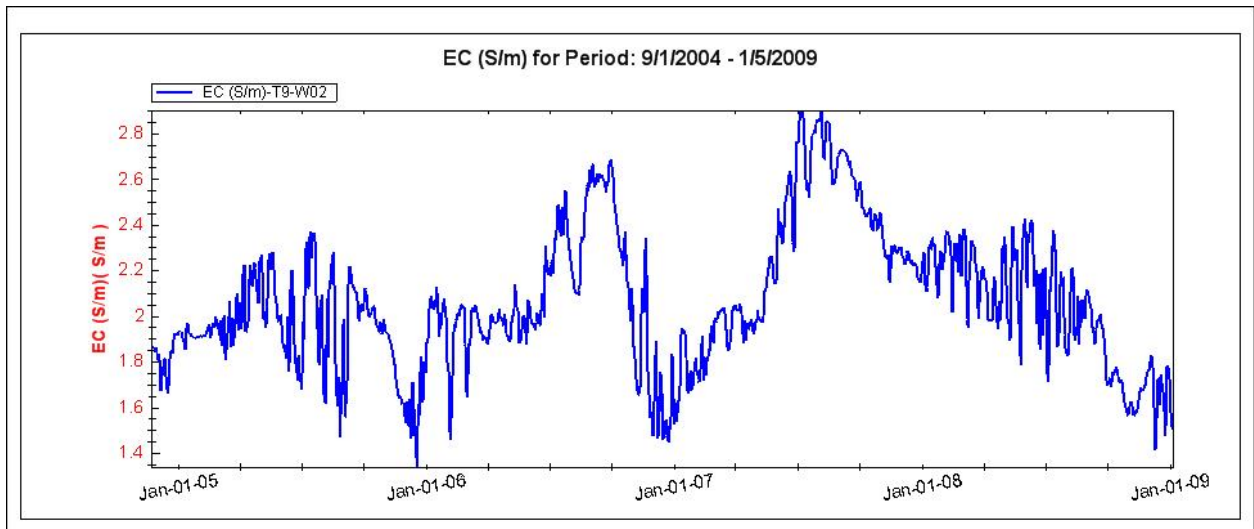


Figure 35. Average daily groundwater EC at well 2 on Transect 9.

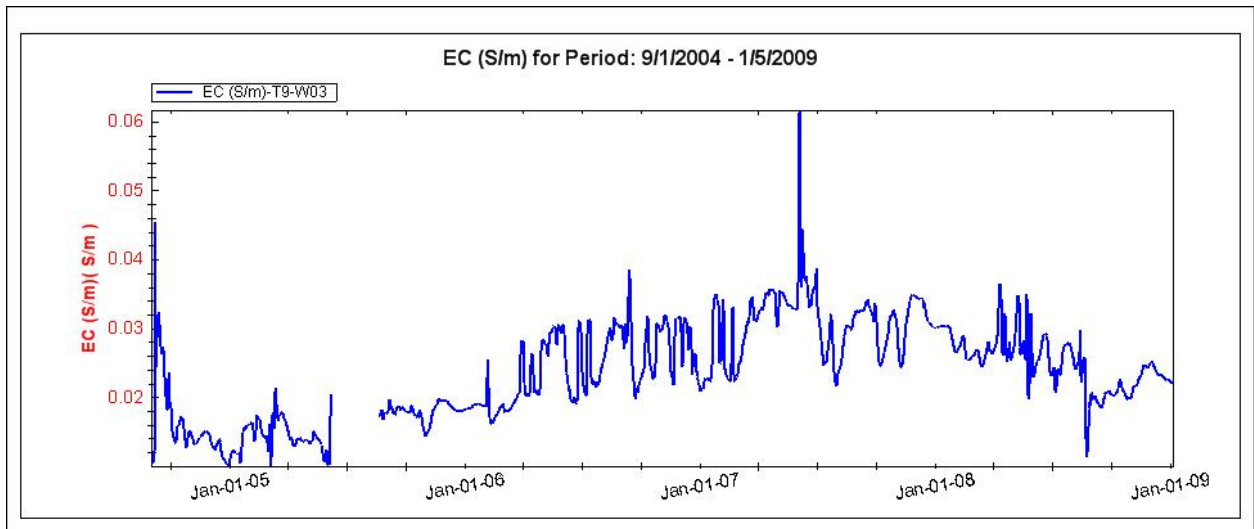


Figure 36. Average daily groundwater EC at well 3 on Transect 9.

Appendix II. Global and Wet/Dry Season Statistics Tables

Summary statistics, including global and wet/dry season means, minima, maxima, variances, and standard deviations are given in tables 1 – 3. Wet and dry season statistics were calculated from monthly data.

Appendix II-A: Global Statistics

Table 1. Global statistics by station over period of record.

T1-W01		Min	Max	Mean	Variance	Std
	WTE (ft, NAVD88)	6.073	12.463	9.063	1.300	1.140
	Temperature (°C)	19.661	25.217	22.739	2.377	1.542
	EC (S/m)	0.045	0.092	0.068	0.000	0.008
T3-W01						
	WTE (ft, NAVD88)	-0.604	5.482	2.272	1.480	1.216
	Temperature (°C)	19.056	27.056	23.236	4.721	2.173
	EC (S/m)	0.017	0.091	0.046	0.000	0.013
T7-W01						
	WTE (ft, NAVD88)	-1.995	2.476	-0.613	0.264	0.514
	Temperature (°C)	20.622	25.283	23.282	1.510	1.229
	EC (S/m)	0.094	0.251	0.148	0.001	0.029
T7-W02						
	WTE (ft, NAVD88)	-1.411	2.182	-0.169	0.147	0.383
	Temperature (°C)	20.306	25.540	23.139	1.769	1.330
	EC (S/m)	0.068	0.348	0.145	0.004	0.060
T7-W03						
	WTE (ft, NAVD88)	-0.987	2.677	-0.062	0.099	0.315
	Temperature (°C)	19.922	26.006	23.246	2.190	1.480
	EC (S/m)	0.048	0.139	0.072	0.000	0.019
T7-W04						
	WTE (ft, NAVD88)	0.761	6.963	3.423	1.334	1.155
	Temperature (°C)	22.011	25.260	23.635	0.935	0.967
	EC (S/m)	0.005	0.012	0.008	0.000	0.002
T8-W01						
	WTE (ft, NAVD88)	-2.871	2.214	-0.504	0.434	0.659
	Temperature (°C)	19.200	25.172	22.856	1.838	1.356
	EC (S/m)	0.077	1.012	0.287	0.032	0.178
T8-W02						
	WTE (ft, NAVD88)	-0.760	2.673	0.136	0.067	0.259
	Temperature (°C)	20.461	24.422	22.885	1.056	1.028
	EC (S/m)	0.061	0.188	0.067	0.000	0.005
T8-W03						
	WTE (ft, NAVD88)	0.068	4.970	1.974	0.916	0.957
	Temperature (°C)	20.717	26.020	23.638	2.100	1.449
	EC (S/m)	0.000	0.046	0.028	0.000	0.006
T9-W01						
	WTE (ft, NAVD88)	-1.999	2.462	-0.667	0.243	0.493
	Temperature (°C)	20.05	26.600	23.622	2.725	1.651
	EC (S/m)	0.355	3.733	1.556	0.594	0.771

T9-W02						
	WTE (ft, NAVD88)	-1.547	2.634	-0.004	0.277	0.526
	Temperature (°C)	18.589	28.111	23.908	4.840	2.200
	EC (S/m)	1.246	2.931	2.066	0.099	0.315
T9-W03						
	WTE (ft, NAVD88)	-1.551	3.186	-0.234	0.546	0.739
	Temperature (°C)	22.633	25.683	24.371	0.530	0.728
	EC (S/m)	0.009	0.077	0.024	0.000	0.007

Appendix II-B: Wet/Dry Season Statistics

Table 2. Water table elevation (ft, NAVD88) wet/dry season statistics.

T1W1	Min	Max	Mean	Variance	Std
11/04 - 4/05 (Dry)	7.563	10.605	8.838	0.401	0.633
5/05 - 10/05 (Wet)	8.141	12.463	10.104	0.391	0.625
11/05 - 4/06 (Dry)	6.759	10.734	8.970	1.631	1.277
5/06 - 10/06 (Wet)	6.338	10.918	8.702	1.595	1.263
11/06 - 4/07 (Dry)	6.368	9.575	7.798	0.603	0.777
5/07 - 10/07 (Wet)	6.073	11.653	9.476	1.877	1.370
11/07 - 4/08 (Dry)	8.048	10.577	9.465	0.123	0.351
5/08 - 10/08 (Wet)	7.126	11.291	9.226	0.440	0.663
11/08 - 1/09 (Dry)*	8.150	9.953	8.758	0.173	0.416
Overall Dry**	6.368	10.734	8.766	0.884	0.940
Overall Wet**	6.073	12.463	9.377	1.201	1.096

T3W1	Min	Max	Mean	Variance	Std
11/04 - 4/05 (Dry)	1.369	3.770	2.438	0.134	0.366
5/05 - 10/05 (Wet)	1.311	5.482	3.397	0.433	0.658
11/05 - 4/06 (Dry)	-0.011	3.828	2.101	1.534	1.239
5/06 - 10/06 (Wet)	-0.358	3.993	1.802	1.480	1.217
11/06 - 4/07 (Dry)	-0.604	3.256	0.891	0.556	0.745
5/07 - 10/07 (Wet)	-0.476	4.710	2.722	2.114	1.454
11/07 - 4/08 (Dry)	1.180	3.909	2.573	0.191	0.438
5/08 - 10/08 (Wet)	0.302	4.440	1.121	2.252	1.501
11/08 - 1/09 (Dry)*	1.500	3.306	1.920	0.218	0.466
Overall Dry**	-0.604	3.909	1.914	0.983	0.991
Overall Wet**	-0.476	5.482	2.589	1.343	1.159

T7W1	Min	Max	Mean	Variance	Std
9/04 - 10/04 (Wet)*	-1.417	2.476	-0.171	0.003	0.055
11/04 - 4/05 (Dry)	-1.826	1.327	-0.534	0.030	0.172
5/05 - 10/05 (Wet)	-1.597	1.333	-0.416	0.135	0.368
11/05 - 4/06 (Dry)	-1.821	0.811	-0.817	0.032	0.179
5/06 - 10/06 (Wet)	-1.995	1.292	-0.693	0.124	0.352
11/06 - 4/07 (Dry)	-1.669	1.171	-0.734	0.051	0.225
5/07 - 10/07 (Wet)	-1.538	1.589	-0.505	0.057	0.238
11/07 - 4/08 (Dry)	-1.831	1.186	-0.814	0.083	0.288
5/08 - 10/08 (Wet)	-1.772	1.481	-0.565	0.163	0.403
11/08 - 1/09 (Dry)*	-1.686	0.669	-0.775	0.134	0.366
Overall Dry**	-1.831	1.327	-0.730	0.007	0.083
Overall Wet**	-1.995	2.476	-0.516	0.012	0.111

* incomplete seasons

** averaged across all wet/dry season months in record

Table 2 (continued).

T7W2	Min	Max	Mean	Variance	Std
9/04 - 10/04 (Wet)*	-0.447	1.488	0.176	0.004	0.059
11/04 - 4/05 (Dry)	-0.869	1.530	-0.160	0.006	0.078
5/05 - 10/05 (Wet)	-0.756	1.812	0.030	0.054	0.233
11/05 - 4/06 (Dry)	-1.198	0.947	-0.342	0.042	0.205
5/06 - 10/06 (Wet)	-1.411	1.471	-0.225	0.042	0.205
11/06 - 4/07 (Dry)	-1.056	1.361	-0.262	0.019	0.138
5/07 - 10/07 (Wet)	-0.802	2.182	-0.002	0.029	0.170
11/07 - 4/08 (Dry)	-1.204	1.748	-0.284	0.088	0.296
5/08 - 10/08 (Wet)	-1.015	1.826	-0.139	0.025	0.158
11/08 - 1/09 (Dry)*	-1.342	0.924	-0.658	0.123	0.350
Overall Dry**	-1.342	1.748	-0.301	0.006	0.076
Overall Wet**	-1.411	2.182	-0.064	0.011	0.103

T7W3	Min	Max	Mean	Variance	Std
9/04 - 10/04 (Wet)*	-0.613	2.677	-0.096	0.008	0.089
11/04 - 4/05 (Dry)	-0.669	1.576	-0.080	0.014	0.119
5/05 - 10/05 (Wet)	-0.485	1.805	0.127	0.035	0.187
11/05 - 4/06 (Dry)	-0.505	1.456	0.106	0.024	0.156
5/06 - 10/06 (Wet)	-0.987	1.303	-0.089	0.031	0.177
11/06 - 4/07 (Dry)	-0.750	1.199	-0.204	0.010	0.100
5/07 - 10/07 (Wet)	-0.550	2.051	-0.004	0.016	0.128
11/07 - 4/08 (Dry)	-0.708	1.625	-0.128	0.045	0.213
5/08 - 10/08 (Wet)	-0.827	1.377	-0.200	0.034	0.184
11/08 - 1/09 (Dry)*	-0.540	1.181	-0.188	0.061	0.247
Overall Dry**	-0.750	1.625	-0.089	0.003	0.057
Overall Wet**	-0.987	2.677	-0.046	0.013	0.116

T7W4	Min	Max	Mean	Variance	Std
11/04 - 4/05 (Dry)	2.484	4.197	3.436	0.181	0.426
5/05 - 10/05 (Wet)	2.537	5.979	4.235	0.524	0.724
11/05 - 4/06 (Dry)	1.903	4.987	3.474	0.772	0.879
5/06 - 10/06 (Wet)	1.287	3.493	2.359	0.506	0.711
11/06 - 4/07 (Dry)	0.996	2.857	1.825	0.343	0.585
5/07 - 10/07 (Wet)	0.761	5.713	3.706	2.334	1.528
11/07 - 4/08 (Dry)	3.165	5.610	3.991	0.235	0.485
5/08 - 10/08 (Wet)	2.732	6.963	4.399	0.329	0.574
11/08 - 1/09 (Dry)*	3.078	4.458	3.515	0.255	0.505
Overall Dry**	0.996	5.610	3.219	0.936	0.968
Overall Wet**	0.761	6.963	3.675	1.474	1.214

* incomplete seasons

** averaged across all wet/dry season months in record

Table 2 (continued).

T8W1	Min	Max	Mean	Variance	Std
11/04 - 4/05 (Dry)	-1.578	0.566	-0.597	0.005	0.070
5/05 - 10/05 (Wet)	-1.696	1.708	-0.347	0.102	0.320
11/05 - 4/06 (Dry)	-2.871	0.950	-1.246	0.261	0.511
5/06 - 10/06 (Wet)	-2.023	1.504	-0.583	0.076	0.275
11/06 - 4/07 (Dry)	-1.642	1.383	-0.580	0.026	0.161
5/07 - 10/07 (Wet)	-1.504	2.116	-0.164	0.064	0.253
11/07 - 4/08 (Dry)	-1.932	1.943	-0.531	0.188	0.433
5/08 - 10/08 (Wet)	-1.770	2.214	-0.177	0.219	0.468
11/08 - 1/09 (Dry)*	-1.436	1.561	-0.266	0.144	0.380
Overall Dry**	-2.871	1.943	-0.701	0.007	0.082
Overall Wet**	-2.023	2.214	-0.318	0.006	0.076

T8W2	Min	Max	Mean	Variance	Std
9/04 - 10/04 (Wet)*	-0.024	2.673	0.586	0.035	0.188
11/04 - 4/05 (Dry)	-0.242	1.428	0.084	0.001	0.035
5/05 - 10/05 (Wet)	-0.274	1.608	0.155	0.013	0.114
11/05 - 4/06 (Dry)	-0.438	1.085	0.029	0.013	0.116
5/06 - 10/06 (Wet)	-0.760	1.396	-0.005	0.019	0.136
11/06 - 4/07 (Dry)	-0.602	1.324	-0.008	0.021	0.143
5/07 - 10/07 (Wet)	-0.254	2.130	0.226	0.010	0.102
11/07 - 4/08 (Dry)	-0.319	1.687	0.179	0.013	0.115
5/08 - 10/08 (Wet)	-0.013	2.438	0.324	0.015	0.122
11/08 - 1/09 (Dry)*	0.001	1.223	0.149	0.019	0.139
Overall Dry**	-0.602	1.687	0.080	0.005	0.068
Overall Wet**	-0.760	2.673	0.197	0.012	0.108

T8W3	Min	Max	Mean	Variance	Std
11/04 - 4/05 (Dry)	1.348	3.404	2.348	0.087	0.296
5/05 - 10/05 (Wet)	0.842	4.564	2.506	0.477	0.691
11/05 - 4/06 (Dry)	0.436	0.682	0.526	---	---
5/06 - 10/06 (Wet)	0.068	3.032	1.166	0.473	0.688
11/06 - 4/07 (Dry)	0.143	2.536	0.806	0.194	0.441
5/07 - 10/07 (Wet)	0.273	4.855	2.689	0.380	0.616
11/07 - 4/08 (Dry)	1.149	4.339	2.209	0.170	0.412
5/08 - 10/08 (Wet)	0.785	4.970	2.502	0.170	0.412
11/08 - 1/09 (Dry)*	1.166	3.179	1.547	0.162	0.403
Overall Dry**	0.143	4.339	1.553	0.035	0.186
Overall Wet**	0.068	4.970	2.195	0.049	0.221

* incomplete seasons

** averaged across all wet/dry season months in record

Table 2 (continued).

T9W1	Min	Max	Mean	Variance	Std
9/04 - 10/04 (Wet)*	-1.121	2.462	-0.278	0.002	0.040
11/04 - 4/05 (Dry)	-1.843	1.215	-0.492	0.087	0.294
5/05 - 10/05 (Wet)	---	---	---	---	---
11/05 - 4/06 (Dry)	-1.331	0.460	-0.709	---	---
5/06 - 10/06 (Wet)	-1.999	1.006	-0.736	0.101	0.318
11/06 - 4/07 (Dry)	-1.855	0.906	-0.848	0.051	0.226
5/07 - 10/07 (Wet)	-1.511	1.686	-0.451	0.031	0.175
11/07 - 4/08 (Dry)	-1.956	1.267	-0.911	0.193	0.439
5/08 - 10/08 (Wet)	-1.707	1.667	-0.531	0.115	0.339
Overall Dry**	-1.956	1.267	-0.778	0.004	0.066
Overall Wet**	-1.999	2.462	-0.543	0.008	0.088

T9W2	Min	Max	Mean	Variance	Std
11/04 - 4/05 (Dry)	-1.547	1.516	-0.354	0.019	0.137
5/05 - 10/05 (Wet)	-1.259	2.137	0.124	0.188	0.434
11/05 - 4/06 (Dry)	-1.240	1.596	-0.136	0.060	0.244
5/06 - 10/06 (Wet)	-1.490	1.891	-0.105	0.123	0.350
11/06 - 4/07 (Dry)	-1.248	1.775	-0.192	0.064	0.253
5/07 - 10/07 (Wet)	-0.855	2.596	0.327	0.050	0.224
11/07 - 4/08 (Dry)	-1.254	2.182	-0.057	0.154	0.393
5/08 - 10/08 (Wet)	-1.048	2.634	0.309	0.177	0.420
11/08 - 1/09 (Dry)*	-1.097	1.730	-0.064	0.258	0.508
Overall Dry**	-1.547	2.182	-0.171	0.005	0.068
Overall Wet**	-1.490	2.634	0.164	0.003	0.055

T9W3	Min	Max	Mean	Variance	Std
9/04 - 10/04 (Wet)*	-0.902	3.186	0.925	0.002	0.049
11/04 - 4/05 (Dry)	-0.900	0.633	-0.216	0.092	0.304
5/05 - 10/05 (Wet)	-0.886	1.764	0.145	0.374	0.611
11/05 - 4/06 (Dry)	-1.246	0.907	-0.513	0.305	0.553
5/06 - 10/06 (Wet)	-1.551	0.025	-0.825	0.134	0.365
11/06 - 4/07 (Dry)	-1.496	-0.265	-0.936	0.082	0.287
5/07 - 10/07 (Wet)	-1.399	1.519	0.204	0.324	0.569
11/07 - 4/08 (Dry)	-1.064	1.444	-0.365	0.296	0.544
5/08 - 10/08 (Wet)	-0.992	2.749	0.255	0.446	0.668
11/08 - 1/09 (Dry)*	-0.667	0.595	-0.191	0.288	0.536
Overall Dry**	-1.496	1.444	-0.472	0.007	0.083
Overall Wet**	-1.551	3.186	0.015	0.064	0.254

* incomplete seasons

** averaged across all wet/dry season months in record

Table 3. Groundwater EC (S/m) wet/dry season statistics.

T1W1	Min	Max	Mean	Variance	Std
11/04 - 4/05 (Dry)	0.051	0.065	0.061	0.000	0.003
5/05 - 10/05 (Wet)	0.054	0.073	0.067	0.000	0.005
11/05 - 4/06 (Dry)	0.064	0.083	0.070	0.000	0.004
5/06 - 10/06 (Wet)	0.048	0.089	0.067	0.000	0.004
11/06 - 4/07 (Dry)	0.062	0.079	0.073	0.000	0.003
5/07 - 10/07 (Wet)	0.047	0.078	0.072	0.000	0.007
11/07 - 4/08 (Dry)	0.052	0.092	0.067	0.000	0.008
5/08 - 10/08 (Wet)	0.045	0.084	0.069	0.000	0.008
11/08 - 1/09 (Dry)*	0.049	0.085	0.065	0.000	0.005
Overall Dry**	0.049	0.092	0.068	0.000	0.006
Overall Wet**	0.045	0.089	0.069	0.000	0.006

T3W1	Min	Max	Mean	Variance	Std
11/04 - 4/05 (Dry)*	0.026	0.055	0.041	0.000	0.006
5/05 - 10/05 (Wet)	0.030	0.068	0.045	0.000	0.008
11/05 - 4/06 (Dry)	0.027	0.052	0.040	0.000	0.006
5/06 - 10/06 (Wet)	0.027	0.072	0.042	0.000	0.010
11/06 - 4/07 (Dry)	0.033	0.059	0.042	0.000	0.005
5/07 - 10/07 (Wet)	0.017	0.091	0.052	0.001	0.025
11/07 - 4/08 (Dry)	0.044	0.084	0.062	0.000	0.007
5/08 - 10/08 (Wet)	0.027	0.054	0.038	0.000	0.007
11/08 - 1/09 (Dry)*	0.038	0.054	0.046	0.000	0.002
Overall Dry**	0.026	0.084	0.046	0.000	0.010
Overall Wet**	0.017	0.091	0.045	0.000	0.014

T7W1	Min	Max	Mean	Variance	Std
9/04 - 10/04 (Wet)*	0.132	0.158	0.145	0.000	0.009
11/04 - 4/05 (Dry)	0.096	0.172	0.152	0.000	0.012
5/05 - 10/05 (Wet)	0.130	0.169	0.150	0.000	0.009
11/05 - 4/06 (Dry)	0.094	0.168	0.119	0.000	0.020
5/06 - 10/06 (Wet)	0.098	0.137	0.120	0.000	0.005
11/06 - 4/07 (Dry)	0.112	0.213	0.137	0.001	0.027
5/07 - 10/07 (Wet)	0.156	0.251	0.183	0.000	0.022
11/07 - 4/08 (Dry)	0.130	0.181	0.160	0.000	0.010
5/08 - 10/08 (Wet)	0.110	0.231	0.161	0.001	0.037
11/08 - 1/09 (Dry)*	0.107	0.232	0.140	0.002	0.039
Overall Dry**	0.094	0.232	0.142	0.000	0.006
Overall Wet**	0.098	0.251	0.153	0.000	0.007

* incomplete seasons

** averaged across all wet/dry season months in record

Table 3 (continued).

T7W2	Min	Max	Mean	Variance	Std
9/04 - 10/04 (Wet)*	0.189	0.220	0.204	0.000	0.001
11/04 - 4/05 (Dry)	0.155	0.232	0.198	0.001	0.028
5/05 - 10/05 (Wet)	0.107	0.155	0.126	0.000	0.013
11/05 - 4/06 (Dry)	0.068	0.076	0.071	0.000	0.002
5/06 - 10/06 (Wet)	0.069	0.141	0.087	0.000	0.016
11/06 - 4/07 (Dry)	0.100	0.146	0.115	0.000	0.010
5/07 - 10/07 (Wet)	0.117	0.348	0.176	0.002	0.048
11/07 - 4/08 (Dry)	0.141	0.339	0.228	0.003	0.057
5/08 - 10/08 (Wet)	0.104	0.142	0.110	0.000	0.007
11/08 - 1/09 (Dry)*	0.094	0.112	0.100	0.000	0.007
Overall Dry**	0.068	0.339	0.157	0.000	0.011
Overall Wet**	0.069	0.348	0.132	0.000	0.013

T7W3	Min	Max	Mean	Variance	Std
9/04 - 10/04 (Wet)*	0.065	0.082	0.070	0.000	0.004
11/04 - 4/05 (Dry)	0.061	0.074	0.066	0.000	0.003
5/05 - 10/05 (Wet)	0.055	0.086	0.069	0.000	0.006
11/05 - 4/06 (Dry)	0.051	0.071	0.057	0.000	0.005
5/06 - 10/06 (Wet)	0.049	0.086	0.059	0.000	0.004
11/06 - 4/07 (Dry)	0.069	0.135	0.101	0.000	0.013
5/07 - 10/07 (Wet)	0.094	0.139	0.106	0.000	0.007
11/07 - 4/08 (Dry)	0.060	0.098	0.069	0.000	0.009
5/08 - 10/08 (Wet)	0.051	0.070	0.059	0.000	0.005
11/08 - 1/09 (Dry)*	0.048	0.052	0.049	0.000	0.001
Overall Dry**	0.048	0.135	0.071	0.000	0.002
Overall Wet**	0.049	0.139	0.073	0.000	0.001

T7W4	Min	Max	Mean	Variance	Std
11/04 - 4/05 (Dry)	0.005	0.010	0.007	0.000	0.002
5/05 - 10/05 (Wet)	0.006	0.010	0.009	0.000	0.000
11/05 - 4/06 (Dry)	0.007	0.010	0.009	0.000	0.001
5/06 - 10/06 (Wet)	0.007	0.009	0.008	0.000	0.001
11/06 - 4/07 (Dry)	0.007	0.012	0.010	0.000	0.001
5/07 - 10/07 (Wet)	0.008	0.012	0.010	0.000	0.000
11/07 - 4/08 (Dry)	0.005	0.012	0.009	0.000	0.002
5/08 - 10/08 (Wet)	0.005	0.007	0.006	0.000	0.001
11/08 - 1/09 (Dry)*	0.006	0.007	0.006	0.000	0.000
Overall Dry**	0.005	0.012	0.008	0.000	0.002
Overall Wet**	0.005	0.012	0.008	0.000	0.002

* incomplete seasons

** averaged across all wet/dry season months in record

Table 3 (continued).

T8W1	Min	Max	Mean	Variance	Std
5/05 - 10/05 (Wet)	0.100	0.279	0.167	0.001	0.037
11/05 - 4/06 (Dry)	0.077	0.335	0.138	0.004	0.063
5/06 - 10/06 (Wet)	0.148	0.669	0.337	0.020	0.140
11/06 - 4/07 (Dry)	0.156	0.663	0.297	0.021	0.145
5/07 - 10/07 (Wet)	0.353	1.012	0.605	0.022	0.150
11/07 - 4/08 (Dry)	0.117	0.437	0.266	0.008	0.088
5/08 - 10/08 (Wet)	0.117	0.351	0.211	0.002	0.042
11/08 - 1/09 (Dry)*	0.142	0.202	0.164	0.000	0.018
Overall Dry**	0.077	0.663	0.224	0.000	0.019
Overall Wet**	0.100	1.012	0.337	0.001	0.034

T8W2	Min	Max	Mean	Variance	Std
9/04 - 10/04 (Wet)*	0.061	0.188	0.067	0.000	0.006
11/04 - 4/05 (Dry)	0.062	0.064	0.063	0.000	0.000
5/05 - 10/05 (Wet)	0.061	0.064	0.063	0.000	0.001
11/05 - 4/06 (Dry)	0.061	0.067	0.063	0.000	0.002
5/06 - 10/06 (Wet)	0.066	0.072	0.069	0.000	0.001
11/06 - 4/07 (Dry)	0.069	0.076	0.071	0.000	0.002
5/07 - 10/07 (Wet)	0.066	0.081	0.072	0.000	0.005
11/07 - 4/08 (Dry)	0.062	0.067	0.064	0.000	0.001
5/08 - 10/08 (Wet)	0.066	0.070	0.067	0.000	0.001
11/08 - 1/09 (Dry)*	0.064	0.068	0.066	0.000	0.001
Overall Dry**	0.061	0.076	0.066	0.000	0.003
Overall Wet**	0.061	0.188	0.067	0.000	0.004

T8W3	Min	Max	Mean	Variance	Std
5/05 - 10/05 (Wet)	0.020	0.030	0.026	0.000	0.001
11/05 - 4/06 (Dry)	0.029	0.030	0.029	---	---
5/06 - 10/06 (Wet)	0.021	0.046	0.035	0.000	0.006
11/06 - 4/07 (Dry)	0.000	0.036	0.031	0.000	0.002
5/07 - 10/07 (Wet)	0.015	0.042	0.027	0.000	0.005
11/07 - 4/08 (Dry)	0.018	0.031	0.025	0.000	0.001
5/08 - 10/08 (Wet)	0.015	0.032	0.024	0.000	0.003
11/08 - 1/09 (Dry)*	0.019	0.029	0.027	0.000	0.003
Overall Dry**	0.000	0.036	0.028	0.000	0.003
Overall Wet**	0.015	0.046	0.028	0.000	0.006

* incomplete seasons

** averaged across all wet/dry season months in record

Table 3 (continued).

T9W1	Min	Max	Mean	Variance	Std
9/04 - 10/04 (Wet)*	2.121	2.964	2.471	0.032	0.179
11/04 - 4/05 (Dry)	1.032	2.186	1.582	0.034	0.184
5/05 - 10/05 (Wet)	0.000	0.000	---	---	---
11/05 - 4/06 (Dry)	1.066	2.135	1.488	---	---
5/06 - 10/06 (Wet)	0.899	3.007	1.796	0.131	0.363
11/06 - 4/07 (Dry)	0.903	3.199	1.817	0.217	0.465
5/07 - 10/07 (Wet)	0.616	3.733	2.221	0.907	0.952
11/07 - 4/08 (Dry)	0.355	1.144	0.582	0.017	0.131
5/08 - 10/08 (Wet)	0.638	1.450	0.980	0.033	0.181
Overall Dry**	0.355	3.199	1.306	0.395	0.629
Overall Wet**	0.616	3.733	1.746	0.596	0.772

T9W2	Min	Max	Mean	Variance	Std
11/04 - 4/05 (Dry)	1.610	2.369	1.930	0.011	0.103
5/05 - 10/05 (Wet)	1.386	2.466	2.002	0.013	0.112
11/05 - 4/06 (Dry)	1.246	2.220	1.863	0.022	0.148
5/06 - 10/06 (Wet)	1.826	2.762	2.269	0.053	0.230
11/06 - 4/07 (Dry)	1.319	2.541	1.822	0.022	0.148
5/07 - 10/07 (Wet)	1.932	2.931	2.532	0.060	0.246
11/07 - 4/08 (Dry)	1.850	2.495	2.218	0.005	0.073
5/08 - 10/08 (Wet)	1.542	2.542	2.009	0.032	0.180
11/08 - 1/09 (Dry)*	1.341	1.861	1.619	0.007	0.082
Overall Dry**	1.246	2.541	1.921	0.046	0.215
Overall Wet**	1.386	2.931	2.203	0.084	0.290

T9W3	Min	Max	Mean	Variance	Std
9/04 - 10/04 (Wet)*	0.009	0.067	0.019	0.000	0.006
11/04 - 4/05 (Dry)	0.010	0.024	0.014	0.000	0.002
5/05 - 10/05 (Wet)	0.010	0.023	0.016	0.000	0.002
11/05 - 4/06 (Dry)	0.014	0.029	0.020	0.000	0.002
5/06 - 10/06 (Wet)	0.019	0.040	0.027	0.000	0.002
11/06 - 4/07 (Dry)	0.021	0.036	0.029	0.000	0.003
5/07 - 10/07 (Wet)	0.021	0.077	0.032	0.000	0.004
11/07 - 4/08 (Dry)	0.024	0.037	0.029	0.000	0.002
5/08 - 10/08 (Wet)	0.011	0.035	0.024	0.000	0.003
11/08 - 1/09 (Dry)*	0.020	0.025	0.023	0.000	0.001
Overall Dry**	0.010	0.037	0.023	0.000	0.006
Overall Wet**	0.009	0.077	0.024	0.000	0.006

* incomplete seasons

** averaged across all wet/dry season months in record